Quantifying the extent of change in extreme weather events in response to global warming

Travis Roger Moore

A Thesis

in

The department

of

Geography, Planning and Environment

Presented in Partial Fulfillment of the Requirements
for the Degree of Master of Science (Geography, Urban, and Environmental Studies) at
Concordia University
Montreal, Quebec, Canada

August 2013

CONCORDIA UNIVERSITY

School of Graduate Studies

This is to certify that the thesis prepared

By: Travis Roger Moore

Entitled: Quantifying the extent of change in extreme weather events in response to global warming

and submitted in partial fulfillment of the requirements for the degree of

M.Sc. Geography, Urban & Environmental Studies

complies with the regulations of the University and meets the accepted standards with respect to originality and quality.

Signed by the final examining committee:

Dr. Pascale Biron_____ Chair
Dr. Hashem Akbari_____ Examiner
Dr. Judith Patterson_____ Examiner
Dr. Damon Matthews____ Supervisor

Approved by _____
Chair of Department or Graduate Program Director

_____
Dean of Faculty

Date _____

Abstract

Quantifying the extent of change in extreme weather events in response to global warming

Travis Moore

Weather extremes have been documented in the context of a warming climate in association with increasing greenhouse gas concentrations. However, there remains much uncertainty as to how these extreme events will respond to future climate warming. In particular, climate modeling studies have predicted changes in the frequency and severity of weather extremes, and the range of changes reported in the literature is very large, and sometimes contradictory, as the nature of many extreme weather phenomena is not fully understood. This uncertainty stems, in part, from the limited ability of coarse resolution climate models to accurately measure and simulate weather events that occur at the microscale level, such as tornadoes and severe thunderstorms. However, some of the range of results reported originates simply from a wide variety of scenarios of future climate change used to drive climate model simulations, which hampers our ability to make generalizations about predicted changes in extreme weather events. The goal of this study is to conduct a meta-analysis of the literature on projected future extreme weather events, so as to identify trends, using global mean temperature change as a common frame of reference. Results indicate that global warming could significantly alter the behavior of multiple extreme weather events, such as mid-latitude drought, severe thunderstorms and tornadoes, as well as the selected important meteorological variables that engender them, into the 21st century.

Acknowledgements

I am deeply thankful to my supervisor, Dr. Damon Matthews, for funding this research, and for his extensive dedication and commitment in guiding me throughout this project, from its preliminary stages to its completion.

I would also like to extend my thanks to Dr. Claudia Tebaldi for kindly preparing and supplying the necessary data pertaining to Figure 4.1 of "Climate Stabilization Targets: Emissions, Concentration and Impacts over Decades to Millennia (2011)". This data was extremely useful in the upscaling process of projected regional temperature changes.

Finally, I would like to offer my heartfelt thanks to my family, friends and colleagues for their support and encouragement throughout the duration of this project.

Table of Contents

List of Figures

List of Tables

List of Acronyms

C	Celsius	49
CAPE	Convective available potential energy	9
CO_2	Carbon dioxide	3
CS	Cool season	61
E	East	26
ENSO	El Nino Southern Oscillation	13
GCM	General Circulation Model	8
hpa	Hectopascals	10
IPCC	Intergovernmental panel on Climate Change	9
JJAS	June, July, August, and September	55
K	Kelvin	9
km	kilometer	10
km/h	kilometer per hour	39
mb	Millibars	9
mm/day	Millimeters per day	42
mph	Miles per hour	6
M/s	Meters per second	7
N	North	16
NDSEV	Number of days in which severe thunderstorm environmental conditions occur	25
NE	Northeast	6
NH	Northern hemisphere	60
NOAA	National Oceanic and Atmospheric Administration	6
NW	Northwest	6
S	South	16
SE	Southeast	19

SH	Southern hemisphere	60
SSTs	Sea-surface temperatures	7
SW	Southwest	11
TC	Tropical cyclone	49
U.S.	United States	1
W	West	26

Introduction

Extreme weather events can be defined as weather phenomena that are at the extremes of the historical distribution, largely severe or unseasonable weather, and are rare occurrences that, by definition, only take place less than 5% of the time (Zhu & Toth). Though rare, extreme weather can dramatically impact society and have significant short and long term repercussions, particularly in terms of loss of life and major environmental, social and economic impacts. From 1990 to 2008, weather extremes accounted for, on average, nearly 35,000 deaths at a global scale annually (Goklany, 2009). In the U.S. (United States) alone, tornadoes and hurricanes combined are responsible for billions of dollars in damage and attributed to over 100 fatalities annually (McNeill, 2012); in 2011, there was a record 12 major weather disasters that each generated costs of over $1 billion while the nation experienced one of the deadliest tornado seasons in recorded history (Rice, 2011).

The response of extreme weather events to anthropogenic climate change has received considerable attention in climate science literature. Recent studies have linked a warming climate to changing frequency and severity of various weather extremes, including severe thunderstorms and tornadoes (Trapp et al., 2007), tropical cyclones (Stowasser et al., 2007; Sugi et al., 2009), heat waves (Gregory et al., 1997; Beniston, 2004), and winter storms at mid-latitudes (Carnell & Senior, 1998; Trapp, et al., 2009; Lambert, 2004). However, the range of changes documented for different events in the literature is large and is likely due to climate models being unable to fully simulate or represent certain extreme weather phenomena, especially those that occur at the microscale level. The uncertainties are also the result of the wide range of scenarios used to drive the models, which increasingly hinders our ability to make assertions about

projected trends in extreme weather events into the 21st century. Thus, the study of climate change science becomes increasingly relevant with respect to the ability of a warming climate to potentially modify extreme weather events for the future.

The science of climate change has rapidly evolved over the last 100 years, and especially over the last 40-50 years. However, the discovery of the science can be traced as early as the beginning of the 18th century, when natural changes in climate were first identified, as well as the role of the natural greenhouse effect (Weart, 2003). The definition of climate change can be described in multiple ways. For the context of this study, however, climate change can be defined as any change that occurs in the statistical distribution of weather patterns at different spatial scales. A distinction should also be made between "weather" and "climate". Weather refers to short term variations in various meteorological parameters (i.e. temperature, air pressure, precipitation, wind, etc.), while the discipline of climatology applies and studies the same meteorological variables over larger time scales, commonly in periods of decadal, centennial or millennial scales, and, for geological temporal scales, millions to even billions of years.

Climate feedbacks are particularly important in climate science in interpreting, for example, potential changing interactions between land-ocean-atmospheric relations, as a result of climate warming. A "climate feedback" is a mechanism by which an initial climate forcing (warming or cooling) is either accelerated or reduced through a response in subsequent climate systems. Although there is now a better understanding of how climate change might influence climate system interactions through climate feedback mechanisms, there remains uncertainty as to which feedbacks will be the most dominant in regulating global and regional climate; this will likely persist in being one of the major

challenges in the field of climate science in future climate modeling studies, primarily because of the complex nature of the climate system, and the interactions that occur between components of the system in response to climate change. In particular, the warming effect associated with increased atmospheric CO_2 (carbon dioxide) is important in terms of the potential response of extreme weather. Global warming related to rapidly increasing atmospheric CO_2 concentrations over the last few decades has been shown to potentially affect extreme weather events in terms of frequency and intensity into the 21st century. For example, warmer global temperatures can lead to an increase in the amount of atmospheric moisture (or water vapor) available for thunderstorm development. An enhancement of moisture can, in turn, contribute to an increase in the number of intense thunderstorms with vigorous updrafts. Similarly, increased atmospheric moisture, through climate warming, can act to increase the intensity of tropical cyclones. Overall, increases in global temperatures can play a significant role in changing the frequency and/or intensity of extreme weather events for the future.

The intent of this study is to explore to what extent changes in extreme weather events can be quantified as a function of global mean temperature change. Other questions of interest that stem from this objective can be related specifically to how individual extreme events may respond to changes in global mean temperature. For example, will tropical cyclones or heat waves becoming increasingly frequent in the future, as a result of a warming climate? Similarly, might we expect an increase or decrease in their overall intensity? Or, are there no significant trends in predictions of the frequency and intensity of specific extreme weather events? Do certain weather extremes appear to be more sensitive to global warming relative to others?

In this study, I have used a meta-analysis to critically evaluate and statistically combine results from climate impacts literature in order to quantify selected weather extremes by using global mean temperature change as a common frame of reference. Most studies use climate modeling techniques to assess how various weather extremes may change over time in response to global warming. Other research employs observational analyses to evaluate past trends to make projections for the future. However, no climate-related work has yet integrated a meta-analysis to study potential future trends in weather extremes.

A meta-analysis incorporates results or findings derived from a collection of research that has a related set of hypotheses, with the purpose of increasing statistical power, increasing the level of reliability of the results, as well as improve estimates of the effect size of an association or intervention (Statistical Solutions, 2011). A meta-analysis is a particularly useful method for the nature of this study, as it combines the ideas and results from a large body of academic literature while making it less influenced by local findings, and it similarly makes it possible to show if publication bias exists (Statistical Solutions, 2011). Meta-analyses make generalizations to the population of studies, and they have the ability to control for between-study variation (Statistical Solutions, 2011). Meta-analyses also offer more precise estimates of the size of any of the effects uncovered (Crombie & Davies, 2009). In addition, this method can show if results are more varied than what is expected from the sample diversity, and it includes moderators to explain variation.

Through the technique of meta-analysis, I have quantified how a warming climate may alter the frequency and severity of extreme weather events at regional to global

scales. I have based some of the methodological approach on a recent study, which used meta-analyses to quantify ecological impacts associated with climate change, focused on the effect of global mean temperature rise on ecosystems (Warren et al., 2010). My research will extend and apply this analysis to changing weather extremes. I have considered individual extreme phenomena based on projected future changes in frequency and intensity, typically by the end of the 21st century. Specifically, I have analyzed the literature on tornadoes, severe thunderstorms, tropical cyclones, the South Asian monsoon, heavy precipitation events, drought, heat waves, and the El Nino Southern Oscillation, through the extraction of model output data that project changes in their frequency and intensity in response to projected changes in global mean temperature. As such, this paper has first provided an overview of the literature pertaining to each event under investigation, followed by a description of the systematic approach used for the meta-analysis. A discussion of the results derived from the statistical analyses employed has then been given.

Literature Review

In this section, I will briefly review the current literature on specific weather extremes.

-Tropical cyclones

A tropical cyclone is defined as an intense area of low pressure consisting of a rotating band of organized thunderstorms that typically initiates in tropical and subtropical waters and has a closed low-level circulation (NOAA, 2012). "Tropical cyclone" is a term used to collectively identify and describe tropical depressions, tropical storms, hurricanes (NE(Northeast) Pacific and Atlantic), cyclones (North Indian Ocean) and typhoons (NW(Northwest) Pacific). Each of these terms is designated to a tropical cyclone based on sustained surface wind speeds and central surface pressures over a given period of time and is contingent with specified thresholds on the Saffir-Simpson scale. Tropical depressions are areas of low pressure with little defined structural characteristics that its superior stages possess, typically a prominent eye. Tropical depressions are upgraded to tropical storms when sustained surface wind speeds achieve and/or surpass 39 mph (miles per hour), while tropical storm status is established when maximum surface sustained winds of between 39-73 mph. Once sustained surface winds exceed tropical storm status, hurricane, typhoon, tropical cyclone, severe tropical storm, or severe cyclonic storm status is attained, depending on the region in question. For all major tropical cyclones (categories 3 through 5), however, NOAA (National Oceanic and Atmospheric Administration) uniformly stipulates an achieved maximum surface wind speed of 111 mph or greater.

Source regions are regions of development where ideal conditions are most suitable for cyclogenesis, a process used to describe and study the formation or evolution of tropical or mid-latitude cyclones over time. The cyclogenesis of a tropical cyclone becomes most favorable under the influence of warm SSTs (sea-surface temperatures) of at least 26.5 degrees Celsius, with generally warm waters that extend to sufficient depths (ideally about 60 meters in depth). The presence of warm SSTs is particularly important because they provide ample amounts of sensible and latent heat to a tropical cyclone (Ahrens, 2007).

Warm SSTs also need to be occurring with strong surface convergence and upper-level divergence, accompanied by sufficient vertical uplift and ample surface/near-surface moisture (Ahrens, 2007). If a tropical cyclone is to initiate successfully, an area of convergence is required to allow tropical squall line thunderstorms to become more organized. Surface convergence may take place with an easterly tropical shortwave trough, or a pre-existing frontal feature, such as a modified cold front that has migrated towards the tropics from mid-latitudes. Little vertical wind shear is also crucial. Vertical wind shear, defined as a change in both speed and direction with increasing altitude, is a meteorological variable that is very important in forecasting the evolution of a tropical cyclone over time. Vertical wind shear values surpassing 15 m/s (meters per second) are considered detrimental to the development of tropical cyclones; this is largely because high levels of vertical wind shear act to disperse heat and moisture, effectively disrupting the vertical structure of a given storm and limiting organized convection from occurring. Consequently, tropical cyclones will gradually weaken when exposed to a zone of high vertical wind shear, even when other ideal environmental conditions are in place.

Tropical cyclones are known to have devastating impacts on society, and potential changes for the future are, thus, of great importance in a warming climate. Over the last two centuries, tropical cyclones have been responsible for nearly two million fatalities, and recent projections show that these storms could potentially account for as much as $109 billion in damage by 2100 (Mendelsohn et al., 2012). Damage costs have also been suggested to increase in the U.S. Gulf and East Coasts by the end of the 21st century due to Atlantic hurricanes (Emanuel, 2011), particularly with respect to storm surge, such as in New York City (Lin et al., 2012). Climate research revealed that the distribution of global tropical cyclones may be changing in response to CO_2-induced warming (Stowasser et al., 2007; Sugi et al., 2009). Atlantic hurricane activity has also been attributed to naturally occurring cycles in tropical climate patterns near the equator (Cheetham, 2011). These natural cycles are referred to as the "tropical multi-decadal signal", and it has been shown that this signal can significantly affect the oceanic and atmospheric conditions in and around the tropical Atlantic. The tropical multi-decadal signal commonly moves through active and inactive phases, lasting for as much as 20-30 years at a time, or perhaps even longer (Cheetham, 2011). Studies have suggested that the increase in active hurricane seasons, particularly since 1995, may be due to a more active phase of the tropical multi-decadal signal, and it is likely that this active phase provided the key conditions necessary for producing an increase in the number of active seasons between 1995 and present day (Beven, et al., 2008).

Several GCM (general circulation modeling) studies that have examined tropical cyclones in the context of a warming climate have done so by typically using a variety of CO_2 scenarios (Knutson et al., 1998; Oouchi et al., 2006; Yoshimura et al., 2006;

Stowasser et al., 2007). Since the early 1990's, increased research efforts have attempted to study how a progressively warming climate may modify the behavior of tropical cyclonic systems. In this sector, studies employ a variety of climate models participating with the IPCC (Intergovernmental Panel on Climate change) to assess and predict changes in storm trajectory, genesis (cyclogenesis), core rainfall, mean surface wind speeds, and general changes in the frequency and intensity of tropical cyclonic systems through these parameters. Experiments that are commonly employed in the literature integrate one or more warming scenarios that are used to simulate tropical cyclone tendencies at various points into the 21st century at different spatial scales. Experimental design is mostly driven by a combination of IPCC and transient greenhouse gas scenarios, as well as prescribed SST changes, typically at tropical latitudes and cyclone development regions. In some cases, the inclusion of a coupled ocean-atmosphere model (e.g. Knutson et al., 2001) is used to study the influence of oceans on the physical processes of cyclogenesis. However, the response of tropical cyclone climatology has differed amongst the findings, largely due to the practical limitation of coarse resolution numerical models (Stowasser at al., 2007). With that said, a trend towards increasing tropical cyclone intensity, as well as increasing intense tropical cyclone frequency is shown in several studies. For example, results given by Knutson et al. (1998) suggested that in a high-CO_2 scenario, surface pressure, on average, for typhoons was 20 mb (millibars) lower, maximum wind speeds increased, and CAPE (convectional available potential energy) increased. Stowasser et al. (2007) showed a substantial warming of tropical surface waters, where SSTs increased by approximately 3 K (Kelvin), and global surface air temperatures increased by 4.5 K under a six-fold increase of present-day

atmospheric CO_2. This resulted in a significant increase in the number of intense tropical cyclones over the entire NW Pacific, while the total number of cyclones in the basin increased only slightly. Yoshimura et al. (2006) have shown that under a doubled CO_2 scenario, the global frequency of weak tropical cyclones may decrease, but the number of intense tropical cyclones could increase in a warmer climate.

In particular, multiple modeling studies show a tendency towards decreasing cyclone frequency at global and regional scales. For instance, Oouchi et al. (2006), Sugi et al., (2009) have shown a consistently large reduction in tropical cyclones at a global scale in a warmer climate, which is similarly projected in Yoshimura et al. (2006) under doubled CO_2 conditions, especially in the Southern hemisphere. Using a 50 km (kilometer)-resolution global atmospheric model, Held & Zhao (2011) similarly found that tropical cyclone frequency decreased by 20% under the combined effect of atmospheric warming, and an increase of 2 K in SSTs. The general reduction in cyclone frequency is shown to be attributed to enhanced upper-tropospheric stability in a warmer climate. Static stability is defined as the stability of the atmosphere in hydrostatic equilibrium with respect to vertical displacement (Peppler, 1988) and determines the buoyancy frequency of dry perturbations in the vertical, and the magnitude of the greenhouse effect (Frierson, 2006). Static stability may also be defined as the difference in potential temperature between two height pressure surfaces, usually between mid- to upper-levels of the atmosphere, most often the 200 to 500 hpa (hectopascals) and surface level (Stowasser et al., 2007; Oouchi et al. 2006; Yoshimura et al., 2006). In the tropics, the moist convection occurring over warm waters alters upper-tropospheric temperature profiles, in which the moist adiabatic structure results in upper-tropospheric amplification

of global warming (Frierson, 2006). Because this warming is principally driven by deep, moist convection, warmer surface temperatures may lead to further warming in the tropical upper-troposphere through greater latent heat release associated with condensation. As such, the tropical upper-tropospheric temperatures would warm proportionally more than those in the boundary layer (Bengtsson et al., 2009), effectively reducing the potential for more numerous tropical cyclone activity across all, or most, storm basins by limiting the potential for deep convection, reducing upward vertical velocities and mid-level vorticity, and weakening the intensity of the tropical circulation flow (Sugi et al., 2002; Stowasser et al., 2007). At the same time, particularly in the Eastern Pacific and tropical Atlantic, other analyses have shown that wind shear increases per degree Celsius global warming, revealing a potential decrease in the number and intensity of Atlantic hurricanes and tropical storms for the future (Vecchi & Soden, 2007; Zhao et al. 2009).

-South Asian monsoon

The Asian monsoon is considered the most spectacular manifestation of the global climate system and is responsible for providing a major percentage of water sources to the largest and most densely populated areas of the world (Ueda et al., 2006). Therefore, how the Asian monsoon may respond to future global warming is of great climatic importance throughout much of the Asian continent. A "monsoon" is widely accepted as a seasonal reversal of wind circulation patterns, and corresponding alterations in precipitation, over a given region. Though the effect of a monsoon is most prominent over much of the Asian continent, monsoons do occur in other regions of the world, such as in Europe, Africa, the SW (Southwest) U.S. and Australia. The Asian monsoon may be

subdivided into region-specific monsoons, such as the South Asian monsoon, as well as the East/NE Asian monsoon. The South/SW Asian monsoon is the most influential of the global monsoons, especially for much of the Indian subcontinent, and it is, consequently, of significant cultural, agricultural and economic importance in India. The monsoon accounts for approximately 55% of the subcontinent's observed annual rainfall (Lal et al., 1998) and, as such, the South Asian and Indian monsoon is of particular interest amongst climate studies.

The Summer South/SW Asian monsoon typically spans from June through to September, with maximum intensity occurring during June, July and August. By late-Spring, as surface temperatures warm much more rapidly, a broad area of low pressure, often termed a "heat low", develops and progressively intensifies over the Indian subcontinent, replacing the anti-cyclone (Siberian High) that is common during the Northern hemisphere Winter. This area of low pressure is also accompanied by a trough of low pressure, called the "Monsoon trough", stationed over the Gangetic Plains, which acts as an important feature for surface convergence and upward vertical motion. Areas of low pressure that move inland along this trough often bring moist convective clouds, inducing intense spells of rainfall (Lal et al., 2001). As the land continues to heat, a steep pressure and temperature gradient becomes established, and because of the circulation around low pressure, prevailing SW winds draw moisture from the Indian Ocean and transport it towards much of South and SW Asia.

Modeling studies have suggested that climate change could strengthen the seasonal monsoon patterns in East Asia (Chen et al., 2004). In a doubled CO_2 scenario, the climate tends to be warmer and wetter and regional climate models have predicted an

overall increase in annual precipitation across much of China, including 23% over Northern China, 21% over central regions, and 8% in southern regions (Chen et al., 2004). Transient greenhouse gas concentration simulations also showed that the effect of El Nino events on the Asian monsoon could decrease due to climate warming (Ashrit et al., 2001), leading to a net increase in rainfall, despite ENSO (El Nino Southern Oscillation) moving into a warmer mean state (Ashrit et al., 2001). Another transient greenhouse warming experiment that used the IPCC IS92 emissions scenario also found an intensification of the Asian monsoon, as well as an increase year-to-year variability, due to an increase in land-sea temperature contrasts, a northward shift in the inter-tropical convergence zone, and a westward shift in the ascending branch of the Walker Circulation (Hu et al., 2000). Kripalani et al., 2003 conversely found, in an observational data analysis, that there is no clear evidence to suggest that both the strength and variability of the Indian monsoon rainfall or its epochal changes (characterized as alternate 30-year periods of above or below normal rainfall) have been impacted by global warming to date.

-Global precipitation and heavy precipitation events

Precipitation is considered to be one of the most important meteorological variables and is of great interest when studying potential changes in extreme precipitation events in a warmer climate, particularly heavy snowfall or convective rainfall events. Precipitation is characterized as having smaller spatial and temporal scales than temperature, and observational data is taken mostly over land (Boer et al., 2000). In many discussions centered on global warming, it is implicitly assumed that the atmosphere will become more energetic as it warms (Held and Soden, 2006), and it is often shown that

precipitation intensity and extreme precipitation scale with column water vapor under climate change (O'Gorman & Muller, 2010).

Precipitable water, also referred to as (integrated) column water vapor, is commonly used as an indicator for the amount of water vapor and moisture in the atmosphere over a particular region or location at different intervals of time. Column water vapor is a useful predictor for favorable conditions associated with deep convection, which is particularly important for lifted parcels experiencing entrainment (Holloway et al., 2009). Higher values of precipitable water have been associated with severe thunderstorms, as the effect of increased water loading from large quantities of water in the main downdraft region of a storm can produce heavy bursts of rain, as well as damaging downdrafts along the gust front. As such, increased precipitable water in the troposphere increases the potential intensity of convective systems by supplying additional moisture or water vapor that could be condensed and precipitated out over a given location. Entrainment plumes have been suggested to become much more buoyant at middle to upper levels of the troposphere when column water vapor values are high, and enhanced free-tropospheric moisture plays an important role in the transition from shallow to deep convection (Holloway et al., 2009). The factors necessary for heavy precipitation events, however, vary by region and season and are, therefore, either dynamically- or thermodynamically-driven (O'Gorman & Muller, 2010; Radermacher & Tomassini, 2012).

The Clausius-Clapeyron relation is used to describe temperature dependence of the saturation vapor pressure and stipulates that a 7% increase in water holding capacity of the atmosphere is produced for every corresponding degree Kelvin change

(Radermacher & Tomassini, 2012). Climate simulations show that warmer temperatures effectively increase the atmosphere's holding capacity of water vapor, consistent with the Clausius-Clapeyron relationship (Boer, 1993; Bosilovich et al., 2005; Held & Soden, 2006). Precipitation, however, is shown not to significantly increase at the Clausius-Clapeyron rate because energy constraints appear to control the strength of the hydrological cycle, though these constraints are much less significant at lower temperatures, suggesting that cool season precipitation increases at a rate more consistent with this relationship (Lorenz & DeWeaver., 2007).

Increased atmospheric moisture content in a warmer climate is shown to enhance precipitation and heavy precipitation events, which may be the result of enhanced moisture convergence (Trenberth, 1998). A comparison of observed and multi-model simulated changes in extreme precipitation over the latter half of the 20th century showed that human-induced increases in greenhouse gases have led to observed intensification of heavy precipitation events over two thirds of the Northern hemisphere land areas (Min et al., 2011). Observational data analysis also shows a trend in increased heavy precipitation in the U.S., with a larger number of days annually exceeding 50.8 mm (Easterling et al., 2000). Over most of Australia, GCM analyses, using an equilibrium-enhanced greenhouse effect, showed that a doubled CO_2 scenario increased the frequency of heavy rainfall events, while decreasing low-rainfall events, implying a greater likelihood of increased flooding (Whetton et al., 1993). Lenderink & Meijgaard (2008) also find in their simulations with a high-resolution regional climate model that one-hour precipitation extremes increase by twice as much with rising temperatures, as well as a

14% increase per degree of warming over large parts of Europe, implying an increase in local flooding.

-Mid-latitude cyclones

Mid-latitude cyclones, also known as extra-tropical cyclones, are cyclonic storms that occur at mid-latitudes (30-55 N (North) and S (South)) as synoptic-scale areas of low pressure. These weather systems are often associated with a variety of extreme weather, including Winter storms, severe thunderstorms, tornadoes, heat waves, and strong winds. Unlike tropical cyclones, mid-latitude cyclones are driven largely by baroclinic instability, where a large pole-equator temperature gradient exists, promoting appreciable to significant warm and cold air advection that is conducive to cyclogenesis. As a cyclone experiences intensification, its precipitation coverage and intensity are also correspondingly enhanced, further promoting cyclonic development.

Moisture availability is also a critical factor that is essential for the development of mid-latitude cyclones. Large amounts of moisture drawn into a mid-latitude cyclone facilitates the release of vast quantities of latent heat, which further promotes atmospheric de-stabilization and allows for potentially vigorous cyclogenesis. It is revealed that about 70% of precipitation associated with mid-latitude cyclones is derived from pre-existing moisture in the atmosphere at the time a given storm formed, while the remaining amount comes from evapotranspiration (Trenberth et al., 2005). With a large quantity of moisture available, enhanced condensation can occur, releasing more latent heat. Reed et al. (1988) showed that over a 24-hour period, latent heating accounted for 40-50% of mid-latitude cyclones' intensification. Consequently, a warming climate can lead to an increased

availability of lower- and mid-tropospheric humidity and moisture content and, therefore, latent heat release (Lambert 1995; Lambert, 2004). The effect of latent heat is also represented in Watterson (2006), where latent heat enhancement occurs with precipitation intensification in a warmer climate, indicating increased genesis in mid-latitude cyclones.

Changes in frequency, intensity and storm track have been documented in various modeling studies (Lambert, 1995; Finnis et al., 1997; Carnell & Senior, 1998; Geng & Sugi, 2003; Lambert et al., 2004; Lambert & Fyfe, 2006). Carnell & Senior (1998), for example, using the Hadley Center coupled ocean-atmosphere model, reported a reduction in the total number of storms during the Northern hemisphere Winter but observed a tendency towards deeper low pressure storm centers, suggesting enhanced intensification of storms. Geng & Sugi (2003) also show that the cyclone density of stronger storms increased by almost 20% in both hemispheres during the June-July-August period. An ensemble of 250-year transient enhanced greenhouse simulations conducted in Lambert (2004) similarly yielded decreases in Winter cyclonic events in both the Northern and Southern hemispheres but an increase in the number of intense events, but the overall reduction in cyclonic frequency was most prevalent in the Southern hemisphere (Lambert & Fyfe, 2006).

In terms of storm track, modeling studies have suggested that storm tracks from the North Pacific and North Atlantic may become shorter and decrease in length at the Northeastern end of the tracks (Carnell & Senior, 1998) in a warmer climate. Compared with the present climate, storms tended to propagate faster, and storm tracks exhibited trajectories that have resulted in storms traveling slightly poleward toward the North Atlantic coast (Geng & Sugi, 2003). Similarly, atmospheric warming may cause

Northwest Atlantic storms to increase in radius, propagate faster, become more severe in nature, and occur in storm tracks that shift slightly poleward (Jiang & Perrie, 2007). It has also been suggested that spatial and structural differences in the distribution of mid-latitude extratropical cyclones in warming-induced conditions exist, where a larger horizontal extent of storms was present as compared to those in the present climate, and stronger wind speeds also tended to occur at greater radii from the storms' center in the climate change scenario simulations (Jiang & Perrie, 2007).

-Drought and heat waves

Drought is not considered an extreme weather event in itself, but it is a condition that is produced by changes in surface and weather patterns, such as deficiencies in soil moisture, rainfall, snowfall, and increased evaporation rates relative to the total amount of precipitation that occurs over a given region or area. Studies that have directly examined drought intensity and frequency in response to future global warming are relatively few in number, and other studies largely explore observational records to identify potential mechanisms behind ongoing drying at regional scales, rather than projecting future changes with global warming.

Soil moisture is an important modulator in the evolution of Summer drought, as well as for surface temperatures. If abundant, moisture stored in the soil evaporates as the surface warms, causing warm, moist air to rise and condense into colder air aloft, which generates late-day rain showers while serving as an additional moisture supply to convective systems. Abundant soil moisture can also significantly contribute to the severity of thunderstorms, as well as tornadic activity in the U.S. When soil moisture is deficient during the late-Spring to Summer, surface evaporation becomes smaller, and the

surface can readily become much hotter because of the lack of evaporative cooling under these conditions, which would otherwise moderate surface temperatures more efficiently. As the snowmelt period ends earlier, the soil, having a lower albedo, is exposed to incoming solar radiation, causing soil moisture stored during the Winter to more quickly evaporate with onset of consistent Spring temperatures. By the late-Spring to Summer period, reduced soil moisture prompts a corresponding decrease in evaporation, and this process is further accelerated by reduced lower-tropospheric relative humidity, which, in turn, prevents saturation and, therefore, rainfall is inhibited (Wetherald & Manabe, 2002). Indeed, we can see that the Winter of 2012 across North America was characterized by very little snow over much of the continent, leading to a deficit in soil moisture, which contributed to extreme drought conditions for much of Canada and the U.S. into the following Summer.

Historical trends, from 1950 to 2010, reveal that progressive global aridity has increased, mostly due to drying taking place over SE (Southeast) Asia, Eastern Australia, Southern Europe, and over much of the African continent (Dai, 2011; Dai, 2013). This upward trend in global drought areas may be attributed to the ongoing warming that had occurred since the 1980s, which prompted an 8% increase in the areas under drought over the first decade of this century (Dai, 2013). Time-dependent coupled ocean-atmosphere GCM studies have shown that with increased levels of CO_2, precipitation and soil moisture are greatly reduced across central North America and Southern Europe (Gregory et al., 1997). Over recent decades, drought events have been linked to changes in tropical SSTs, particularly those of the tropical and equatorial Pacific (Dai, 2011). Therefore, historical changes in ENSO patterns (Dai, 2011) have been an important

climatic factor in global drought since the 1950s, where La Nina events have been associated with drying in North America, while El Nino has often generated drought conditions over much of Asia, particularly East Asia, when it is present, possibly due to a weaker monsoon circulation when an El Nino event occurs.

Because of climatological variations at the regional scale, there is generally no universal definition that characterizes a heat wave. However, the World Meteorological Organization defines a heat wave as when maximum temperatures for more than five consecutive days exceed five degrees Celsius, relative to the climatological norm for a given location or region (usually with respect to 1961-1990 climatology). However, different regions establish different standards as to when a heat wave formally occurs; a hot, moist climate, which is common in equatorial and tropical regions of the globe, may define a heat wave much more differently than a given location stationed in the mid-latitudes. Heat waves may also have different thresholds within the same country. In Canada, for example, a heat wave is declared when at least three consecutive days attain 32 Celsius or more, but in the province of Quebec, the threshold is 30 Celsius over the same period of time.

Heat waves during the late-Spring to Summer season at mid-latitudes are common under a variety of meteorological conditions. Heat waves are largely associated with a combination of dynamic and thermodynamic processes interacting with hydrological changes at the land surface (Lau & Nath, 2012). Most frequently, high pressure developing at mid-levels of the troposphere provide the most favorable conditions for the development of a heat wave. Building high pressure at mid- to high-levels of the troposphere that become stationary often induce air subsidence towards the surface and

creates a “lid” (a temperature inversion) at mid-levels of the atmosphere, causing building heat to be trapped near the surface while preventing the rising motion of air, and, therefore, convection, from occurring for as much as several days to even over a week. Such conditions would also produce positive geopotential height anomalies (Huth et al., 2000; Lau & Nath, 2012; Meehl & Tebaldi, 2004). Because of the extreme dry conditions associated with air subsidence, soil moisture is quickly exhausted, leading to further drying through a decline in surface and near-surface relative humidity. In other cases, a heat wave may be accompanied by sweltering humidity. In North America, for instance, when a strengthening area of high pressure that displaces over the Atlantic and becomes stationary, the Southwesterly circulation located at its back end allows for very warm and moist air to flow into much of the central and Eastern sections of the continent, aided by areas of low pressure forming to the West.

Soil moisture, like drought, is a determinant for the intensity and frequency of heat waves, especially for mid-latitude regions. In particular, the European and North American continents have received attention with respect to potential changes in heat waves and drought in a warmer climate, notably in Europe. Observational and modeling studies that focus on European heat waves have also been emerging over the last decade, and the motivation for this research was primarily due to the extreme Summer heat of 2003 that affected much of the continent. As is the case for drought-like conditions, a lack of soil moisture during the Winter can create extremely dry conditions in time for the late-Spring to Summer period. It is suggested that the frequency of very hot days could increase tenfold in Summer under drier soil conditions (Attinger, 2012). Regional climate models running simulations of increased greenhouse gas concentrations have also

revealed that temperature variability increased by up to 100% in future European climate, with maximum changes occurring in Eastern and central Europe (Schar et al., 2004). Other findings similarly suggest that European Summers will become progressively as hot as the heat wave of 2003 by the latter part of the 21st century (Beniston, 2004; Beniston & Diaz, 2004). Similarly other projections estimate that under a doubled CO_2 scenario, the resultant Summer temperature could be as high as 4.5 Celsius over South Moravia (Czech Republic), which could induce a five-fold increase in the frequency of tropical days, and a larger number of heat waves and dry spells globally (Huth et al., 2000). Climate studies have shown that the snowmelt period could end sooner in a warmer climate (Wetherald & Manabe, 2002), suggesting that soil moisture would have more time to evaporate, as an increase in solar radiation would be absorbed by the surface for a prolonged period. This corresponds to a decrease in annual soil moisture at regional scales, especially mid-latitudes and semi-arid regions. However, most of the annual decrease in soil moisture is attributed to large decreases found during the warmer months.

-Severe thunderstorms and tornadoes

Severe thunderstorms and tornadoes are some of the most violent and destructive weather events on Earth and accounted for nearly $20 billion in damage from 1950-1994 in the U.S. alone (NOAA, 2013). Yet, in spite of their destructive power, and the significant impacts associated with them, they have received considerably less attention in the literature, as compared to other forms of extreme weather, such as tropical cyclones. This is likely because of very limited data availability, and climate models' inability to fully simulate those weather events that occur at such small spatial scales. Severe thunderstorms can, with the exception of Antarctica, occur on any continent, but a

major proportion of these storms principally develop in the U.S. every year and take place largely during the Northern hemisphere Spring, where the vast majority of annual average number of tornadoes (approximately 1000) occur. Tornadoes are defined as a spinning vortex of air that extend from the base of a severe thunderstorm (as a funnel) and makes contact with the surface. The strength rating of a tornado is estimated by using the Fujita scale, or Enhanced Fujita scale, which are both scales entirely based on the nature of the damage a given tornado induces. Both the Fujita and Enhanced Fujita scales are subdivided into six categories, ranging from F0/EF0 to F5/EF5, representing the weakest to strongest rating, respectively.

Severe thunderstorms are largely associated with enhanced atmospheric baroclinicity, in which boundary layer and mid-level tropospheric cool and warm air advection is occurring. The degree of baroclinicity is most often at its peak during the Spring season, when cold air to the North and warm air to the South strongly interact, often generating a defined meridional temperature and pressure gradient that supports vigorous cyclogenesis. The U.S. offers a classic, yet unique, atmospheric and geographic combination for conflicting air mass interactions to occur. During the tornado season within the tornado alley of the U.S., maritime tropical air masses originating from the Gulf of Mexico circulate farther North, which commonly mingle with cold, drier air to the North. It is this interaction that facilitates vigorous cyclogenesis to take place across much of the U.S. Midwest and Great Plains, in addition to the occasional presence of dry air migration from the U.S. SW. In addition, the NE-SW orientation of the Appalachians to the East and North-South extent of the Rockies to the West means that warm, moist air

from the South is not hindered in its Northward migration, allowing these air masses to frequently collide with colder air to the North.

As air masses of differing densities collide at low- to mid- levels of the troposphere, this favors the development of strong, deep areas of low pressure, as well as creating suitable low-level and deep-layer vertical wind shear, in which, as specified previously, winds change in both direction and speed with increasing elevation within the troposphere. A high amount of vertical shear is crucial for long-lasting severe thunderstorms to occur, as it acts to displace the storms' downdraft from their main updraft region, thereby preventing any significant weakening of the storms' updraft associated with the downward motion of air, an effect that does not occur within ordinary single-cell thunderstorms. As deep-layer vertical shear becomes increasingly favorable, the likelihood for vertically-defined mesocyclonic activity (rotating updraft) within supercell thunderstorms becomes enhanced.

In addition to sufficient vertical wind shear, severe thunderstorms also require suitable levels of CAPE in order to successfully develop. CAPE is a thermodynamic measure that assesses the degree of instability, or buoyant energy, that is present in the troposphere over a given period of time. High levels of CAPE, measured in units of Joules per kilogram (J/kg) often result when strong thermodynamic instability is occurring in a given area. When CAPE values are in excess of 2500 J/kg, significant levels of atmospheric instability are occurring, and any thunderstorms in development within this environment will possess vigorous updrafts, reducing the effect of water loading on a storm's updraft. Larger levels of boundary layer moisture and surface heating drive large surface-based thermodynamic instability. Thus, the most severe

thunderstorms are mostly found in environments where sufficient vertical wind shear and large amounts of CAPE are occurring concurrently. Abundant soil moisture can also enhance CAPE by releasing more water vapor to the atmosphere. Consequently, warm seasons with abundant soil moisture can yield a greater number of days where higher levels of CAPE can exist.

Ongoing greenhouse warming has been documented as a factor in influencing thunderstorm and tornadic activity at regional scales. However, data availability and reliability is a very limiting factor in small-scale meteorological phenomena (Davis & Walsh, 2008). Research has considered the transient response of severe thunderstorms to increased greenhouse gas concentrations and have shown that severe thunderstorms increased with time in response to climate warming (Trapp et al., 2007; Trapp et al., 2009), particularly East of the North American Rocky mountains (e.g. Diffenbaugh et al., 2008). "NDSEV" refers to the number of days in which severe thunderstorm environmental conditions occur and is the product of wind shear and CAPE (Trapp et al., 2007). Modeling studies have revealed that by the end of the 21st century, NDSEV may increase significantly in some locations of the U.S. (Trapp et al., 2007), suggesting an increase in both severe thunderstorm and tornadic occurrences in the U.S.

Water vapor in the atmosphere is also an important factor in the development of thunderstorms and supercells. GCM studies predicted that increased warming associated with doubled CO_2 could lead to greater evaporation from the oceans, which would increase atmospheric water vapor concentration and enhance surface warming and, therefore, thunderstorm development (Rind, 1998; Held & Soden, 2000; Held & Soden, 2006).

To another extent, lightning frequency has been used as an indicator to predict thunderstorm occurrence trends for the future (Fosberg et al., 1990; Michalon et al., 1999; Vellinga et al., 2001; Price, 2009). It has been suggested that lightning frequency may increase across the Northern hemisphere with warmer mean temperature anomalies due to a corresponding increase in convective activity (Fosberg et al., 1990). In a doubled CO_2 climate, with a corresponding 4.2 Celsius warming, another study found that global cloud-to-ground lightning could increase by as much as 72% over continental regions (Vellinga et al., 2001).

-El Nino Southern Oscillation

ENSO, or the El Nino Southern Oscillation, is the most important climatic modulator on global inter-annual variability (Carnell & Senior, 1998; Timmermann et al., 1999). ENSO variability is monitored throughout the equatorial and tropical Pacific Ocean, typically between 80 W (West) and 120 E (East) longitudes, where variations in SSTs between the Eastern and Western equatorial Pacific determine the overall phase of the oscillation. When the central and Eastern sections of the equatorial and tropical Pacific are at least a few degrees warmer relative to the Western Pacific, El Nino conditions dominate, whereas the reverse occurs for La Nina. Both El Nino and La Nina events are commonly categorized as weak, moderate and strong, and these sub-divisions are determined based on the persistence of SST departures in the Nino3.4 (5 N to 5 S and 170 to 120 W) to Nino3 region (5 N to 5 S and 90-150 W) over a given period of time. If cooler than normal SSTs are present over the central and Eastern equatorial Pacific, then a La Nina event is established. An El Nino or La Nina event is declared when SSTs in the Nino3.4 region exhibit departures (relative to 1961-1990 climatology) of at least above or

below 0.5 degrees Celsius and endure for a minimum of five consecutive months. SST anomalies are measured as three-month running means.

Changes in the variability of ENSO dictate convective patterns across the equatorial Pacific. During an El Nino event, convection is enhanced across the central and Eastern equatorial Pacific, resulting in more convective rains and pronounced thunderstorm activity there. The warmer SST anomalies also result in a deepening of the thermocline, as above average SSTs extend to greater depths. The presence of El Nino also weakens the Walker circulation by weakening the surface trade winds, as well as the upper-level westerlies. The Walker circulation is characterized by vertical and horizontal winds (upper and lower level), and the circulation changes in response to changes in ENSO variability. During an El Nino (or ENSO warm phase), the weakening of the trade winds prevents upwelling of cool, nutrient-rich waters from occurring in the Eastern equatorial Pacific. The Western Pacific, under these conditions, is marked by cooler than normal SST anomalies, whose occurrence is aided by the anomalous surface easterlies that are common during a given El Nino event. At the same time, convection is suppressed over this region. During a La Nina phase, these conditions are reversed, with convection suppressed over the Eastern and central equatorial Pacific, while enhanced over Western sections. Both El Nino and La Nina occur, on average, on intervals of three to seven years.

El Nino and La Nina events control temperature and precipitation variability at a global scale. In years where an El Nino event is occurring, drought, or reduced precipitation occur over regions located in the Western Pacific, where Australia, especially Eastern sections, often experience severe to extreme drought. At the same time

in South and SE Asia, the weakening of the Walker circulation associated with El Nino subsequently weakens the Summer monsoon circulation by causing a reversal in the lower-tropospheric wind patterns, where easterly winds replace the climatological Southwesterlies that commonly circulate warm, moist air from the Indian Ocean. Elsewhere, the likelihood for increased flooding occurs in North America, and the North American Winter is usually marked by above-normal temperatures and reduced snowfall. Atlantic tropical cyclone activity is also often significantly reduced during El Nino years, owing to an enhancement of vertical wind shear over much of the tropical Atlantic. Tornado and severe thunderstorm activity North America have also been correlated with El Nino and La Nina events (Marzban & Schaefer, 2001).

In recent decades, ENSO variability has shown an increase in the number of El Nino events, including an increase in the number of stronger El Nino events (Marzan & Schaeffer, 2001, Kug et al., 2008). This has raised the fundamental question as to whether anthropogenic warming could affect El Nino dynamics (Kug et al., 2008). Potential future ENSO statistics (amplitude and period), however, have been debated due to the inability of the models to fully simulate ENSO (Timmermann et al., 1999), and some authors have suggested that it is crucial to explore the parameter space of the coupled climate models used to make predictions (e.g. Collins, 2000).

Climate modeling studies have found that as global air temperatures increase, the mean state of the Pacific shifts toward a more prevalent El Nino state, with greater relative surface warming in the equatorial Eastern Pacific (Kug et al., 2008). In another study, Collins et al. (2000) used an ocean-atmosphere coupled model (HadCM2) and found that a CO_2 quadrupling resulted in dramatic changes to ENSO statistics. However,

a later study conducted with the HadCM3 model revealed opposite results with a quadrupling of CO_2, where no changes in ENSO statistics were observed (Collins, 2000b). Other studies also showed that, under global warming, the mean climate of the Pacific may undergo significant changes, including weakened tropical easterly winds, faster warming taking place near the equator, and temperature gradients becoming steeper between surface and sub-surface waters (Collins et al., 2010).

Methodology

In order to conduct a meta-analysis, this study required a systematic approach that collects, compiles and organizes data through the searching, scanning and analysis of peer reviewed literature pertaining to potential future changes in weather extremes.

-Search and scanning phase

In the scanning process, I used a set of criteria to include and exclude articles from the study. I have considered only peer reviewed articles, collected from a large variety of journals in the environmental sciences. These journals include the Journal of Climate, Nature Climate Change, Geophysical Research Letters, Global and Planetary Change, Atmospheric Research, Nature Geoscience, Natural Hazards, International Journal of Climatology, Climate Dynamics, Science, Nature, Tellus, and the Bulletin of the American Meteorological Society. I have used a combination of specific keyword searches using the Web of Science search engine in order to retrieve the selected various articles of interest. Keywords include "climate change", "greenhouse warming", or "global warming", or "doubled CO_2". The specific weather events under investigation would then be attached to these keywords in order to refine the search. Because this study is focused on examining weather extremes in a global context, I have only included specific regions, as several extreme weather events under study are most dominant on certain regions. I have also focused on relatively recent research; consequently, articles published prior to 1990 were excluded. Studies during the 1990's had begun to increasingly focus on the relationship between global warming and extreme weather events; however, much of the research dedicated towards tropical cyclones began to particularly surface beyond 2004, following the dramatic hurricane seasons of 2004 and

2005. 1995 also exhibited an active Atlantic hurricane season, leading to more research efforts following that year, not only with respect to tropical storms, but for other forms of weather extremes, as well.

In the next phase of the scanning process, I have first identified and collected academic climate research papers that typically utilize climate modeling experiments to project various levels of global warming based on prescribed greenhouse gas concentration increases. Ideally, the intent of the research articles gathered for this study was to simulate and quantify projected changes in various weather extremes that correspond to proposed scenarios of greenhouse gas increases for the future. CO_2 is one of the most important greenhouse gases, due to its ability to strongly absorb near-infrared and infrared radiation, and its long residence time in the atmosphere. CO_2 is, therefore, frequently used in climate impacts studies to forecast potential future climate trends, including in terms of weather extremes. Specific CO_2 scenarios used in the climate modeling research include a doubling, tripling, quadrupling, or even a six-fold increase in atmospheric CO_2 towards various points of the 21st century, relative to pre-industrial values, 1961-1990 climatology, or specified present-day concentrations.

In general, I have retrieved articles which focus on weather extreme occurrences consistent with the definition of "extreme weather", that is, weather phenomena that are at the extremes of the historical distribution, such as severe or unseasonable weather. Certain weather extremes, however, can be grouped with those considered in this study. For example, changes in the frequency or intensity of mid-latitude cyclones can also be used as an indicator for drought, or an increase/decrease in the number of major snowfall events. Strong winds (sustained and gusts) have also been classified as an extreme

weather phenomenon. Strong winds are frequently attributed to a strong air pressure gradient and are, apart from tropical cyclones and tornadoes, usually associated with intense mid-latitude cyclonic storms. As such, changes in the number of intense mid-latitude cyclones can reflect changes in extreme wind events.

In situations where specific articles are of particular importance, I have also retrieved research that had been cited in these papers, especially for weather events where keyword searches did not readily display a sufficient number of focused articles, or when search results became less varied. Similarly, I have used cited reference searches in Web of Science to identify and retrieve more recent articles which have cited key studies. Conversely, I have excluded articles that only draw on results or findings from other literature, but these articles may be useful to retrieve the original research articles in order to gather additional data. In total, 124 articles were used for all extreme weather events considered in this study.

-Selected weather extremes

The extreme weather events that I have considered in this study are the following:

-Tropical cyclones
-Severe thunderstorms
-Tornadoes
-Heavy precipitation (rainfall) events
-Heat waves
-Drought
-Tropical monsoons
-Mid-latitude cyclones (seasonal)
-ENSO

For a number of these events, I used a variety of proxies to assist in the assessment of how these extreme events may change in response to future climate warming. Parameters, such as wind shear, precipitable water, severe thunderstorm

development days, or soil moisture, are also helpful as proxies for multiple extreme weather events mentioned above. I have categorized these parameters based on the weather event(s) that they are commonly associated with, as well as those events that depend on their presence in order to occur. For example, wind shear, soil moisture and precipitable water are important determinants and indicators in the development of severe thunderstorms, heavy rainfall events, tornadoes, and tropical cyclones. Heat waves and drought can be related to soil moisture reductions. Many climate impacts literature use this approach to help explain how, for instance, severe thunderstorms may change for the future based on how the variables that are conducive to their development respond to greenhouse warming.

I have also included the El Nino Southern Oscillation in this study, as it is one of the most influential climate modulators at a global scale. Many studies have classified El Nino and La Nina phases as being extreme events of ENSO, which, in turn, can contribute to the development of weather extremes at a global scale at regular intervals of 3 to 7 years. Therefore, it is of interest to assess how ENSO may change in response to climate warming in this study. It is also worth noting that I have included mid-latitude cyclonic storms as a potential weather extreme. Mid-latitude cyclones may not necessarily be considered an extreme event in themselves, but they can be categorized as such if they are expected to become more numerous or increasingly intense. Furthermore, mid-latitude cyclones are responsible for many of the weather extremes that occur at mid-latitudes, including severe thunderstorms, strong winds, tornadoes or heat waves, and, during the winter, they are attributed to major snowfall events, especially in the Northern hemisphere.

-Data collection and interpretation

I have gathered principal findings from research papers, either from the abstract, results, or concluding sections. I have examined the methods to identify the greenhouse gas concentration scenarios used, as well as the corresponding global temperature increase that was projected. I have also considered other climate studies that use observational data analysis for context but have not include these as part of the data collection process. When retrieving results, I have focused on identifying the specified change in intensity and/or frequency in selected weather events for different regions. Many articles typically use coupled GCM analyses, driven by either transient or equilibrium greenhouse gas increases. Greenhouse gas scenarios include the IPCC Second Report on Emissions Scenarios (A1B, A1T, A1FI, A2, B1, B2), as well as the IS92 scenario from the IPCC Second Assessment Report. In some cases, experimentation details do not include how global mean temperatures would change in response to specified greenhouse gas increases. Here, it is possible that the authors of those papers assumed that the resultant temperature increases are easily accessible; this may be particularly true for studies that use the IPCC scenarios in their experiments, where resulting temperature increases can be found in the original IPCC reports. When this information was not readily available, I have attempted to contact the author(s) of those articles directly to request the necessary data.

The majority of the literature that I surveyed included information about global mean temperature change and was centered within a global context. However, there are some studies that report temperature changes at a regional, rather than a global scale. Where regional mean temperatures are provided, it was necessary to apply upscaling

techniques in order to estimate the global mean temperature associated with a given regional temperature change. To achieve this upscaling process, I have made use of information on the spatial pattern of temperature changes per unit global temperature change, available as part of the report: "Climate Stabilization Targets: Emissions, Concentration and Impacts over Decades to Millennia (2011)" from the National Research Council (2011). As shown in the figure below, this information is available for both annual mean regional temperatures, as well as for seasonal regional temperature change per degree of global warming. Raw data corresponding to this figure is provided by Tebaldi (2011) in tabular format as an Excel spreadsheet.

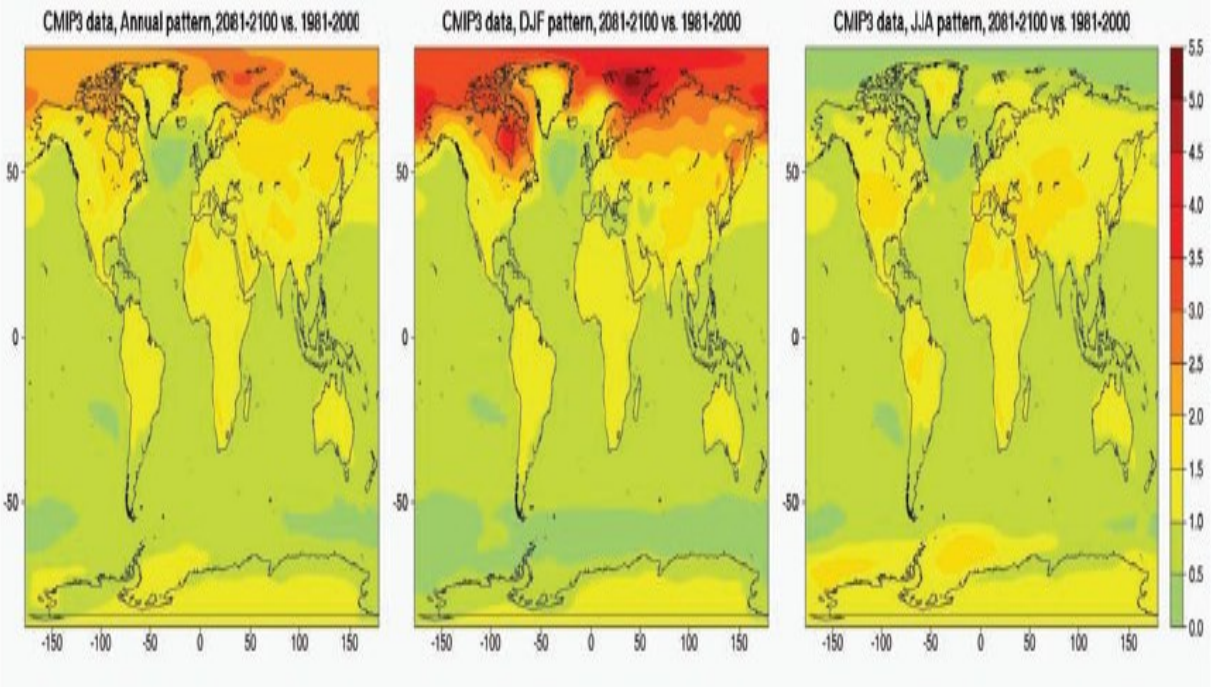

Figure 1. Geographical patterns of warming per degree Celsius of global warming over the globe. The figure on the left represents patterns of average annual temperature. The figure in the middle illustrates average temperature patterns during the Northern Hemisphere winter (December, January and February), whereas the figure on the right shows average temperature patterns for the Northern Hemisphere summer (June, July and August). Patterns are obtained by scaling end-21st century changes relative to end 20th century changes by global average annual temperature over the same period, using surface temperature from the 18 CMIP models, whose output is available for the SRES scenarios of A2, A1B, and B1. Source: Tebaldi, 2011 (Figure 4.1 of Climate Stabilization Targets: Emissions, Concentration and Impacts over Decades to Millennia (2011)).

Warm SSTs are an important parameter for the development of a tropical cyclone. As such, prescribed SSTs, or resultant SSTs from global warming scenarios, are commonly used in climate modeling studies that simulate and project changes in tropical cyclone behavior. Because this study focused on global mean temperature changes, I have used upscaling methods to convert projected SST warming, either globally or regionally, into a global mean air temperature change. I have employed upscaling methods by using combined air temperature anomaly data (water + land), and global air temperature anomaly data over water alone. The data that I used was supplied by the Climate Research Unit and covers a time series from 1850 to the present, and it shows a total estimated warming of 0.6 Celsius between the 1850-1879 and 1981-2010 climatologies. It also assumes that air temperature anomalies directly over water are identical to SST anomalies. Thus, it was feasible to convert a given SST change, relative to a prescribed baseline period, into an approximate global warming by using these available historical SST anomalies. In cases where only regional or local SSTs were given, I used data from Tebaldi (2011) and interpolated it in GIS software to calculate relevant average temperature changes, so that a conversion factor may be found for a given area of interest. As such, I upscaled a regional or local SST change into a global mean temperature change in this way. Again, I have assumed that SST warming is similar to the warming of the air directly above the sea-surface. Data is provided in this manner because marine air temperatures lack consistency in coverage and are, consequently, not spatially homogeneous, as compared to SSTs (Climate Research Unit, 2013).

For this study, the data that I collected for all the selected variables is expressed as a percentage change, which is relative to given prescribed baseline periods adhering to

their respective climate modeling studies. In many cases, data is originally given as a percent change in climate studies, but absolute values are not provided. Where data is expressed as absolute changes, however, I have derived a percent change. As a result, all changes, both global mean temperature, and corresponding (percent) changes for a given extreme weather event, is provided relative to various reference periods for the different studies considered. Once percentage changes are gathered, I have converted them into a percent change per degree Celsius of global warming. In some cases, multiple studies use different climate change scenarios for the same model(s). Under these circumstances, associated results are not considered to be independent, and the effect of pseudo-replication exists. To account for replicated data, I averaged data given for scenarios corresponding to the same model into a single data point. I have then placed a discussion of the results given by the output of the statistical tests, followed by a synthesis of meteorological factors that may be attributed to the changes.

All of the studies that I considered in this paper, as well as their documented changes per degree Celsius of global warming, are presented in Table 9 (Appendix), and all variables used, along with a brief description and number of data points for each, are outlined in the following table (Table 1). The number of data points for each selected parameter is defined as a collection of results gathered from the body of climate impacts literature. Data points do not represent the total number of studies for a given parameter but instead reflect the total number of results derived from the studies for that particular parameter. This is especially true where studies use multiple models to assess changes in a specified variable with respect to global warming; thus, results from individual models from the same study represent a separate data point. Each individual data point represents

a change (percent or absolute) per degree Celsius of global warming. In cases of replicated results, these data points were averaged into a single point.

-Statistical analysis

Once the necessary data is compiled for each extreme weather event, I have employed the one-sample t-test, as well as its non-parametric counterpart, the Wilcoxon Rank Sum test, using R software. "R" is a programming software used largely for statistical computing and graphics. These tests were particularly useful to statistically evaluate the degree of significance associated with a derived change in intensity and/or frequency of selected extreme weather events per degree Celsius of global warming. The one-sample t-test is a widely used statistical test to compare the means of groups and primarily assumes that data is normally distributed, and that random sampling has no selection bias. The Wilcoxon Rank Sum test, on the other hand, assumes that the data is not normally distributed and is only based on the ranking of observations of a given sample. As such, the test statistic given by the Wilcoxon Rank Sum test is based on the sum of ranks for observations from a sample. The null hypothesis would be that there is no significant change in a given extreme weather event per degree Celsius of global warming. Small p-value results derived from these tests would, thus, indicate statistically significant changes in the patterns of a given extreme weather event per degree Celsius of global warming. Before the appropriate statistical test could be determined, however, I have used the Normal Quantile-Quantile diagnostic plot to test and verify if the various collected datasets are of normally distributed nature. Here, the normality of a given dataset can be determined based on linearity exhibited by the Normal Quantile-Qunatile plots. Thus, when these plots show a data distribution that is linear in nature, the data

would be considered normally distributed. Conversely, if non-linearity is produced, then the data is not normally distributed. As such, based on the results given by these plots, it is possible to determine which statistical test would be most appropriate. Because the one-sample t-test assumes normality, it is used when plots generally show linear patterns with the data.

Table 1. Selected variables considered in research. Variables names are listed in the left-hand column, followed by a description (middle column), and the number of data points collected (right-hand column) for each.

Variable name	Description	# of data points
Global tropical cyclone frequency	Tropical cyclones of all types and strengths across all basins, principally the tropical Atlantic, the Indian Ocean, and the NW Pacific and East/NE Pacific. Changes are given as a percentage per degree Celsius of global warming.	26
Global intense tropical cyclone frequency	Tropical cyclones that have achieved strong tropical storm status or greater; therefore, storms that generate sustained surface/near-surface wind speeds of about 90 km/h (kilometers per hour) (25 m/s) or more. Changes are given as a percentage per degree Celsius of global warming.	16
Most intense global tropical cyclone frequency	Global tropical cyclones with maximum surface wind speeds greater than 50 m/s (category 4 and 5 storms)	15

Global tropical cyclone intensity	Considers the intensity of global tropical cyclones by taking into account mean maximum sustained surface/near-surface wind speeds (in units of m/s) at a global scale. Changes are given as a percentage per degree Celsius of global warming.	12
NW Pacific tropical cyclone frequency	Tropical cyclones of all types and strengths in the NW Pacific basin (0-45 N, 100 E-180). Changes are given as a percentage per degree Celsius of global warming.	19
Intense NW Pacific tropical cyclone frequency	Tropical cyclones that have achieved strong tropical storm status or greater (surface/near-surface winds speeds of about 90 km/h (25 m/s) or more) in the NW Pacific basin. Changes are given as a percentage per degree Celsius of global warming.	13
Most intense NW Pacific tropical cyclone frequency	Tropical cyclones with maximum surface wind speeds greater than 50 m/s (category 4 and 5 storms) in the NW Pacific basin	11
NW Pacific tropical cyclone intensity	Considers the intensity of a tropical cyclone in the NW Pacific basin by taking into account mean maximum sustained surface/near-surface wind speeds (in units of m/s). Changes are given as a percentage per degree Celsius of global warming.	19

North Atlantic tropical cyclone frequency	Tropical cyclones of all types and strengths in the North Atlantic basin (0-45 N, 90 W-0). Changes are given as a percentage per degree Celsius of global warming.	25
Most intense Atlantic tropical cyclone frequency	Tropical cyclones with maximum surface wind speeds greater than 50 m/s (category 4 and 5 storms) in the Atlantic basin.	9
Intense Atlantic tropical cyclone frequency	Tropical cyclones that have achieved strong tropical storm status or greater (surface/near-surface winds speeds of about 90 km/h (25 m/s) or more) in the North Atlantic basin. Changes are given as a percentage per degree Celsius of global warming.	6
North Atlantic tropical cyclone intensity	Considers the intensity of a tropical cyclone in the North Atlantic basin by taking into account mean maximum sustained surface/near-surface wind speeds (in units of m/s). Changes are given as a percentage per degree Celsius of global warming.	8
South Asian warm season zonal winds	South Asian warm season (June-September) monsoon zonal winds are defined as low-level, or boundary layer, monsoonal wind patterns (typically between the surface to the 850 hpa geopotential height). Absolute changes are given in this study and are expressed in units of m/s per degree Celsius of global warming.	11

South Asian monsoon warm season rainfall	South Asian monsoon warm season (June-September) rainfall. Units for Summer rainfall are typically expressed as mm/day (millimeters per day) and are given as percent changes in this study.	56
Global precipitation	Global precipitation of all types. Units are in mm/day and given as a percentage change per degree Celsius of global warming.	72
Global precipitable water	Referred to as the depth of water that could be precipitated out of a column of air as rain. This variable can be used to broadly examine changes in the frequency intensity of heavy precipitation events, and particularly deep convective systems. Changes are given as a percentage per degree Celsius of global warming.	22
Global convective rainfall	Global rainfall associated with deep convective systems and is used to broadly assess changes in thunderstorm frequency or intensity. Changes are given as a percentage per degree Celsius of global warming.	7
Northern hemisphere mid-latitude cyclone annual frequency	Annual Northern hemisphere mid-latitude (30-55 N) cyclonic storm frequency of all intensities. Changes are given as a percentage per degree Celsius of global warming.	7

Northern hemisphere cool season mid-latitude cyclone frequency	Northern hemisphere cool season (November-March) mid-latitude cyclone frequency of all intensities. Absolute changes are given per cool season per degree Celsius of global warming.	24
Intense Northern hemisphere cool season mid-latitude cyclone frequency	Northern hemisphere intense cool season cyclone frequency. Intense cyclones are defined as having central surface pressures of 970-980 hpa or less. Changes are given per degree Celsius of global warming.	23
Southern hemisphere annual mid-latitude cyclone frequency	Annual Northern hemisphere mid-latitude (30-55 S) cyclonic storm frequency of all intensities. Changes are given as a percentage per degree Celsius of global warming.	6
Southern hemisphere cool season mid-latitude cyclone frequency	Southern hemisphere cool season (May-September) mid-latitude cyclone frequency of all intensities. Absolute changes are given per cool season per degree Celsius of global warming.	18
Intense Southern hemisphere cool season mid-latitude cyclone frequency	Southern hemisphere intense cool season cyclone frequency. Intense cyclones are defined as having central surface pressures of 970-980 hpa or less. Changes are given per degree Celsius of global warming.	18

European soil moisture	Used to broadly assess changes in heat wave and drought frequency and intensity in the European region. Soil moisture is commonly measured as the uppermost 10 centimeters of soil. Changes are given as a percentage change per degree Celsius of global warming.	8
North American soil moisture	Used to broadly assess changes in heat wave and drought frequency and intensity in the Northern American region. Soil moisture is commonly measured as the uppermost 10 centimeters of soil. Changes are given as a percentage per degree Celsius of global warming.	7
European 30 Celsius days	Number of days that reach 30 Celsius or more in the European region. This parameter is used as a proxy to gauge European heat wave frequency. Changes are given as a percentage per degree Celsius of global warming.	5
U.S. vertical wind shear	Vertical wind shear is used to examine changes in the intensity and frequency of severe thunderstorms and tornadoes. Vertical wind shear is defined as winds changing in both speed and a direction with increasing altitude between the 850 and 200 hpa geopotential height and is given as a percentage change per degree Celsius of global warming.	5

U.S. severe thunderstorm development days	Defined as the number of days where severe thunderstorm development is favorable and takes into account both changes in vertical wind shear and convective available potential energy (CAPE). Changes are given as a percent per degree Celsius of global warming.	8
El Nino Southern Oscillation amplitude	Referred to as equatorial SST departures, commonly in the Nino3.4 (5 N-5 S and 170 W 120 W) to Nino3 region (5 N-5 S and 90-150 W). Changes are given as a percentage per degree Celsius of global warming are usually relative to 1961-1990 climatology.	31
El Nino Southern Oscillation period	Referred to as the period, or cycle, between warm (El Nino) and cool (La Nina) phases. The equatorial Pacific is considered in this study, with a focus on the Nino3.4 to Nino3 region. Changes are given as a percentage per degree Celsius of global warming and are usually relative to 1961-1990 climatology.	19

Results

-Global and regional tropical cyclones

This section draws on the findings provided for the frequency of global and regional tropical cyclones, the number of intense storms, the number of the most intense storms, as well as changes in storm intensity per degree Celsius of global warming, which is represented in figures 2, 3, 4 and 5. Table 2 summarizes the significance results for the selected variables used to assess global and regional tropical cyclone frequency and intensity, along with corresponding statistical tests (either the one-sample t-test or Wilcoxon Rank Sum test).

Global and regional tropical cyclone frequency is first examined. Figure 2a shows a trend towards decreasing global tropical cyclones, where the majority of data points (20 out of 26) favor a decline with global warming, with an average decrease of 7.2% per degree Celsius of global warming. The results given by the one-sample t-test show that the decrease in global tropical cyclone frequency is highly statistically significant at the 1% significance level (p=0.01), as shown in Table 2.

When analyzing regional variations in tropical cyclone frequency in the Atlantic and NW Pacific basins, the overall distribution of these frequencies follows a similar pattern to that exhibited at the global scale, mostly for the NW Pacific, as shown in figure 2b. Like global patterns, a trend towards a decrease in tropical cyclones is observed in the NW Pacific, with most data points (11 out of 19) indicating a decline, with an average decrease of -5.5% per degree Celsius of global warming. However, the results are not statistically significant (p=0.18), as noted in Table 2. In the Atlantic basin, a similar trend towards a decrease in tropical cyclones can be seen per degree Celsius of global warming

(figure 2c), where a large number of the total data points (16 out of 25) suggests a decrease, although the result, much like for the NW Pacific, is not significant (p=0.60).

In contrast to tropical cyclone frequency at global and regional scales, the findings show that there is an increase in the number of intense storms at regional scales. At the global scale, no apparent change (p=0.91) in the number of intense storms is obvious (figure 3a), where a near-even divide in the number of data points shows an increase and decrease. At regional scales, however, the results are shown to differ. In the NW Pacific, for example, as shown in figure 3b, the number of intense storms favors a significant increasing trend (p=0.03), with a mean increase of 12.3%. By comparison, for intense tropical cyclone frequency, with respect to the Atlantic basin (figure 3c), a decrease in the number of these storms is given, where most of the data points (7 out of 9) support a decline, with an average decrease of about 6.7%. This decrease is also shown to be significant within the 5% significance level (p=0.04). When specifically examining the most intense tropical cyclones, that is, category 4 and 5 cyclones, the patterns are shown to be generally similar to the number of intense storms. Globally, an average increase of 13% in the most intense storms is shown, though the results are not significant (p=0.15), as given in Table 2. Figure 4b, by contrast, illustrates a clearer trend towards an increase in the most intense storms for the NW Pacific basin, where all of the data points (11) indicate an increase, with an average increase of 18.7% per degree Celsius of global warming. This increase is shown to be highly statistically significant (p<0.01). In the Atlantic, a similar average increase (about 20%), as shown in figure 4c, is observed, but the result is not significant (p=0.22).

Next, an assessment of the results for tropical cyclone *intensity* trends is given for global and regional scales. In the literature, tropical cyclone intensity is most commonly evaluated based on the change in mean maximum surface wind speeds, which also broadly acts as an indicator for surface cyclonic central pressure changes. The results in this study suggest a general increase (average increase of 1.7%) in the intensity (mean maximum surface/near-surface wind speeds) at a global scale, as well as across the NW Pacific and Atlantic basins (Table 2). From figures 5a to 5c, the increases in the intensity of tropical cyclones at the global scale, as well as individually for the Atlantic and NW Pacific basins, are highlighted, where most data points show increases for every degree Celsius of global warming. At the global scale, the increase in intensity is shown to not be statistically significant (p=0.12), but for the NW Pacific and Atlantic basins, results are significant within the 1% and 5% significance level, respectively, per degree Celsius of global warming. The average intensity increase for NW Pacific and Atlantic tropical cyclones is 3.8% and 3.5%, respectively. These findings are also generally consistent with those given by Knutson et al. (2010), who document a 2-11% increase in global tropical cyclone intensity, and a 6-34% decrease in the frequency of global tropical cyclones.

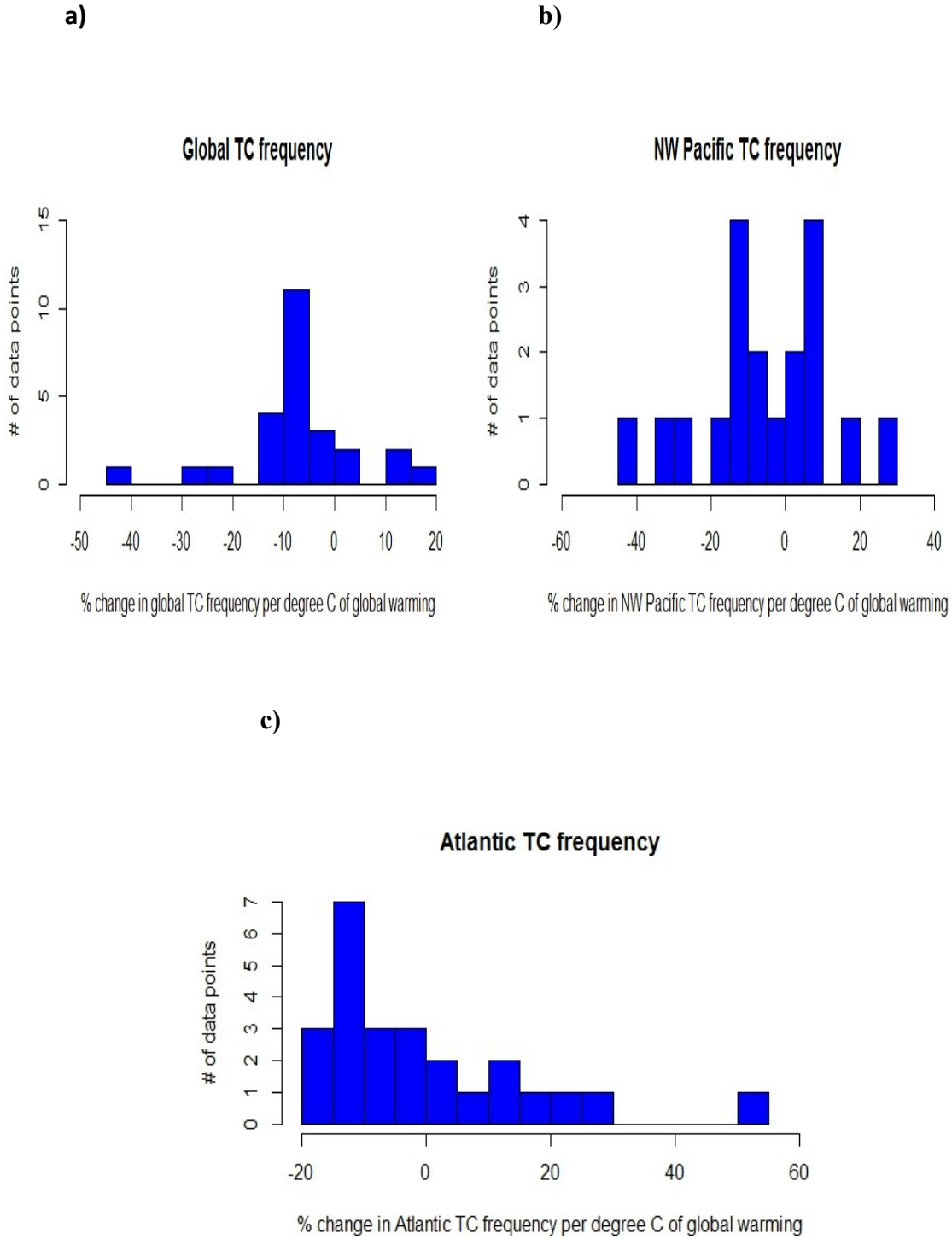

Figure 2. Global and regional tropical cyclone (TC) frequency changes. Histograms show percentage changes in tropical cyclone (TC) frequency per degree Celsius (C) of global warming for the (a), global scale, (b) NW Pacific and (c) Atlantic basin.

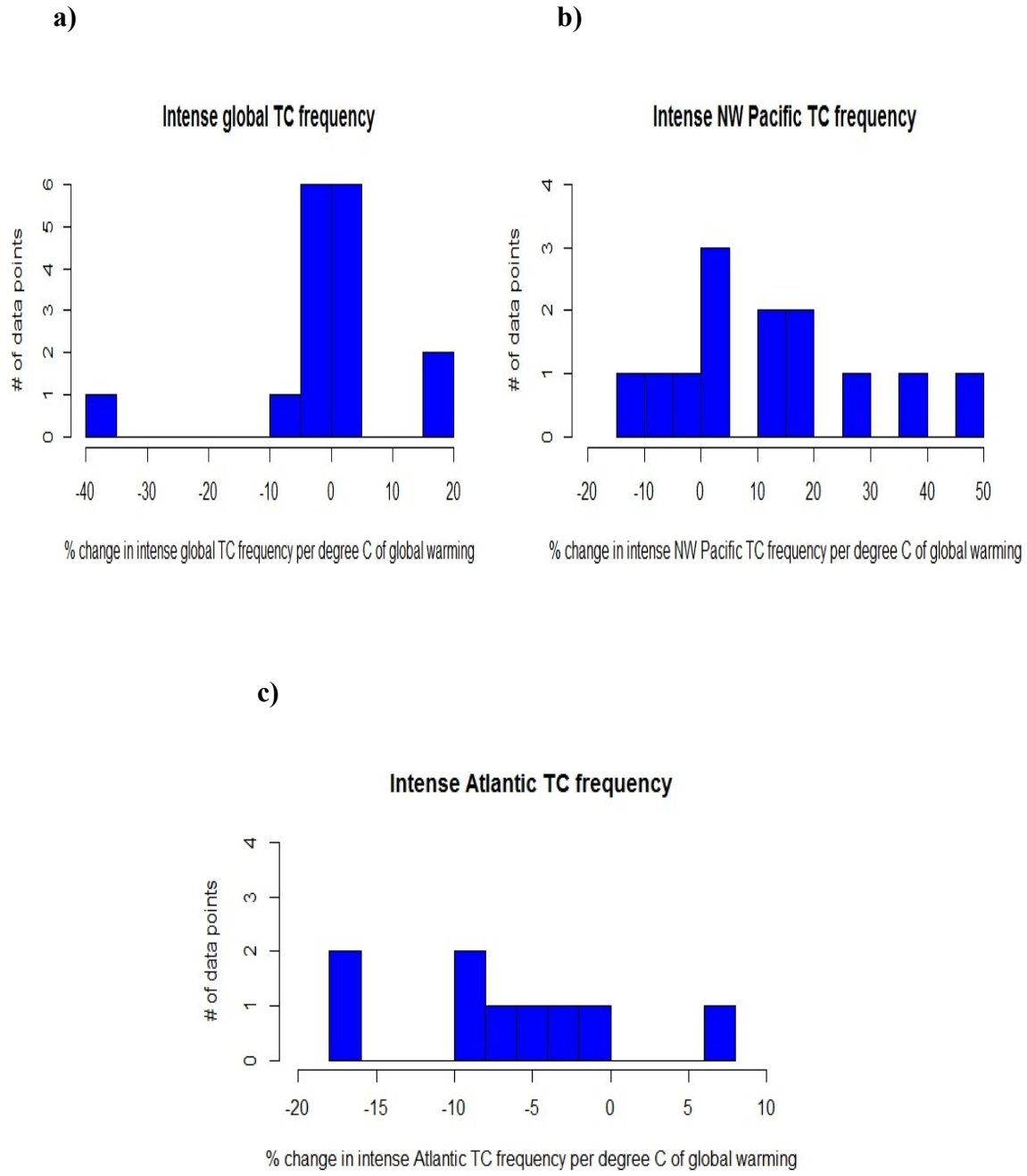

Figure 3. Global and regional intense tropical cyclone (TC) frequency changes. Histograms display percentage changes in intense tropical cyclone frequency per degree Celsius of global warming for the (a), global scale, (b) NW Pacific and (c) Atlantic basins.

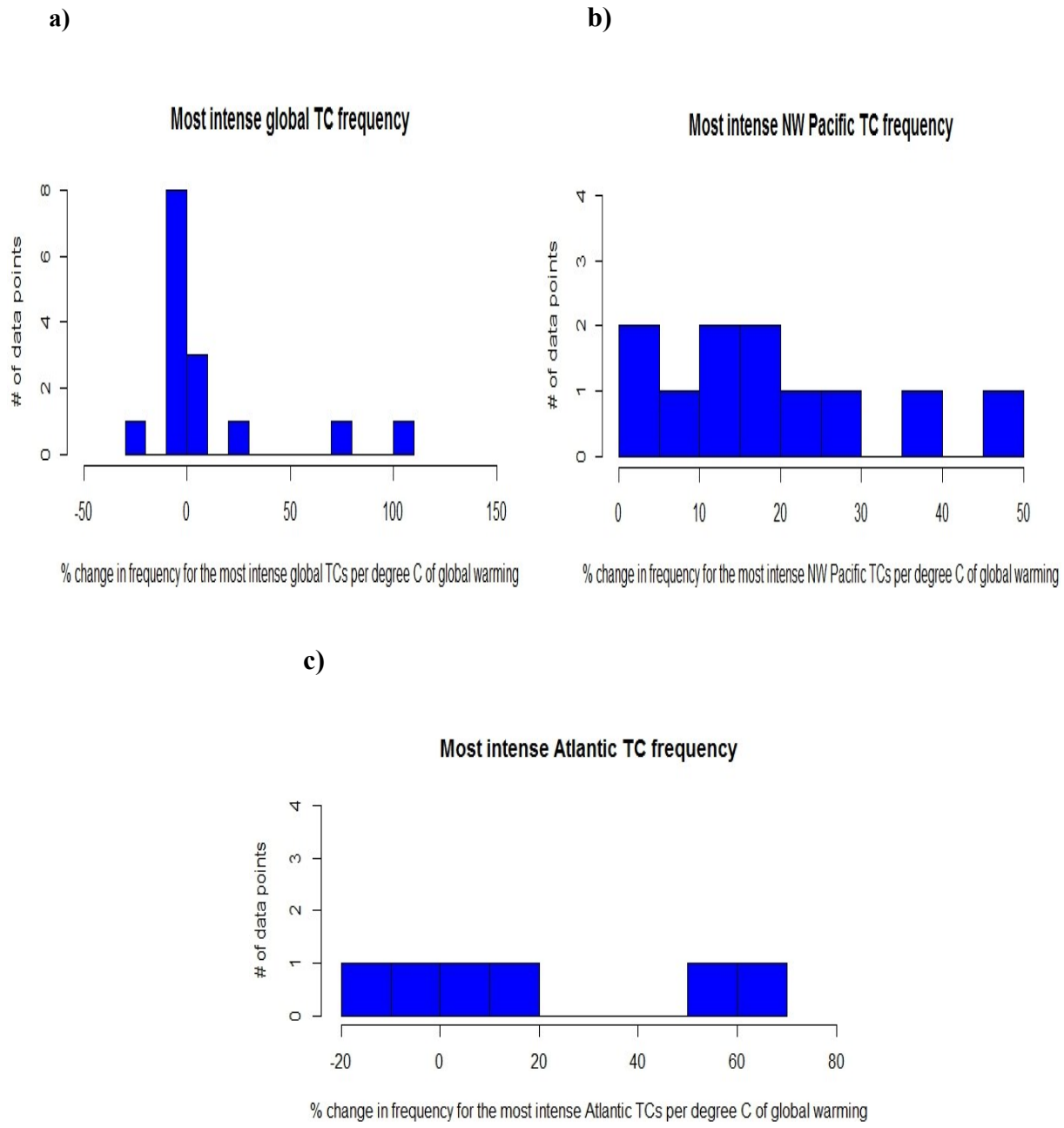

Figure 4. Most intense global and regional tropical cyclone (TC) frequency changes, based on maximum sustained surface winds greater than 50 m/s, or category 4 and 5 cyclones. Histograms display percentage changes for the frequency of the most intense tropical cyclones per degree Celsius of global warming for the (a), global scale, (b) NW Pacific and (c) Atlantic basins.

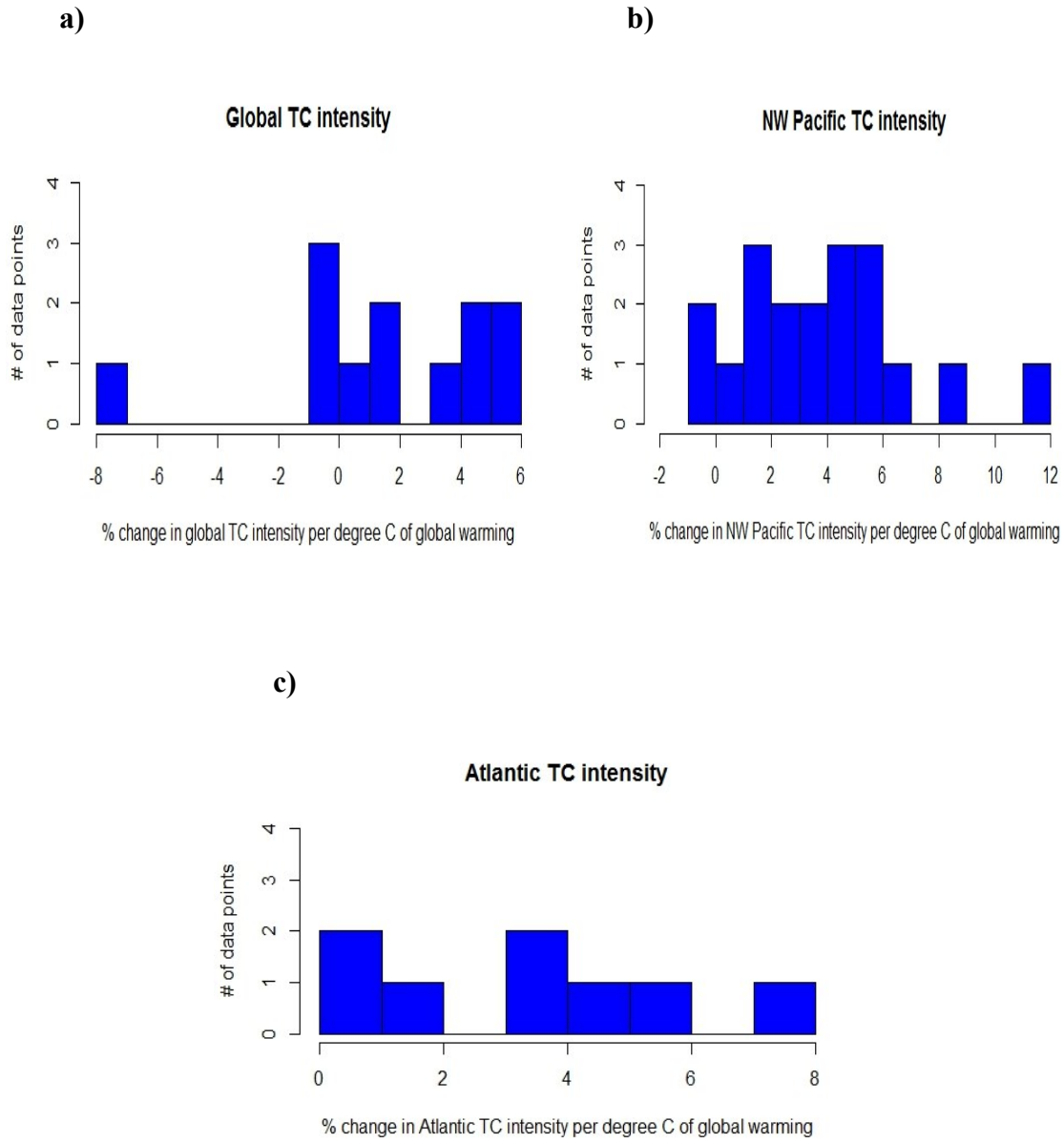

Figure 5. Global and regional tropical cyclone (TC) intensity changes. Histograms show percentage changes in tropical cyclone (TC) intensity per degree Celsius of global warming for the (a), global scale, (b) NW Pacific and (c) Atlantic basins.

Table 2. Results for global and regional tropical cyclone patterns. Results are given for global and regional (NW Pacific and Atlantic basins) tropical cyclone frequency, intense storm frequency, the most intense storms (category 4 and 5), and tropical cyclone intensity changes (based on mean maximum surface wind speeds) per degree Celsius of global warming. Means and standard deviations are given as percent changes. "**", and "***" indicate results that are statistically significant at or within the 5% and 1% significance levels, respectively.

Global tropical cyclones						
Variable name	Change	# of data points	Mean change	Standard deviation	Statistical test	p-value
Frequency	Decrease***	26	-7.22	12.06	t-test	0.01
Frequency (intense storms)	No change	16	0.31	11.14	t-test	0.91
Frequency (category 4 and 5)	No change	15	12.89	34.47	Wilcoxon	0.15
Intensity	No change	12	1.70	3.57	Wilcoxon	0.12
NW Pacific tropical cyclones						
Variable name	Change	# of data points	Mean change	Standard deviation	Statistical test	p-value
Frequency	No change	19	-5.45	17.05	t-test	0.18
Frequency (intense storms)	Increase**	13	12.30	17.92	t-test	0.03
Frequency (category 4 and 5)	Increase***	11	18.71	14.87	Wilcoxon	<0.01
Intensity	Increase***	19	3.83	2.89	t-test	<0.01
Atlantic tropical cyclones						
Variable name	Change	# of data points	Mean change	Standard deviation	Statistical test	p-value
Frequency	No change	25	-0.004	17.26	Wilcoxon	0.60
Frequency (intense storms)	Decrease**	9	-6.72	7.46	Wilcoxon	0.04
Frequency (category 4 and5)	No change	6	20.45	31.15	Wilcoxon	0.22
Intensity	Increase**	8	3.46	2.54	Wilcoxon	0.02

-South Asian monsoon

The South Asian monsoon's activity is studied based on the average low-level (boundary layer) zonal wind component, as well as rainfall changes, for the warm season. The findings suggested here indicate that the South Asian monsoonal boundary layer zonal wind weakens with global warming, as represented in figure 6a. Here, the average decrease in the monsoonal zonal wind is 0.23 m/s per degree Celsius of global warming, and the results are statistically significant within the 10 % significance level (p=0.08).

Changes in the South Asian monsoon Summer rainfall in a future warming climate are also considered to verify if they are consistent with alterations in the mean zonal wind. Figure 6b indicates that a trend towards increased warm season monsoonal rainfall occurs over South Asia. The average increase in South Asian Summer rainfall is about 3.6% per degree Celsius of global warming. The p-values given by the Wilcoxon Rank Sum test are also very significant (p<0.01). As a result, in spite of weakened zonal winds (figure 6a) in a warming climate, total warm season rainfall is shown to be enhanced significantly. Table 3 provides a summary of the results obtained for the South Asian monsoon circulation (zonal wind) changes, as well as alterations for warm season (June-September) rainfall per degree Celsius of global warming.

a) **b)**

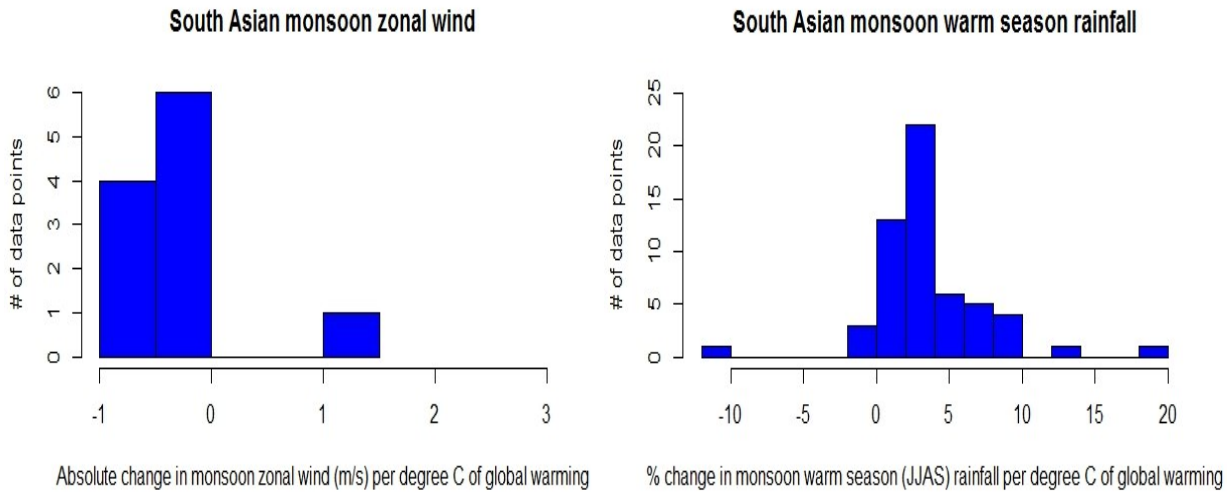

Figure 6. South Asian monsoon pattern changes. Histograms display the South Asian Summer (JJAS) - June, July, August, and September)) mean monsoon per degree Celsius of global warming in terms of (a) absolute change in zonal wind and (b) percentages changes in Summer rainfall.

Table 3. Results for South Asian monsoon patterns. Findings are provided for the South Asian monsoon boundary layer zonal wind (in m/s) and warm season (JJAS) rainfall changes per degree Celsius of global warming. Means and standard deviations are given as absolute changes (in m/s) for zonal winds and percent changes for rainfall. "*" and "***" indicates results that are statistically significant at or within the 10% and 1% significance level, respectively.

South Asian monsoon zonal wind and warm season precipitation and global warming						
Variable name	Change	# of data points	Mean change	Standard deviation	Statistical test	p-value
Zonal wind	Decrease*	11	-0.23	0.51	Wilcoxon	0.08
Warm season precipitation	Increase***	56	3.55	3.88	t-test	<0.01

-Global precipitation and heavy precipitation events

Heavy precipitation changes are examined in a warming climate in this study. Results for the selected variables are provided in Table 4. Changes in global precipitation are first studied as a predictor for potential changes in extreme precipitation events; if

global precipitation increases, for example, it may imply that intense precipitation could subsequently become enhanced with global warming, thereby contributing to the overall increase in global precipitation amounts. Here, the results suggest that global precipitation increases significantly per degree Celsius of global warming (figure 7a), which is statistically significant within the 1% significance level ($p<0.01$), as shown in Table 4. As suggested in figure 7a, the majority of data points favors a 0.5-2.5% increase in global precipitation for every degree Celsius of global warming, with an average increase of 1.5%.

Heavy precipitation events, however, are particularly associated with convective systems. This study also presents results related specifically as to how convective precipitation, at a global scale, may change with global warming. One method to examine such changes is to examine modifications in precipitable water, which is a useful proxy in evaluating changes in the amount of atmospheric convective available potential energy (CAPE). In figure 7b, the patterns show that average global precipitable water increases, with most studies showing a 6-8.5% enhancement (average increase of 7.5%) in the amount of global precipitable water for every degree Celsius of global warming, suggesting that more buoyant energy would be available for deep convective systems in the future climate, such as thunderstorms. Here, the results for global precipitable water are statistically significant within the 1% significance level ($p<0.01$). The trends illustrated for convective rainfall (figure 7c) also indicate an increase per degree Celsius of global warming, with 6 out of 7 data points exhibiting an increase (an average increase of 5.4%). The results given for global convective rainfall are also shown to be statistically

significant (p=0.05), which is consistent with the highly significant increase found for global precipitable water.

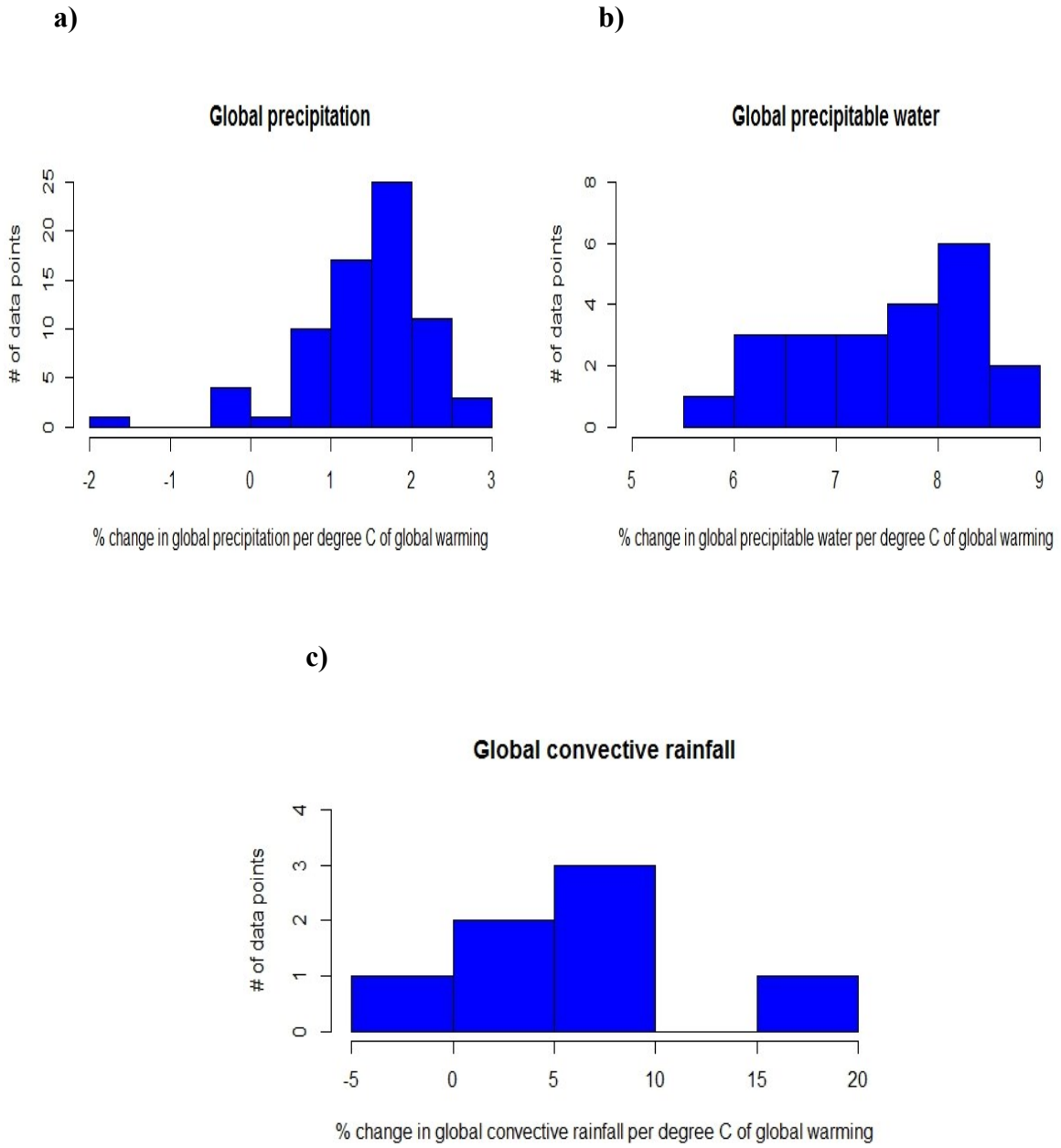

Figure 7. Global precipitation, global precipitable water, and global convective rainfall changes. Histograms show percentage changes in precipitation per degree Celsius of global warming for (a) the globe, (b) global precipitable water, and (c) global convective rainfall.

Table 4. Results for selected global precipitation variables. Findings include global precipitation, global precipitable water, and global convective precipitation per degree Celsius of global warming. Means and standard deviations are given as percent changes. "**" and "***" indicates results that are statistically significant at or within the 5% and 1% significance levels, respectively.

Precipitation and global warming						
Variable name	Change	# of data points	Mean change	Standard deviation	Statistical test	p-value
Global precipitation	Increase***	72	1.46	0.76	t-test	<0.01
Global precipitable water	Increase***	22	7.45	0.84	t-test	<0.01
Global convective rainfall	Increase**	7	5.83	6.52	Wilcoxon	0.05

-Mid-latitude cyclones

Results presented in this section are based on changes in hemispheric mid-latitude cyclone frequency, as well as intense cyclone frequency for annual and mainly cool season cyclonic events.

The findings show that global warming significantly affects the frequency of mid-latitude cyclones, as well as the number of intense storms (defined as central, or storm center, surface pressures of 970-980 hpa or less), particularly in the cool seasons of the respective hemispheres. Table 5 highlights the significance of these findings. For cool season cyclones, including for intense storms, absolute change per degree Celsius of global warming is applied for both hemispheres.

Figures 8a, 9a 10a show changes for Northern hemisphere mid-latitude cyclones, in terms of annual frequency (figure 8a), cool season frequency (figure 9a), and the number of intense cool season storm systems (figure 10a). At the annual temporal scale,

the average total number of storms is projected to decrease in a warmer climate in the Northern hemisphere. Figure 8a shows that most data points (6 out of 7) indicate a 0.5-2% decrease in the average number of total annual storms, with an average decline of 1%. Similarly, the total annual number of cool season storms exhibits a decrease in a warmer climate, as shown in figure 9a, which illustrates absolute changes in storm counts per Winter/cool season for every degree Celsius of global warming. All of the 24 data points show reductions in annual Northern hemisphere cool season storm counts, with most showing decreases of 25 to 100 storms per degree Celsius of global warming. In both the Northern hemisphere annual and cool season temporal scales, the results are statistically significant within the 5% (p=0.02) and 1% (p<0.01) significance level, respectively, as shown in Table 5. In contrast, the average total number of intense Northern hemisphere cool season cyclones show a distinct increase with global warming, as represented in figure 10a (units are similar to figure 9a). Here, the results are also statistically significant, though at the 5% significance level (p=0.05), with most data points (15 out of 23) indicating annual intense cool season storm increases, most of which are within the 0 to 20 range (figure 10a). The average increase is about seven cyclones for the Northern hemisphere cool season intense storms.

In the Southern hemisphere, similar patterns are found for mid-latitude cyclones. Figures 8b, 9b and 10b show changes in Southern hemisphere annual cyclone frequency, annual cool season frequency, and intense cool season cyclone frequency, respectively.

For Southern hemisphere annual cyclone frequency (figure 8b), much like the Northern hemisphere (figure 8a), a trend towards a decrease is observed, though the results are not statistically significant (p=0.11), as compared to the degree of significance

for Northern hemisphere mid-latitude cyclone frequency change (p=0.02). With respect to the average total number of cool season Southern hemisphere mid-latitude cyclonic systems (figure 9b), storms are also shown to decrease in number, with most data points, similarly to annual Northern hemisphere cool season cyclone frequency, favoring decreases between 0-100 storms per year with rising global temperatures. The results given are statistically significant within the 5% significance level (p=0.03). Conversely, in the case of Southern hemisphere intense cool season storms, the total number shows a marked increase with global warming, as represented in figure 10b. Here, the results are highly significant (p<0.01), with most (about 55%) of the data points indicating annual intense cool season storm increases of as much as 20 to 40 storms, with an average increase of approximately 27 cyclones.

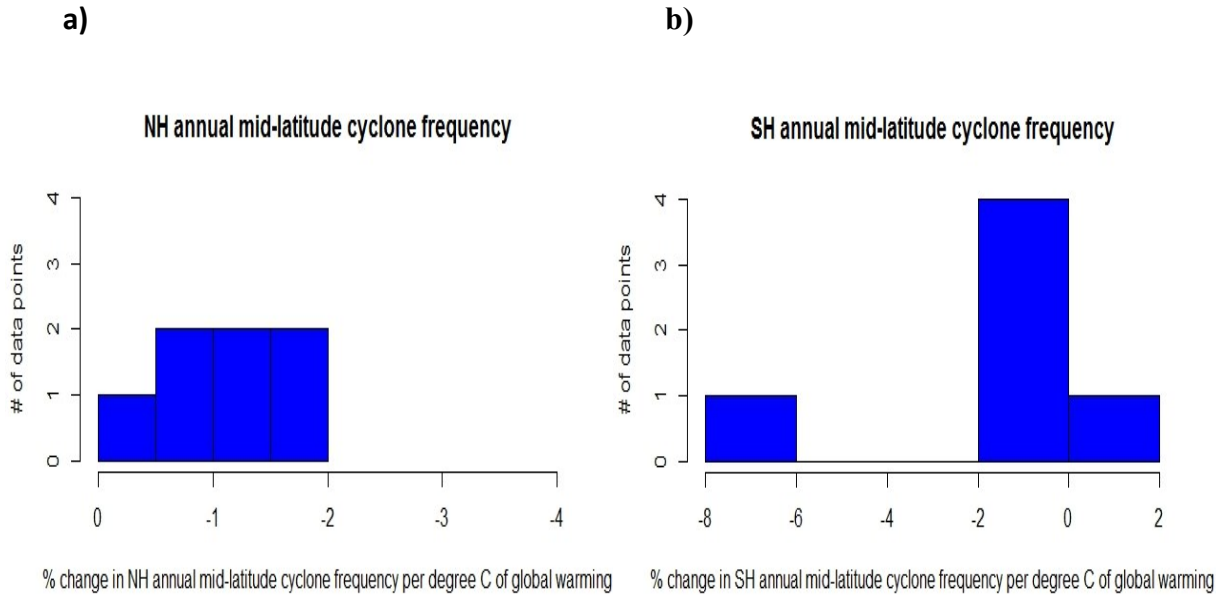

Figure 8. Hemispheric annual mid-latitude cyclone frequency changes. Histograms display percentage changes of annual mid-latitude cyclone frequency per degree Celsius of global warming for the (a) NH (Northern hemisphere) and (b) SH (Southern hemisphere).

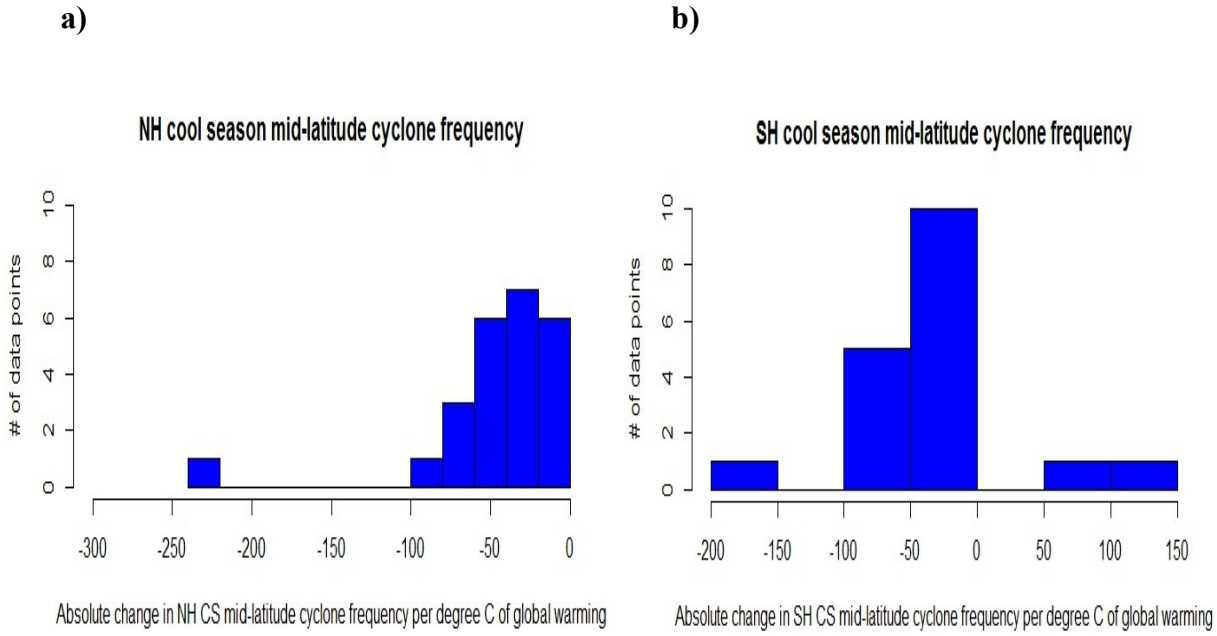

Figure 9. Hemispheric CS (cool season) mid-latitude cyclone frequency changes. Histograms show absolute changes (in number of storms per cool season) in cool season mid-latitude cyclone frequency per degree Celsius of global warming for the (a) NH (Northern hemisphere) and (b) SH (Southern hemisphere). Changes are representative of annual cool seasons.

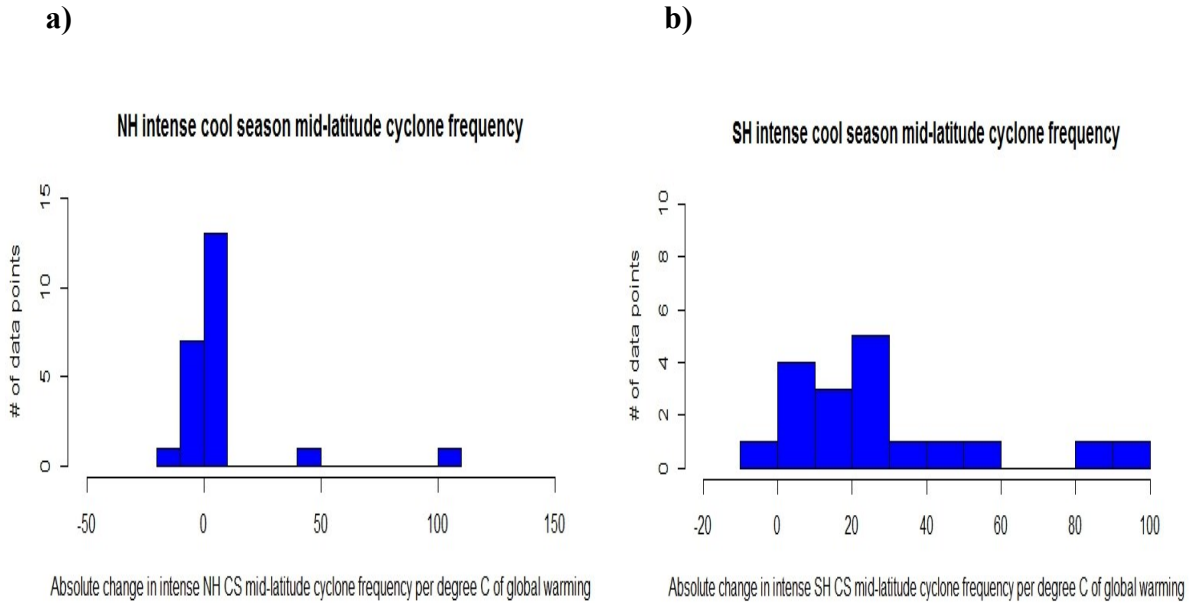

Figure 10. Hemispheric intense CS (cool season) mid-latitude cyclone frequency changes. Histograms highlight absolute changes (in number of storms per cool season) in intense cool mid-latitude cyclone frequency per degree Celsius of global warming for the (a) NH (Northern hemisphere) and (b) SH (Southern hemisphere). Changes are representative of annual cool seasons.

Table 5. Results for hemispheric mid-latitude cyclone patterns. Findings include mid-latitude cyclone frequency (annual and cool season) changes, as well as with respect to the number of cool season intense storms. Means and standard deviations are given as percent changes for annual frequencies, and absolute changes are provided for cool season cyclone frequency and intense cool season cyclone frequency (in number of storms per cool season). "**" and "***" indicate results that are statistically significant at or within the 5%, and 1% significance levels, respectively.

NH mid-latitude cyclones						
Variable name	Change	# of data points	Mean change	Standard deviation	Statistical test	p-value
Annual frequency	Decrease**	7	-1.03	0.60	Wilcoxon	0.04
Cool season cyclone frequency	Decrease***	24	-46.65	48.37	Wilcoxon	<0.01
Cool season intense cyclone frequency	Increase**	23	6.90	22.86	Wilcoxon	0.05
SH mid-latitude cyclones						
Variable name	Change	# of data points	Mean change	Standard deviation	Statistical test	p-value
Annual frequency	No change	6	-1.96	3.02	Wilcoxon	0.11
Cool season cyclone frequency	Decrease**	18	-35.14	64.73	t-test	0.03
Cool season intense cyclone frequency	Increase***	18	28.94	27.35	Wilcoxon	<0.01

-Drought and heat waves

Soil moisture data is used to assess changes in drought/heat wave frequency and intensity in response to global warming into the 21st century. In this study, the North American and European continents were selected for global representation. For Europe, in addition to soil moisture, heat wave frequency is evaluated based on changes in the number of days attaining 30 Celsius or more in the European region (figure 11c). For

European soil moisture (figure 11a), the results derived from the Wilcoxon test indicate a general decrease in a warmer climate, and these findings are shown to be statistically significant (p=0.01). Similarly, for North American soil moisture (figure 11b), a general reduction is also shown, with all data points exhibiting a 2 to 14% decrease per degree Celsius of global warming. Here, results are significant within the 5% level (p=0.02). When examining the percentage changes corresponding to the number of days reaching 30 Celsius or more in Europe, as shown in figure 11c, all of the five data points show an increase, with statistically significant results given from the Wilcoxon test within the 10% significance level (p=0.06). Table 6 shows the obtained results for both changes in soil moisture across Europe and North America, as well as for the number of European 30 C day changes with global warming.

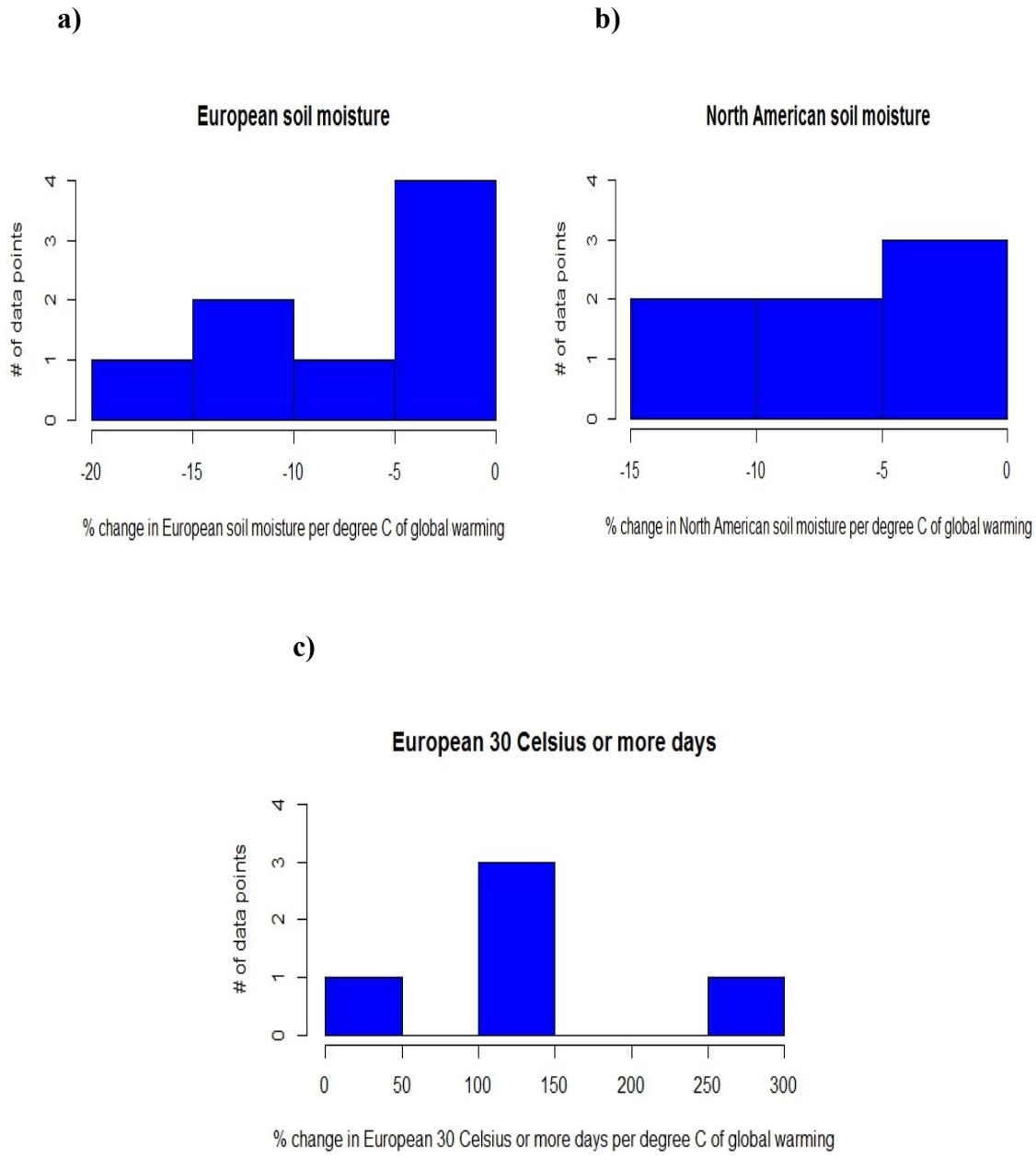

Figure 11. Regional soil moisture changes, and changes in the number of European 30 C or more days. Histograms display percentage changes in soil moisture per degree Celsius of global warming for (a) Europe and (b) North America. (c) Percentage changes in days reaching 30 C or more per degree Celsius of global warming.

Table 6. Results for European and North American soil moisture changes, and European 30 Celsius or more days. Findings are given as percent changes per degree Celsius of global warming. Means and standard deviations are also given as percent changes. "*", "**" and "***" indicate results that are statistically significant at or within the 10%, 5%, and 1% significance levels, respectively.

European soil moisture						
Variable name	Change	# of data points	Mean change	Standard deviation	Statistical test	p-value
Soil moisture	Decrease***	8	-7.40	6.06	Wilcoxon	0.01
North American soil moisture						
Variable name	Change	# of data points	Mean change	Standard deviation	Statistical test	p-value
Soil moisture	Decrease**	7	-7.19	5.62	Wilcoxon	0.02
European 30 Celsius (or more) days						
Variable name	Change	# of data points	Mean change	Standard deviation	Statistical test	p-value
30 Celsius days	Increase*	5	128.50	85.13	Wilcoxon	0.06

-Severe thunderstorms and tornadoes

Severe thunderstorms and tornadoes are assessed, with a summary of principal results noted in Table 7 for the selected variables. Here, results are presented based on changes in vertical wind shear (figure 12a), and changes in the number of severe thunderstorm development days (figure 12b). For every degree Celsius of global warming, the findings show declines in the amount of vertical wind shear, relative to the climatological mean, with data points displaying decreases of between 0 to 5%, and an average reduction of 1.8%. These findings are statistically significant at the 10% significance level. In contrast to vertical wind shear patterns, the number of severe thunderstorm development days shows an increase, with all of the data points favoring an enhancement in the number of these types of days in a warmer climate, with an average

increase of 6.5%. Results for severe thunderstorm development days are statistically significant within the 5% significance level (p=0.02).

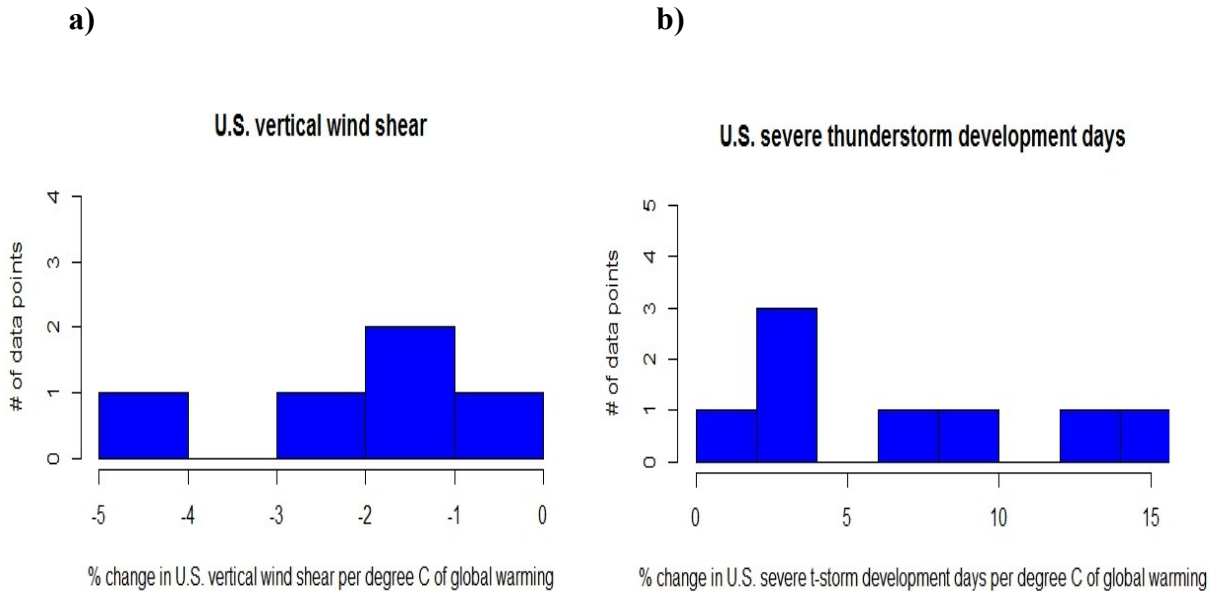

Figure 12. U.S. vertical wind shear and severe thunderstorm development day changes. Histograms highlight percentage changes per degree Celsius of global warming in terms of (a) vertical wind shear and (b) severe thunderstorm development days.

Table 7. Results for selected severe thunderstorm and tornado variables. Results include changes in severe thunderstorm development days, and changes in mean vertical wind shear (measured between the 850 and 200 hpa geopotential heights). Means and standard deviations are given as percent changes. "*" and "**" indicate results that are statistically significant at or within the 10% and 5% significance levels, respectively.

U.S. Severe thunderstorm development days and mean vertical wind shear						
Variable	Change	# of data points	Mean change	Standard deviation	Statistical test	p-value
Mean vertical shear	Decrease*	5	-1.78	1.48	Wilcoxon	0.10
# of severe thunderstorm development days	Increase**	8	6.53	5.21	Wilcoxon	0.02

-El Nino Southern Oscillation

Changes in the behavior of ENSO with global warming can be utilized to assess future changes in regional drought, Atlantic tropical cyclone activity, the South Asian monsoon, as well as, to some extent, severe thunderstorms and tornadoes. Figures 13a and 13b show percent changes in ENSO amplitude and period per degree Celsius of global warming, respectively. ENSO amplitude shows no significant change (p=0.91). More distinct, however, is the significant trend towards a decrease in ENSO period per degree Celsius of global warming, as represented in figure 13b, indicating an increase in both El Nino and La Nina events. Here, the results are statistically significant at the 1% significance level (p=0.01), and a large number of data points (14 out of 19) show a trend towards a decrease of between 0 to 10% for ENSO period in a warmer climate (figure 13b), with an average decrease of 3.4%. Table 8 summarizes the results for ENSO amplitude and period per degree Celsius of global warming.

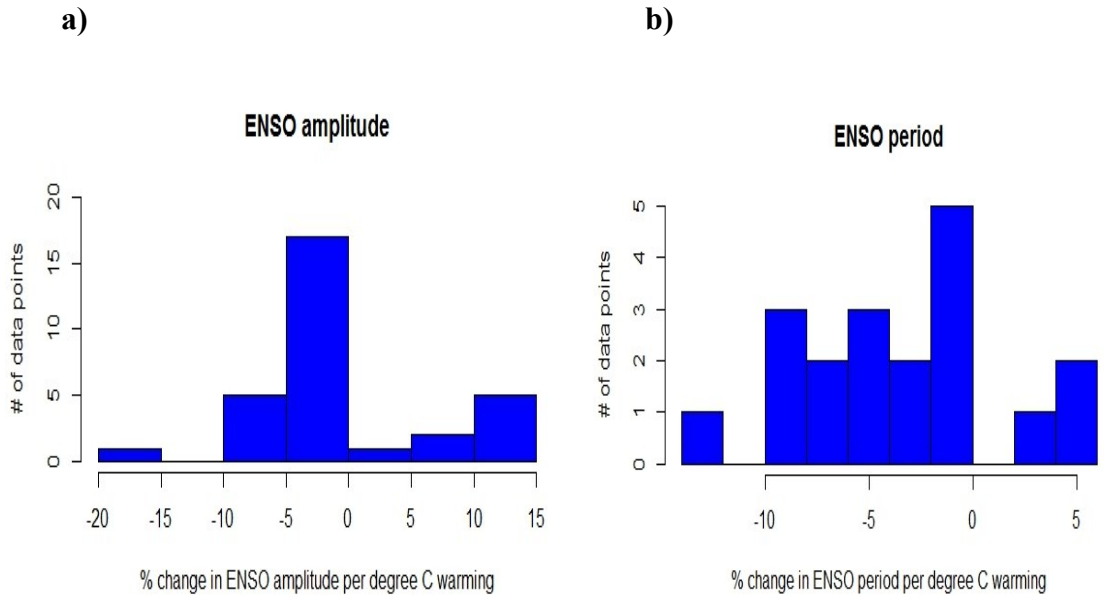

Figure 13. ENSO pattern changes. Histograms show percentage changes of ENSO behavior per degree Celsius of global warming for (a) ENSO amplitude and (b) period.

Table 8. Results for ENSO patterns. The findings provide changes in amplitude and period per degree Celsius of global warming. Means and standard deviations are given as percent changes. "***" indicates results that are statistically significant at the 1% significance level.

ENSO amplitude and period						
Variable name	Change	# of data points	Mean change	Standard deviation	Statistical test	p-value
ENSO amplitude	No change	31	-0.13	6.77	t-test	0.91
ENSO period	Decrease***	19	-3.38	5.12	t-test	0.01

Discussion

-Tropical cyclones

It is widely suggested in the literature that the frequency of global tropical cyclones will decrease in response to different levels of global warming, along with an increase in intensity, as well as an increase in the number of intense storms. The results in this study indicate that tropical cyclone numbers, at a global scale, decrease significantly per degree Celsius of global warming, and though there is no statistically significant change in intensity, the intensity of storms is shown to significantly increase in both the Atlantic and Pacific basins. As a result, in spite of the global decline in tropical cyclones in a warmer climate, as well as generally statistically insignificant changes for regional frequency, the storms that do occur, at least in the NW Pacific and Atlantic, could potentially become more severe and, thus, damaging, as consistently shown through an enhancement in storm intensity in these basins, with results that are all statistically significant in this study. The increase in storm intensification could also imply a shift towards more intense tropical cyclones, where a larger number of storms attain higher category strength. This is particularly evident for the NW Pacific basin, where the number of category 4 and 5 storms is shown to increase significantly with global warming. The increase in cyclonic intensification is also consistent with the significant increase in intense storms, in general, in the NW Pacific. By contrast, in the Atlantic, an increase in intensification is shown to occur in conjunction with a significant decrease in the frequency of intense storms, as well as no statistically significant change in the frequency of the most intense storms. This combination may imply that the cyclones that do form could become more intense with global warming, even in spite of a decrease in the number of intense storms shown for the basin. However, the degree of intensification

may mostly not be enough for cyclones to commonly advance into higher category storms, as compared to the NW Pacific, where the number of intense storms increases significantly.

The significant decline in global tropical cyclone frequency and consistent increase in intensity at regional scales with global warming may be explained through multiple factors, but the trend towards increased tropical upper-tropospheric stability in a warming climate appears to play a leading role in the decreasing pattern shown by global tropical cyclone frequency. Modeling studies (e.g. Knutson & Tuleya, 2004) have projected that rising global mean temperatures into the 21st century favor an increase in warming throughout much of the troposphere, but it is illustrated that the rate of warming in the tropical upper-troposphere is significantly larger than that of which occurs at or near the surface over these regions, enhancing the effect of static stability.

Despite decreased global tropical cyclone frequency, the significant increase in intensity noted in this study for the Atlantic and NW Pacific implies that the impact of an enhanced thermodynamically stable environment is effectively offset by changes in other specific environmental conditions that are important for cyclogenesis. As such, while global tropical cyclone frequency is likely more sensitive to enhanced upper-tropospheric warming, increased severity of Atlantic and NW Pacific tropical cyclones, as well as the number of intense storms in the NW Pacific, could be driven more so by an increase in potency of dynamical features, such as boundary layer moistening, decreased wind shear, and SST warming, such that the negative effects of atmospheric stability would be offset.

Increased global atmospheric moisture may be a significant contributor in the intensification of tropical cyclones in a warmer climate, which could lead to an increase in CAPE, especially in tropical regions. A warming climate may, thus, act to supply more buoyant energy to tropical cyclones through enhanced moisture content. This effect has been documented in Knutson et al. (1998), highlighting that tropical cyclone intensification in the NW Pacific basin in their simulations is primarily due to increases in CAPE and tropical SSTs, which compensate for the impact of tropospheric stability at upper-levels. Gualdi et al. (2008) also note a 24% increase in CAPE, relative to the pre-industrial period, due to an increase in lower-tropospheric water vapor with CO_2 doubling. In this study, global precipitable water serves as a proxy for global moisture and is related to the amount of CAPE present in the atmosphere. As shown in Table 4, global precipitable water increases significantly per degree Celsius of global warming, suggesting a correspondingly significant increase in CAPE through boundary layer moistening. Consequently, the increase in precipitable water, as per the results of this study, could explain general patterns in tropical cyclone intensification with global warming at regional and global scales.

In summary, the significant decline of global tropical cyclones found here may be related to the dominating effect of mid- to upper-tropospheric warming in a warmer climate. By comparison, the consistent and very significant increase in tropical cyclone intensity given for regional-scale storms, as well as for both the NW Pacific and Atlantic basins, may be attributed to an increase in tropical CAPE and warmer SSTs, which, together, could act to overcome the hindering effect associated with predicted tropospheric stability. In the NW Pacific, however, in addition to the highly significant

increase in storm intensification, there is also a very significant increase in the frequency of category 4 and 5 storms, as well as in terms of the number of intense storms, in general. This could likely be due to the combination of increased tropical CAPE, warmer SSTs, and a tendency towards decreased vertical wind shear projected to occur simultaneously with global warming (e.g. Stowasser et al., 2007); this would suggest that tropical cyclone intensification would be most pronounced in this region while fostering ideal environmental conditions that promote an enhancement in the number of intense storms. Indeed, these patterns are consistent with the results presented in this study with respect to NW Pacific cyclones, where the increase in intense storms, the most intense tropical cyclone frequency and general storm intensification are shown to be most statistically significant. In the Atlantic, differing results are given. Because Atlantic tropical cyclone frequency remains largely unchanged with global warming, the increase in intensification would suggest typically more intense storms with global warming. However, the degree of intensification may mostly not be enough for cyclones to commonly advance into higher category storms, as compared to the NW Pacific, where the number of intense storms increases significantly.

The observational record shows that there has been no distinct trend highlighting any increases in global and regional land-falling tropical cyclone frequency, and with respect to the number of the most intense storms, since the 1950s (Weinkle et al., 2012), though there is some tendency towards an increase in cyclone frequency in the Atlantic since the mid-1990s. The patterns exhibited in the historical record are, therefore, somewhat similar to the results provided in this study, in that there is generally no statistically significant change in the frequency of intense or most intense cyclones (with

the exception of the NW Pacific), as well as in terms of the NW Pacific cyclone frequency.

-South Asian monsoon

For the South Asian monsoon, an increasingly warmer climate is shown to weaken the general monsoonal circulation during the warm season (JJAS). The results presented here indicate that the zonal wind component of this circulation will decrease as a result of global warming. However, a simultaneous increase in warm season monsoonal rainfall is shown to significantly increase in a warmer climate, suggesting that rainfall exhibits a trend towards an increase, in spite of weakened monsoon circulation.

The increased monsoonal rainfall finding follows well with the clear trend towards global precipitation increases, which implies an increase in more heavy rainfall events associated with the South Asian Summer monsoon. Also, due to the significant increase in global precipitable water, we might expect enhanced convective rainfall associated with the South Asian Summer monsoon, which is consistent with the significant increase in global convective rainfall found in this study. The increased rainfall tendencies might also be related to a weakened ENSO-monsoon relationship with global warming, suggesting that the effect of ENSO, in terms of ENSO-warm phases (El Nino events), may have little effect on South Asian Summer precipitation (this effect is further discussed in the ENSO section). As such, although monsoonal circulation is to significantly weaken with global warming through a decline in mean warm season zonal wind flow, this trend is likely to be counteracted by an enhancement in convective activity, with respect to more moisture availability (precipitable water) and moisture

convergence, while a more enduring and increased land-ocean pressure gradient, as is documented in many studies (e.g. Meehl & Washington, 1993; Lal et al., 2000), could also increase the potential for more heavy rainfall events through surface convergence.

-Global precipitation

The results indicate that a very significant increase in global precipitation is expected in a warmer climate. This finding adheres to the increase in observed global precipitation shown over nearly the last century, as given in Kumar et al. (2013), who show an average global increase of 0.78 mm/decade during the 1930-2004 period.

To assess potential trends in heavier precipitation events, changes in precipitable water and convective rainfall, at a global scale, are examined. Like global precipitation, the findings suggest that precipitable water increases significantly with global warming and are consistent with the Clausius-Clapeyron relationship. Similarly, a significant increase in convective rainfall is also shown per degree Celsius of global warming. In the historical record, atmospheric moisture has also been particularly increasing from 1973 to 1995 (Trenberth et al., 2005).

From the results given, the increase in global precipitation may be significantly attributed to a rise in precipitable water. Because convection is dominant in tropical and equatorial regions, we might expect that most of the increase in global precipitation in a warmer climate would occur over those latitudes, as compared to farther North or South towards mid-latitudes. Indeed, annual mid-latitude cyclonic systems, as discussed in the following section, are shown to significantly decrease, especially in the Northern hemisphere, and there is also a significant decline in both European and North American

soil moisture; the combination of these factors would imply a decrease in annual precipitation at mid-latitudes, in spite of a significant global increase in precipitation. By contrast, because mid-latitude cyclones are heavily dependent on moisture availability, an increase in global precipitable water could, like tropical cyclones, lead to an increased intensification of these storms through greater latent heat release, which is shown to significantly increase the number of intense storms in a warmer climate. This would also indicate that convection, at least in tropical to equatorial regions, becomes enhanced in a warmer climate because of more moisture availability in the atmosphere, which would lead to greater latent heat release of condensation and, therefore, promoting further atmospheric instability. Increased moisture may also lead to more severe thunderstorm development days. As discussed in the previous sub-sections, tropical cyclonic intensification may similarly be attributed to increases in atmospheric moisture, which, in turn, favor an enhancement in CAPE. At the same time, the South Asian monsoonal rainfall may become enhanced in a warmer climate with more moisture availability and increased convective activity.

-Mid-latitude cyclones

The findings indicate that global mean temperature rise will likely act to reduce mid-latitude cyclones for the future but will conversely increase the number of intense cool season storms, a trend that is highlighted mostly for the Northern hemisphere in this study. For Northern hemisphere mid-latitude cyclones, a consistent decrease in the annual number of storms is found. At seasonal scales, similar patterns are also observed for the Northern hemisphere cool season, showing a notable decrease in the number of storms per cool season in a warming climate. In terms of intense storm counts, an increase is

shown per cool season. Similar results are also found for the Southern hemisphere, although there is no statistically significant change in annual cyclone frequency in the Southern hemisphere.

The decreasing trend in mid-latitude cyclones may be related to a projected decrease in baroclinicity at mid-latitudes (e.g. Konig et al., 1993; Beersma et al., 1997; Geng & Sugi, 2003; Catto et al., 2011), which, in turn, may be linked to the weakening of the equatorward meridional temperature gradient associated with reduced Winter sea ice and snow coverage in a warmer climate. As per the results of this study, weakened baroclinicity may be a particularly important factor contributing to the decrease in annual cyclones shown for the Northern hemisphere. With a weakened latitudinal temperature gradient, mid-latitude Rossby waves (specifically troughs), which are crucial for the development of cyclonic development at the surface, could subsequently become less prominent and, thus, increase the likelihood for a decrease in the number of cyclones that do occur. To another extent, the significant reduction of global tropical cyclone frequency may also partly explain the general declining pattern of mid-latitude cyclones. In the Northern hemisphere, for example, as tropical cyclones mature and propagate North to Northeastward, they undergo a gradual weakening that is attributed to either prolonged exposure to cooler SSTs, or boundary layer frictional influences associated with land surfaces. It is this cyclonic weakening that transpires into storm systems that assume extra-tropical cyclone characteristics. Consequently, the significant decrease in global tropical cyclones could partly contribute to the overall decrease of mid-latitude storms, principally during the warm season.

That said, an increase in the number of intense storms could yield more significant snowfall events, along with a subsequently elevated number of strong wind incidences, as the pressure gradient associated with these systems would be stronger. This trend could likely become more pronounced in the Southern hemisphere, as the increase in the number of cool season intense storms appears to respond more significantly to global warming there. The increase in the number of hemispheric intense cool season storms may also, in part, be due to increased moisture availability. The significant increase in precipitable water and, therefore, atmospheric moisture content found in this study could explain this increase, as it would act to fuel the development of cool season mid-latitude cyclones in a warmer climate and, consequently, enhance the potential for heavier snowfall events. As a result, the increase in precipitable water is consistent with the increase in intense hemispheric cool season mid-latitude cyclones. This tendency is also highlighted in Sinclair & Watterson (1999) and Geng & Sugi (2003), who show that increased water vapor and humidity in a warmer climate favors the development of more intense mid-latitude cyclonic storms. The increase in the number of intense storms during the austral Winter could be that the poleward storm track allows for easier accessibility to Antarctic air masses, thereby increasing the available potential energy for storms, as suggested in Bengtsson et al., (2006).

Decreased mid-latitude cyclone frequency may also be related to a change in storm track with global warming. Because of a poleward increase in temperature gradients in a warmer climate, as documented in multiple studies, the increase in the number of intense storms, as well as potentially enhanced cyclone frequency, in general, is more likely to occur farther towards higher latitudes and poleward due to a more active

storm track. Mizuta et al. (2011), for instance, show in their simulations that the number of intense storms during the Northern hemisphere Winter in a warmer climate is found on the polar side, North of the storm track. Similarly, Bengtsson et al. (2006) find that Southern and Northern hemisphere mid-latitude cyclones are reduced slightly due to a poleward shift in the maximum SST gradient, prompting an approximately 5 degree Southward or Northward shift in storm track induced by a corresponding change in the upper-tropospheric jet stream. This shift is also represented in Fyfe (2003) for the Southern hemisphere in the sub-Antarctic Ocean, showing a poleward shift in baroclinicity towards the Antarctic Ocean, resulting in increased cyclone frequency there.

As such, the decreases in mid-latitude cyclone frequency found in this study are likely associated with decreases in mid-latitude baroclinicity, which, in turn, are related to a reduced temperature gradient. In addition, because the strongest temperature gradients shift farther poleward, the polar jet stream would also correspondingly migrate poleward, as well, resulting in more pronounced temperature variability and increasing the potential for more intense cyclogenesis over these regions. As a result, though the significant increase in the number of intense storms shown here may lead to more heavy snowfall events in a warmer climate, these storms may be found farther poleward near high-latitudes, or the poleward extent of mid-latitudes, due to a shift in storm track, while leaving more rainfall for mid-latitudes because of increased exposure to associated warm sectors of these storms. In another context, despite a significant global increase in precipitation, the findings presented for mid-latitude cyclones would suggest that most of this increase occurs over tropical regions, given the decline in annual cyclonic frequency at mid-latitudes (mostly in the Northern hemisphere), especially during the cool season.

Also, because of a poleward shift in temperature gradients, we might expect an increase in precipitation towards the poleward extent of mid-latitudes and Northward (Southward) in the Northern hemisphere (Southern hemisphere) into high latitudes, which has been projected to occur in some studies (e.g. Lau et al., 2013).

Wang et al. (2013) show that extra-tropical cyclones, in both hemisphere, have exhibited signs of increasing over the 1871-2010 period for both the Northern and Southern hemisphere, with the greatest increase in the Southern hemisphere. Though the results in this study largely favor a significant decrease in cyclone frequency in the Northern hemisphere per degree Celsius of global warming, as well as for cool season cyclones in both hemispheres, an increase in cyclones towards poleward sections of mid-latitudes could occur in a warmer climate, due to a shift in baroclinicity.

-Drought and heat waves

A significant decrease in soil moisture is found for the European continent in this study. Nearly similar decreases are displayed for the North American continent. It has been shown that decreased soil moisture, especially at mid-latitudes, may be attributed to an increase in the rain to snow ratio during the cooler seasons, coupled with earlier snowmelt in the Spring, which prompts a deficit in soil moisture during the Summer (Sheffield & Wood, 2008). Indeed, the significant decline in soil moisture in the results presented here is consistent with a trend towards decreased mid-latitude cyclone frequency, both annually, and during the Northern hemisphere cool season. As discussed in the previous section, particularly notable is the decrease in cyclonic frequency during the cool season over mid-latitudes. By contrast, though the number of intense storms is

shown to increase, the shift towards a more poleward track of these storms, as suggested in the literature, would imply a decreased likelihood for heavy snowfall events to occur farther South because of a rise in boundary layer temperatures. This would then result in less Winter precipitation in the form of snow over the mid-latitudes of the Northern hemisphere, including Europe and North America, mostly with respect to total snowfall and, thus, snow coverage, which are important in the soil moisture recharge process. As a result, drought and heat waves would increase in both frequency and intensity under these conditions in time for the warm season.

Though soil moisture is shown to decrease, this study, counter-intuitively, also finds a significant increase in global precipitation per degree Celsius of global warming, as previously discussed, which would alternatively suggest a corresponding decline in drought through an increase in soil moisture. This effect may be related to a simultaneous increase in the rate of potential evapotranspiration with global warming, which offsets the increase in precipitation, as shown in Rind et al. (1990). In this study, most of the global precipitation increase may be associated with significant increases in precipitable water, which could increase the intensity and frequency of convective precipitation. At mid-latitudes, however, annual precipitation may decrease due to a decrease in cyclonic storms (as described in the previous section), but because of increases in global precipitable water, the frequency of heavy precipitation events could increase, allowing for a subsequent increase in flooding (or flash-flooding) events during the warm season. This occurs due to the combination of drier soils and a significant increase in the intensity and frequency of heavy (convective) rainfall, as dry soils cannot efficiently accommodate the intensified nature of heavier rainfall events.

Heat waves are shown to change in frequency and severity into the future over Europe and North America (Meehl & Tebaldi, 2004). As with drought, regional heat waves are also found to increase, at least in North America and Europe, with global warming through a significant reduction in soil moisture. According to historical data pertaining to daily high temperatures for the contiguous U.S. from the 1950s to 2000s, for example, the number of record daily highs and record daily highs have increased since the 1970s, with unusually hot Summer days becoming more common, as well as a higher frequency of warmer Summer overnight lows (EPA, 2013). The results presented here for North American heat waves, therefore, further this trend with future global warming. Similarly, the number of days reaching 30 Celsius or more across the European continent is shown to increase significantly. This result is consistent with the decrease in soil moisture content over the region, which would also lead to a declining rate of evaporative cooling. These patterns are represented in Schar et al. (2004), where future temperature and precipitation patterns for 2071-2090 are similar to those present during the anomalously hot Summer of 2003 across much of Europe, likely attributed to increased soil moisture depletion and convective inhibition.

Because positively strong geopotential heights, especially at the 500 hpa level, are commonly associated with distinct warming episodes (warm air advection), the results suggested here could imply that a trend towards more of these anomalies could occur through increased air expansion. This effect is found in Meehl & Tebaldi (2004), where the 500 hpa geopotential height increases by 55 and 50 geopotential meters over areas near the upper U.S. Midwest and France, respectively, with end-21st century warming. Nearly identical tendencies have been found into the Southern U.S. and Mediterranean,

as well as areas near Moravia, Czech Republic (Huth et al., 2000). Similar mid-tropospheric anomalies are also displayed in Lau & Nath (2012), who show that the anti-cyclonic circulation associated with the blocking ridge patterns at the 500 hpa level hinders the movement of synoptic-scale systems throughout many regions of the U.S., while decreased eddy motion projected in their model simulations suggest a more stagnant environment that favors prolonged conditions that are warm and dry.

Though solely two continents are used to assess drought and heat waves, the results provided here may be valid at a global scale, as well, especially at mid-latitudes, where snow coverage could significantly decrease with a significant decline in cool season mid-latitude tropical cyclones. Indeed, Mueller & Seneviratne (2012) show in their findings that for many areas of the globe, there is a strong relationship between the number of hot days during the hottest month, and preceding precipitation deficits.

-Severe thunderstorms and tornadoes

An overall trend towards an increasing frequency of severe thunderstorms over the U.S. in this study is shown to occur with rising global mean temperatures, and results for this increase are highly significant. This is particularly evident when examining the results given for the number of days where severe thunderstorm development takes place, in which case, an increase occurs in a warmer climate. However, the increase in severe thunderstorm development days coincides with a consistent significant decrease in deep-layer vertical wind shear with global warming, which would, intuitively, act to suppress the overall severity of thunderstorms. The results, then, suggest that severe thunderstorm frequency would increase in response to global warming, in spite of decreasing levels of

wind shear. One explanation for this contradiction could be that precipitable water increases significantly, which would largely contribute to an elevated amount of CAPE distributed in the troposphere in a warmer climate. In this study, the amount of precipitable water, at a global scale, is shown to be enhanced substantially per degree Celsius of global warming, with statistically significant increases. Consequently, it is likely that the increase in precipitable water and, therefore, CAPE, is leading to an increase in the number of severe thunderstorm days occurring across the U.S., enough to offset the negative effect associated with decreased vertical wind shear. The influence of increased buoyancy on thunderstorm development in a warmer climate has also been suggested in Trenberth (2012). Thus, the net effect is an increase in the number of severe thunderstorm development days, which is consistent with the findings presented in Trapp et al. (2007), as well as Trapp et al. (2009), who show that NDSEV increases, in spite of decreases in vertical wind shear with global warming. On the other hand, decreases in wind shear in a warmer climate may restrict the number of tornadic (or supercell) thunderstorms that do develop, while suppressing the potential for severe tornadoes, and limiting the endurance and/or organization of severe thunderstorms. Limited thunderstorm and tornado intensity may also be attributed to statistically significant decreases in North American soil moisture. Decreased soil moisture content could act to moderate, to some extent, the regional precipitable water, which may lead to less water vapor that could be released to the atmosphere during the warm season and, as a consequence, weakening atmospheric instability, and the overall severity of thunderstorms and tornadoes with global warming.

The increase in severe thunderstorm development days is also not consistent with a decrease in annual Northern hemisphere mid-latitude cyclones in a warmer climate, as severe thunderstorm and tornadic activity are often associated with these cyclonic storms. The declining tendencies exhibited by mid-latitude cyclone frequency, as noted previously, are likely related to decreasing baroclinicity and may also be associated with a decrease in the North-South temperature gradient developing at low- to mid-levels of the troposphere (e.g. Van klooster & Roebber, 2009). The decreasing trend in mid-latitude cyclones is, by contrast, consistent with reductions in vertical wind shear, as the presence of these cyclones, especially the stronger storms, enhances deep-layer shear profiles, particularly in terms of the directional component. However, Finnis et al. (2007) and Trapp et al. (2009) find that the general decrease in mid-latitude cyclones is more pronounced in the cool season, as compared to the warm season. A tendency towards significant decreases in cool season cyclone frequency at Northern hemisphere mid-latitudes is also shown here. Furthermore, Trapp et al. (2009) note that severe thunderstorms can develop in the absence of synoptic-scale systems, and the projected changes (decreases or any increases) in warm season mid-latitude cyclone frequency in their study are found to be statistically insignificant. In Lee (2012), an increase of U.S. F2 or greater tornado days is found due to changes in synoptic-scale activity, though much of this increase is shown to occur during the late-Northern hemisphere Winter to early-Spring period (February to April) because of a shift in seasonality with end-21st century global warming. As such, it may be that, based on the results of this study, as well as those findings in other works, severe thunderstorms and tornadoes could increase in frequency in the U.S. in a warmer climate, as the degree of instability increases with

enhanced atmospheric moistening (precipitable water), even with a decline in mid-latitude cyclone frequency. The increased moistening would generate more CAPE during the warm season, which could lead to powerful thunderstorm development because of potentially stronger updrafts more frequently present inside thunderstorms. However, because of the potential northward shift in baroclinicity with global warming, it is possible that most of the increase in severe thunderstorm development days would be located farther North into Northern regions of the U.S. and Southern Canada.

Alternatively, based on the results found here, the trend of decreased vertical wind shear would suggest a generally more limited potential for vigorous mesocyclonic development that is conducive to more violent tornadoes and longer sustained thunderstorm updrafts, as larger degrees of shear would otherwise provide conditions more suitable for enduring single and multi-cellular thunderstorm cells, and related storm modes (such as squall lines or derechos). In addition, although increased moisture content would favor larger surface-based CAPE, the effect of increased precipitable water content could also act to weaken stronger updrafts due to the increasing influence of water loading, though the negative effect associated with water loading will ultimately depend on the vertical distribution of CAPE throughout the troposphere. Consequently, thunderstorms that do form in such environments will have an enhanced capability of producing flash-flooding, frequent lightning and stronger downdrafts (outflow) because of a greater quantity of water being condensed into the thunderstorms. The potential for flash-flooding may be further exacerbated by weaker speed shear, which could cause storms to propagate at a slower rate and, therefore, allowing them to remain over areas for a prolonged period of time. In another scenario, as North American soil moisture

content is shown to be significantly reduced with global warming, regional precipitable water could also be reduced in this way. With decreased moisture availability, severe thunderstorm development days may not necessarily decrease but could, instead, have a more dominant storm mode, that is, thunderstorms that have a greater potential of producing stronger downdrafts and larger hail due to enhanced mid-level evaporative cooling associated with drier air. That said, tornadoes would generally be weaker under these circumstances, since cloud bases are more elevated when supercells are of the low-precipitation variety.

Historical decadal tornado counts spanning from the early 20th century to present day would suggest that tornado frequency, including the number of intense tornadoes, has increased sharply in the U.S. (NOAA, 2013). However, much of this drastic change is likely attributed to increases in densely populated areas, storm spotters, weather watchers, storm chasers, as well as communication systems (warning systems formally introduced in the 1970s). The combination of these factors has mostly contributed to the increase in tornadoes observed in the historical record due to enhanced detection. A closer inspection of recent decades, however, shows that there is no significant change in tornado frequency, or in terms of the most intense tornadoes (EF3 to EF5), though, since the 1980s, there has been a trend towards a slight decline in the most intense tornadoes. As a result, tornado trends over the last few decades are inconsistent with those results found in this study. However, there are some similarities between the results shown for intense tornadoes, and the trend towards a slight decrease in the strongest tornadoes depicted in the most recent decades.

-El Nino Southern Oscillation

The results outlined here show that ENSO could significantly decrease in period, while ENSO amplitude exhibits no significant change. These findings imply that global warming could alter ENSO-warm and cool cycles but leave the amplitude largely unchanged, indicating an increase in both ENSO warm and cool phases (i.e. more El Nino and La Nina events), but with similar intensities to the present climate. The decrease in ENSO period may be associated with a greater rate of heat content entering and leaving through a larger meridional temperature gradient on either side of the equator, as suggested by Collins (2000a). ENSO period changes may also be driven by an enhancement in the equatorial wave speed caused by increased stratification associated with the surface-intensified nature of ocean warming, which is found in Chen et al. (2005) and Merryfield (2006).

In a recent study that used tree-ring data from the American Southwest to re-construct a 1,100-year history of ENSO cycles, the records revealed a 50-90-year cycle of strengthening and weakening of El Nino intensity (Li et al., 2011). The records also showed that the variance between El Nino and La Nina events becomes more pronounced when the background temperature is warmer, and less during cooler periods; this suggests that future warming could enhance ENSO variability, as well as more extreme global climate conditions (Li et al., 2011), which is consistent with the results presented here, in terms of ENSO period.

-NW Pacific and Atlantic tropical cyclones and ENSO

The Pacific Walker circulation is driven by zonal and vertical pressure differences occurring between the East and West tropical Pacific, and its circulatory intensity is principally controlled by ENSO. The weakening of the Pacific Walker circulation in climate experiments has been attributed to decreased wind shear over the NW Pacific development region, which favors an increase in tropical cyclone frequency and intensity. When an El Nino event is present, vertical wind shear weakens over much of the tropical NW Pacific basin, including over the main development region for cyclones. It has been shown by Saunders et al. (2000) that El Nino years foster conditions that are conducive for more land-falling typhoons to occur in the NW Pacific. Consequently, during El Nino years, decreased wind shear considerably increases the likelihood for storm formation, often allowing tropical storms to evolve into full-fledged typhoons. In this study, the intense and most intense tropical cyclones, and storm intensification, are shown to significantly increase per degree Celsius of global warming and could be related to the statistically significant decrease in ENSO period with a warming climate, where an increase in El Nino events could lead to a greater number of years for active typhoon seasons. As a result, modifications to ENSO period with global warming may partly explain the significant intensification of NW Pacific tropical cyclones shown in this study, as well as with respect to the significant increase in the number of category 4 and 5 storms in this basin, and strong storms, in general.

Similarly, in the Atlantic basin, a decrease in ENSO period in a warmer climate may lead to an increase in years where Atlantic tropical cyclones undergo an increase in intensification, which may, in part, explain the significant increase found for Atlantic

cyclone intensity because of decreased vertical wind shear associated with more La Nina years. An increase in La Nina events would ideally strengthen the Walker circulation and, thus, enhance ENSO-neutral conditions. Consequently, weaker vertical shear profiles generated over the Atlantic basin during these years would more frequently favor further intensification of tropical Atlantic cyclones. On the other hand, the significant decrease in the number of Atlantic intense storms in a warmer climate may be related to an increase in El Nino years, which could decrease the frequency for favorable cyclogenesis. That said, the results between both the NW Pacific and Atlantic suggest that changes in ENSO period may have more of an influence in decreasing intense storm counts in the Atlantic, as compared to the Pacific. This may be that the increase in vertical wind shear associated with La Nina events over the NW Pacific in a warming climate may not be as significant as the increase in shear that occurs over the tropical Atlantic during an El Nino, allowing tropical cyclone development to remain active over the NW Pacific, even during La Nina years.

-South Asian monsoon zonal circulation and ENSO

The Asian monsoon can be influenced by various climatic factors, such as ENSO. The ENSO-monsoon relationship has been extensively documented in the literature as a major influence on the Summer South Asian monsoon (e.g. Kripalani et al., 2007), as an increase in ENSO-warm phases in a warmer climate may act to suppress precipitation increases over the region. When ENSO exhibits El Nino-like patterns, the Walker circulation 850 hpa winds weaken due to a reversal of SST differential heating between the central and East tropical Pacific, and the West tropical Pacific and East Indian Ocean. These changes manifest themselves as anomalous low-level easterly winds in place of the

climatological low-level Southwesterlies that are typical of the Summer Asian monsoon. This is likely attributed to strengthening subsidence associated with cooler SSTs present in the Eastern Indian Ocean and Western Pacific relative to the central and East Pacific. These patterns are also represented by precipitation patterns in the tropical Pacific, where central and Eastern sections show an increase in convective activity, while suppression occurs in the West. The reverse holds true during the course of La Nina years. Of particular interest are potential changes in the Walker circulation.

The results found in this study suggest that the overall South Asian Summer monsoonal circulation, in terms of its zonal component, is reduced, indicating a weakening in the overall circulation with global warming. This would imply that boundary layer easterlies in the Indian Ocean become more pronounced in a warmer climate, which, in turn, would suggest that the Walker circulation weakens to promote these anomalous easterlies. A further examination of ENSO tendencies in this study would also support changes in the Walker circulation in a warmer climate, particularly in terms of ENSO period. The results presented here show that ENSO period is significantly reduced in a warming climate. This, as mentioned above, represents an increase in both El Nino and La Nina events. However, an increase in the number of El Nino phases would explain more frequent modifications to the Summer monsoon climatological boundary layer zonal winds, in which case, they would more often weaken in a warmer climate. With a significant weakening in the boundary layer zonal winds of the Summer South Asian monsoon circulation shown in this study, one would hypothesize that warm season rainfall would considerably be reduced in a warmer climate. As shown in figure 6b and Table 3, this is not the case, as the results yield an increase in Summer monsoonal

rainfall. The implication is that other climatic factors may be playing an important role in order to offset the weakened monsoon circulation with global warming, as well as the increase in El Nino events in a warmer climate. It is projected that the ENSO-monsoon relationship could weaken in a warmer climate (Ashrit et al., 2001; Vecchi et al., 2006; Kripalani et al., 2007), as increased moisture transport into South Asia, reduced Eurasian snow depth/coverage during the Northern hemisphere Winter associated with enhanced Eurasian warming, and a stronger land-ocean temperature and pressure contrast between the Indian subcontinent and Indian Ocean, may lead to a net-increase in the South Asian monsoon circulation. As such, the cumulative effect of these factors may offset the potential increase in warmer ENSO events, as well as possible tropical upper-tropospheric warming in a warmer climate. Increased evaporation over the tropical Pacific could also be a more important factor to monsoon variability, where increased precipitation and, therefore, latent heat release in the central tropical Pacific is transmitted to the Indian Ocean by the anomalous East-West lower atmospheric circulation in a warmer climate, subsequently inducing an increase in upward vertical velocity in the Indian Ocean. Thus, warmer tropical Pacific SSTs may suggest an increase in monsoon precipitation, even in the absence of a strong Walker circulation and, therefore, more El Nino-like patterns. In addition, the significant increases in global precipitable water found here also suggest that convection, at the global scale, would be considerably enhanced in a warming climate, which could act to increase the intensity of heavy rainfall events from deep convective systems during the Summer monsoon season.

-Drought, heat waves and ENSO

Changes in ENSO patterns were also considered in this study to examine how they might influence heat waves and drought in a warmer climate. An increase in ENSO period would result in more episodes of drought and heat waves for many regions, including North America, Europe, and Australia. With more El Nino events, Australia could see more occurrences of drought, while more La Nina events would favor increased drying and heat wave potential in sections of North America. That said, ENSO has been exhibiting a trend towards cooler phases since 1999 (Dai, 2013). Over Asia, increased El Nino events could also lead to more drought conditions there through the weakening of the monsoonal circulation in a warmer climate. However, the weakened ENSO-monsoon relationship, as described in the sub-section above, through increases in warm season rainfall, indicates that Asia, at least South Asia, would not be affected significantly by an increase in El Nino (or ENSO-warm) events, while increased La Nina events would amplify the overall strength of the circulation with global warming. The impact of ENSO may also amplify heat wave frequency and/or intensity in a similar manner to drought, that is, increased El Nino events would favor an increase in Australian heat waves, while more La Nina episodes may enhance heat waves over parts of North America.

-Severe thunderstorms changes and ENSO

The effect of changing ENSO patterns in a warming climate is explored to explain trends in severe thunderstorm development days. Marzban & Schaefer (2001) show in their study that cooler equatorial SSTs, or La Nina events, tend to increase the number of tornado and, therefore, severe thunderstorm days across the U.S., particularly into the

U.S. NE and SE Canada due to the dominant influence of the mid-latitude jet stream persisting over the regions. In this study, the statistically significant reduction in ENSO period would lead to an increase in the number of El Nino and La Nina events. This would suggest more years with an enhanced frequency of severe thunderstorm/tornado days during the tornado season due to an increase in La Nina years. The increase in these severe weather days through decreased ENSO period is consistent with the significant increase in severe thunderstorm development days, and it is, therefore, possible that ENSO may be an important contributor to North American severe thunderstorm development in a warmer climate in this way.

Summary and conclusion

In this study, I have employed a meta-analysis to quantify trends for specific extreme weather events in response to global warming. Using a combination of the one-sample t-test and Wilcoxon Rank Sum test on datasets collected for a wide variety of selected variables representing specific weather phenomena, it was possible to identify potential trends of weather extremes and statistically measure their degree of significance with 21st century global warming.

For global tropical cyclones, the results indicate that the overall frequency of these storms will decrease significantly, while their intensity will increase in a warmer climate. In terms of both the Atlantic and NW Pacific basins, the changes in tropical cyclone intensity are shown to also be significant, but unlike global tropical cyclone frequency, no obvious trend is shown for these basins. For the number of intense tropical cyclones, no significant trend is identified at a global scale, nor for the Pacific and Atlantic basins. That said, a clear pattern towards an increase in the most intense tropical cyclones is highlighted per degree Celsius of global warming for the NW Pacific. The decreased global tropical cyclone frequency with global warming may be the result of increasing upper-tropospheric stability, while the general intensification of storms is more likely associated with increased levels of tropical CAPE and warmer SSTs offsetting the effects of increased thermodynamic stability. Decreases in ENSO period may also play a role in intensification, mostly in the NW Pacific and Atlantic. These factors may be most pronounced in the NW Pacific, which could be related to the significant increase in the most intense tropical cyclones there.

The South Asian Summer monsoon and heavy precipitation events are also shown to be altered in a warmer climate. With global warming, the zonal wind component of the Summer monsoon significantly weakens and may be attributed to a transition from climatological boundary layer southwesterlies to largely easterlies, reducing moisture transport to South Asia. By contrast, despite this weakening, the results also show an increase in Summer rainfall per degree Celsius of global warming. This enhancement likely arises from more moisture available in a warmer climate, as shown by significant increases in global precipitable water, which may act to suppress the hindering effect of weaker zonal winds and instead increase the intensity of deep convective systems, notably thunderstorms. Increased monsoonal rainfall in a warmer climate may also be due to a steeper land-ocean temperature gradient being more established, and a significant increase in global convective rainfall. These results imply that the increase in global precipitation can be largely related to the increase in atmospheric moisture, which, like the enhancement in South Asian monsoon warm season rainfall, may be related to increased precipitable water, especially in tropical and equatorial regions.

Mid-latitude cyclones were also explored for both the Northern and Southern hemisphere. The findings indicate that annual Northern hemisphere mid-latitude cyclonic events decrease significantly in frequency with global warming, with similar results given for cool season mid-latitude cyclone events. By contrast, the number of intense cool season cyclones is shown to increase. In the Southern hemisphere, the results are also significant for the cool season mid-latitude cyclone frequencies, though the level of significance is less, as compared to the Northern hemisphere. However, the increase in intense cool season cyclonic events is shown to be even more significant than that of the

Northern hemisphere. The decreased tendency represented for global mid-latitude cyclone frequency, especially in the Northern hemisphere, may be related to a decreased equator-pole boundary layer and upper-tropospheric temperature gradient associated with global warming, resulting in reduced baroclinicity. Because the strongest temperature gradient may be found farther poleward, a more active storm track should also become more prominent for those regions. Thus, the significant increase in intense storms found for both hemispheres, especially in the Southern hemisphere, could be more prevalent towards higher latitudes, where temperature gradients are most pronounced. This would imply that heavy snowfall events increase with global warming, but the overall cool season snowfall could decline in equatorward sections of mid-latitudes, owing to a potential poleward shift in cyclonic activity in a warmer climate, including the significant increase in the number of intense cyclones.

Trends in heat waves and drought were also assessed with a changing climate through modifications in soil moisture. This study shows that soil moisture, at least for both Europe and North America, significantly decreases per degree Celsius of global warming, with significant decreases for the European continent, and for North America. The decreases in soil moisture are consistent with decreases in mid-latitude cyclone frequency in the Northern hemisphere, leading to less cool season snowfall coverage for mid-latitudes and more rapid melting (due to an increase in bare ground) that would occur into the late-Winter to Spring period, which subsequently induces faster moisture withdrawal rates at the surface over the course of the warm season. Significant increases in 30 Celsius or more days for Europe also correspond well with soil moisture declines found in this study and may, therefore, be the result of less evaporative cooling. In

addition, the combination of increased convective rainfall (through increased precipitable water) and drier/unsaturated surfaces could yield more incidences of flooding during the warmer seasons.

Global warming is also shown to significantly affect severe thunderstorm and tornado days. The results presented here show that U.S./North American vertical wind shear decreases with global warming, but the number of severe thunderstorm development days significantly increases, in spite of weakened levels of vertical wind shear. The decrease in North American soil moisture also would suggest less energy available for thunderstorm development. The increase in severe thunderstorm development days would, conversely, suggest that a stronger thermodynamic environment (or enhanced atmospheric instability) would compensate for decreases in vertical wind shear, as well as decreases in soil moisture. This indicates that CAPE would increase considerably in magnitude in a warmer climate, which may, in part, be reflected by significant increases in moisture through global precipitable water. That being said, because of decreasing levels of vertical wind shear, or deep-layer shear, this would suggest that mesocyclonic activity is reduced, leading to potentially less tornadic thunderstorms in a warmer climate, or declines with respect to the number of more intense tornadoes. Increases in precipitable water may also play a role in weakening thunderstorm updrafts due to enhanced water loading but increasing the overall strength of the downdraft and flash flooding potential. In a drier environment, which may occur with decreased warm season soil moisture, severe thunderstorms that do form may produce strong downdrafts and damaging hail.

Finally, ENSO was examined in this study in a warming climate to potentially provide more insight as to the changes in extreme weather events. Here, this study shows that ENSO amplitude remains unchanged in a warmer climate, but there is a distinct decrease in the oscillation's period. The decrease in period, along with constant amplitude would suggest more El Nino and La Nina events, with degrees of intensity similar to the present-day climate. Because several extreme weather events, at a global scale, are largely dependent on changes in ENSO, this would imply an increase in the number of extreme events. For example, more El Nino episodes could explain the increase in the number of the most intense NW Pacific cyclones and cyclonic intensification in the NW Pacific basin by weakening vertical shear. Similarly, more La Nina events in a warmer climate could also explain the significant increase in cyclone intensity found for the Atlantic basin. An increase in El Nino may also suggest more drought and heat wave occurrences across Australia and South Asia, though with significant increases in rainfall during the South Asian Summer monsoon found here, this would suggest a weakened ENSO-monsoon relationship with global warming. In parts of North America, an increase in drought and heat waves may also take place with an increase in the number of La Nina events, as well as increases in severe thunderstorm/tornado days for the central-East U.S., especially towards the U.S NE.

The results presented herein imply that global warming could significantly influence all of the selected extreme weather events chosen for this study through a number of important metrics, particularly those that relate to both frequency and intensity. This study, therefore, would suggest that all events examined may be very sensitive to differing levels of global warming, including in smaller amounts, and because

most of the events studied are interconnected, their frequency and intensity could ultimately be affected by subsequent changes in other extreme weather events. This is particularly evident with respect to potential increases in drought and heat waves through decreases in soil moisture, which may lead to considerable losses in the agricultural sector, most notably at mid-latitudes, where precipitation may decrease because of decreases in cyclonic events. The combination of unsaturated soil surfaces and heavy rainfall events could also lead to more localized flooding, including in South Asia, where warm season monsoonal rains are shown to increase in a warmer climate. In another context, consistently significant increases in tropical cyclone intensification with global warming, in spite of either decreased or unchanged cyclone frequency at both a global and regional scale, may lead to more incidences of coastal inundation, as well as enhanced property damage, because of stronger sustained land-falling tropical cyclone surface winds. More severe thunderstorm development days through increased moisture availability could also lead to more costly severe weather seasons for sections of the U.S. in a warmer climate, not just in terms of tornadoes, but also with respect to other hazardous elements that constitute severe thunderstorms, such as hail, damaging winds, or heavy rainfall, during the Spring to early-Summer. Though other important parameters that are conducive to the development of extreme weather are not explicitly taken into account to explain trends, mostly due to limited data availability, the findings provide some representation as to how certain events may change with global warming and, as such, show significant global implications for the future. These effects may further be amplified through changes in ENSO teleconnections, especially in terms of ENSO period. As shown here, the effects of global warming on ENSO behavior is of particular

importance, as ENSO plays a critical role in governing the frequency and severity of extreme weather at a global scale. This study also highlights the significant role of atmospheric moisture in the intensification of multiple weather events, especially with respect to tropical cyclones, mid-latitude cyclones, severe thunderstorms, and tornadoes.

As such, with global temperatures projected to continue rising throughout the 21st century, it is important to consider mitigation measures that would reduce impacts associated with a potentially more extreme future climate, as per the results presented in this study. On the other hand, this work also indirectly demonstrates where more research is needed to be focused, mostly in terms of those weather events or parameters that have a more restrictive availability of data. This is especially true for the events that occur at the microscale level, such as severe thunderstorms and tornadoes, as well as with respect to the meteorological variables that engender them. Enhancing data quality and availability is particularly crucial because of the relatively low predictability associated with tornadic thunderstorms, and other related phenomena. Also, other necessary variables should be accounted for in order to examine certain extreme weather events, as it may very well be that some of these are equally (or even more) significant to their development. More importantly, many uncertainties are also present with respect to ENSO behavior in a warming climate, simply because the fundamental physical processes that drive this phenomenon are not yet understood and are, thus, not fully represented amongst climate models in a completely meaningful way. Understanding ENSO in a warmer climate is, arguably, at the forefront for assessing future trends in extreme weather, as this can significantly improve short- and long-term predictability of these events.

References

Ahrens, D. (2007). *Meteorology Today: An introduction to Weather, Climate, and the Environment* (8th ed). Belmont, CA: Thompson/Brooks/Cole.

An, S., Kug, J., Ham, Y., & Kang, I. (2008). Successive modulation of ENSO to the future greenhouse warming. *Journal of Climate, 21*(1), 3-21. doi: 10.1175/2007JCLI1500.1

Andre, J., Royer, J., & Chauvin, F. (2008). Tropical cyclones and climate change. *Comptes Rendus Geoscience, 340*(9-10), 575-583. doi: 10.1016/j.crte.2008.07.003

Ashrit, R., Douville, H., & Kumar, K. (2003). Response of the Indian monsoon and ENSO-monsoon teleconnection to enhanced greenhouse effect in the CNRM coupled model. *Journal of the Meteorological Society of Japan, 81*(4), 779-803. doi: 10.2151/jmsj.81.779

Ashrit, R., Kumar, K., & Kumar, K. (2001). ENSO-monsoon relationships in a greenhouse warming scenario. *Geophysical Research Letters, 28*(9), 1727-1730. doi: 10.1029/2000GL012489

Attinger, G. (2012). Soil responsible for heat waves. http://www.ethlife.ethz.ch/archive_articles/101213_hitzewellen_paper_ga/index_EN Retrieved on February 3rd, 2013.

Beersma, J., Rider, K., Komen, G., Kaas, E., & Kharin, V. (1997). An analysis of extra-tropical storms in the north atlantic region as simulated in a control and 2xCO(2) time-slice experiment with a high-resolution atmospheric model. *Tellus Series A-Dynamic Meteorology and Oceanography, 49*(3), 347-361. doi: 10.1034/j.1600-0870.1997.t01-2-00003.x

Bender, M. A., Knutson, T. R., Tuleya, R. E., Sirutis, J. J., Vecchi, G. A., Garner, S. T., & Held, I. M. (2010). Modeled impact of anthropogenic warming on the frequency of intense atlantic hurricanes. *Science, 327*(5964), 454-458. doi: 10.1126/science.1180568

Bengtsson, L., Botzet, M., & Esch, M. (1996). Will greenhouse gas-induced warming over the next 50 years lead to higher frequency and greater intensity of hurricanes? *Tellus Series A-Dynamic Meteorology and Oceanography, 48*(1), 57-73. doi: 10.1034/j.1600-0870.1996.00004.x

Bengtsson, L., Hodges, K. I., Esch, M., Keenlyside, N., Kornblueh, L., Luo, J., & Yamagata, T. (2007). How may tropical cyclones change in a warmer climate? *Tellus Series A-Dynamic Meteorology and Oceanography, 59*(4), 539-561. doi: 10.1111/j.1600-0870.2007.00251.x

Bengtsson, L., Hodges, K. I., & Keenlyside, N. (2009). Will extratropical storms intensify in a warmer climate? *Journal of Climate, 22*(9), 2276-2301. doi: 10.1175/2008JCLI2678.1

Bengtsson, L., Hodges, K. I., & Roeckner, E. (2006). Storm tracks and climate change. *Journal of Climate, 19*(15), 3518-3543. doi: 10.1175/JCLI3815.1

Beniston, M. (2004). The 2003 heat wave in Europe: A shape of things to come? an analysis based on swiss climatological data and model simulations. *Geophysical Research Letters, 31*(2), L02202. doi: 10.1029/2003GL018857

Beniston, M., & Diaz, H. (2004). The 2003 heat wave as an example of summers in a greenhouse climate? observations and climate model simulations for basel, switzerland. *Global and Planetary Change, 44*(1-4), 73-81. doi: 10.1016/j.gloplacha.2004.06.006

Beniston, M., & Goyette, S. (2007). Changes in variability and persistence of climate in switzerland: Exploring 20th century observations and 21st century simulations. *Global and Planetary Change, 57*(1-2), 1-15. doi: 10.1016/j.gloplacha.2006.11.004

Beven, J. et al. (2008). "Atlantic Hurricane Season of 2005". *Monthly Weather Review, 136* (2), p.1109-1173.

Bhaskaran, B., Mitchell, J., Lavery, J., & Lal, M. (1995). Climatic response of the Indian subcontinent to doubled Co2 concentrations. *International Journal of Climatology, 15*(8), 873-892. doi: 10.1002/joc.3370150804

Boer, G. (1993). Climate change and the regulation of the surface moisture and energy budgets. *Climate Dynamics, 8*(5), 225-239.

Boer, G., Flato, G., & Ramsden, D. (2000). A transient climate change simulation with greenhouse gas and aerosol forcing: Projected climate to the twenty-first century. *Climate Dynamics, 16*(6), 427-450. doi: 10.1007/s003820050338

Boer, G., Flato, G., Reader, M., & Ramsden, D. (2000). A transient climate change simulation with greenhouse gas and aerosol forcing: Experimental design and comparison with the instrumental record for the twentieth century. *Climate Dynamics, 16*(6), 405-425. doi: 10.1007/s003820050337

Boer, G., McFarlane, N., & Lazare, M. (1992). Greenhouse gas induced climate change simulated with the ccc 2nd-generation general-circulation model. *Journal of Climate, 5*(10), 1045-1077. doi: 10.1175/1520-0442(1992)005<1045:GGCCSW>2.0.CO;2

Bosilovich, M., Schubert, S., & Walker, G. (2005). Global changes of the water cycle intensity. *Journal of Climate, 18*(10), 1591-1608. doi: 10.1175/JCLI3357.1

Carnell, R., & Senior, C. (1998). Changes in mid latitude variability due to increasing greenhouse gases and sulphate aerosols. *Climate Dynamics, 14*(5), 369-383. doi: 10.1007/s003820050229

Catto, J. L., Shaffrey, L. C., & Hodges, K. I. (2011). Northern hemisphere extratropical cyclones in a warming climate in the HiGEM high-resolution climate model. *Journal of Climate, 24*(20), 5336-5352. doi: 10.1175/2011JCLI4181.1

Cheetham, A. (2011). Climatic Events – Hurricanes. *Global Warming Science.* http://www.appinsys.com/GlobalWarming/GW_4CE_Hurricanes.htm

Chen, H. et al, (2004). Regional Climate Change in East Asia Simulated by an Interactive-Soil-Vegetation Model. *Journal of Climate, 17*(3). p. 557-572.

Chen, X., Kimoto, M., & Takahashi, M. (2005). Changes in ENSO in response to greenhouse warming as simulated by the CCSR/NIES/FRCGC coupled GCM. *Sola, 1*, 149-152. doi: 10.2151/sola.2005-039

Climate Research Unit. (2013). Temperature. http://www.cru.uea.ac.uk/cru/data/temperature/#faq4 Retrieved on June 8th, 2012.

Collins, M. (2000). The El Nino-Southern Oscillation in the second Hadley Centre coupled model and its response to greenhouse warming. *Journal of Climate, 13*(7), 1299-1312. doi: 10.1175/1520-0442(2000)013<1299:TENOSO>2.0.CO;2

Collins, M. (2000). Understanding uncertainties in the response of ENSO to greenhouse warming. *Geophysical Research Letters, 27*(21), 3509-3512. doi: 10.1029/2000GL011747

Collins, M., et al. (2010). The impact of global warming on the tropical Pacific Ocean and El Nino. *Nature Geoscience, 3.* p. 391-397.

Crombie, L. & Davies, H. (2009). What is Meta-Analysis? http://www.medicine.ox.ac.uk/bandolier/painres/download/whatis/Meta-An.pdf

Dai, A., Meehl, G., Washington, W., & Wigley, T. (2001). Climate changes in the 21st century over the Asia-Pacific region simulated by the NCAR CSM and PCM. *Advances in Atmospheric Sciences, 18*(5), 639-658.

Dai, A., Washington, W., Meehl, G., Bettge, T., & Strand, W. (2004). The ACPI climate change simulations. *Climatic Change, 62*(1-3), 29-43. doi: 10.1023/B:CLIM.0000013679.74883.e6

Dai, A., Wigley, T., Boville, B., Kiehl, J., & Buja, L. (2001). Climates of the twentieth and twenty-first centuries simulated by the NCAR climate system model. *Journal of Climate,*

Dai, A., Wigley, T., Meehl, G., & Washington, W. (2001). Effects of stabilizing atmospheric CO2 on global climate in the next two centuries. *Geophysical Research Letters, 28*(23), 4511-4514. doi: 10.1029/2001GL013359 *14*(4), 485-519. doi: 10.1175/1520-0442(2001)014<0485:COTTAT>2.0.CO;2

Dai, A. (2011). Characteristics and trends in various forms of the palmer drought severity index during 1900-2008. *Journal of Geophysical Research-Atmospheres, 116*, D12115. doi: 10.1029/2010JD015541

Dai, A. (2013). Increasing drought under global warming in observations and models. *Nature Climate Change, 3*(1), 52-58. doi: 10.1038/NCLIMATE1633

Dairaku, K., & Emori, S. (2006). Dynamic and thermodynamic influences on intensified daily rainfall during the asian summer monsoon under doubled atmospheric CO2 conditions. *Geophysical Research Letters, 33*(1), L01704. doi: 10.1029/2005GL024754

Davis, S. & Walsh, K.J.E. (2008). Southeast Australian thunderstorms: are they increasing in frequency? *Australian Meteorological Magazine, 57.* p. 1-11.

Del Genio, A. D., Yao, M., & Jonas, J. (2007). Will moist convection be stronger in a warmer climate? *Geophysical Research Letters, 34*(16), L16703. doi: 10.1029/2007GL030525

Diffenbaugh, N., Pal, J., Trapp, R., & Giorgi, F. (2005). Fine-scale processes regulate the response of extreme events to global climate change. *Proceedings of the National Academy of Sciences of the United States of America, 102*(44), 15774-15778. doi: 10.1073/pnas.0506042102

Diffenbaugh et al. (2008). Does Global Warming Influence Tornado Activity? *American Geophysical Union, 89*(53), 553-554. DOI: 10.1029/2008EO530001

Easterling, D. et al. (2000). Observed Variability and Trends in Extreme Climate Events: A Brief Review. *Bulletin of the American Meteorological Society.* p. 417-425.

Emanuel, K. (2011). Global warming effects on US hurricane damage. *Weather Climate and Society, 3*(4), 261-268. doi: 10.1175/WCAS-D-11-00007.1

EPA (2013). Climate Change Indicators in the United States: High and Low Temperatures. http://www.epa.gov/climatechange/science/indicators/weather-climate/high-low-temps.html Retrieved on August 3rd, 2013

Emanuel, K. (2013). Downscaling CMIP5 climate models shows increased tropical cyclone activity over the 21st century. *PNAS.* www.pnas.org/cgi/doi/10.1073/pnas.1301293110

Fischer, E. M., & Schaer, C. (2009). Future changes in daily summer temperature variability: Driving processes and role for temperature extremes. *Climate Dynamics, 33*(7-8), 917-935. doi: 10.1007/s00382-008-0473-8

Finnis, J., Holland, M. M., Serreze, M. C., & Cassano, J. J. (2007). Response of northern hemisphere extratropical cyclone activity and associated precipitation to climate change, as represented by the community climate system model. *Journal of Geophysical Research-Biogeosciences, 112*(G4), G04S42. doi: 10.1029/2006JG000286

Fosberg, M. et al. (1990) Global change: effects on forest ecosystems and wildfire severity. Page 463-486 in J.G. Goldammer, ed. Fire in the Tropical Biota: Ecosystem Processes and Global Challenges.

Frierson, D. M. W. (2006). Robust increases in midlatitude static stability in simulations of global warming. *Geophysical Research Letters, 33*(24), L24816. doi: 10.1029/2006GL027504

Fyfe, J. (2003). Extratropical southern hemisphere cyclones: Harbingers of climate change? *Journal of Climate, 16*(17), 2802-2805. doi: 10.1175/1520-0442(2003)016<2802:ESHCHO>2.0.CO;2

Geng, Q., & Sugi, M. (2003). Possible change of extratropical cyclone activity due to enhanced greenhouse gases and sulfate aerosols - study with a high-resolution AGCM. *Journal of Climate, 16*(13), 2262-2274. doi: 10.1175/1520-0442(2003)16<2262:PCOECA>2.0.CO;2

Goklany, I. (2009). Deaths and Death Rates from Extreme Weather Events: 1900-2008. *Journal of American Physicians and Surgeons, 14*(4). p. 102-109.

Gordon, H., Whetton, P., Pittock, A., Fowler, A., & Haylock, M. (1992). Simulated changes in daily rainfall intensity due to the enhanced greenhouse-effect - implications for extreme rainfall events. *Climate Dynamics, 8*(2), 83-102.

Gregory, J., Mitchell, J., & Brady, A. (1997). Summer drought in northern midlatitudes in a time-dependent CO2 climate experiment. *Journal of Climate, 10*(4), 662-686. doi: 10.1175/1520-0442(1997)010<0662:SDINMI>2.0.CO;2

Gualdi, S., Scoccimarro, E., & Navarra, A. (2008). Changes in tropical cyclone activity due to global warming: Results from a high-resolution coupled general circulation model. *Journal of Climate, 21*(20), 5204-5228. doi: 10.1175/2008JCLI1921.1

Haarsma, R., Mitchell, J., & Senior, C. (1993). Tropical disturbances in a gcm. *Climate Dynamics, 8*(5), 247-257.

Hart, T., Bourke, W., McAvaney, B., Forgan, B., & McGregor, J. (1990). Atmospheric general-circulation simulations with the bmrc global spectral model - the impact of revised physical parameterizations. *Journal of Climate, 3*(4), 436-459. doi: 10.1175/1520-0442(1990)003<0436:AGCSWT>2.0.CO;2

Held & Soden. (2000). Water Vapor Feedback And Global Warming. *Annual Review of Energy and the Environment, 25.* p. 441-475.

Held, I. M., & Soden, B. J. (2006). Robust responses of the hydrological cycle to global warming. *Journal of Climate, 19*(21), 5686-5699. doi: 10.1175/JCLI3990.1

Held, I. M., & Zhao, M. (2011). The response of tropical cyclone statistics to an increase in CO2 with fixed sea surface temperatures. *Journal of Climate, 24*(20), 5353-5364. doi: 10.1175/JCLI-D-11-00050.1

Henderson-Sellers, A., Dickinson, R., Durbidge, T., Kennedy, P., McGuffie, K., & Pitman, A. (1993). Tropical deforestation - modeling local-scale to regional-scale climate change. *Journal of Geophysical Research-Atmospheres, 98*(D4), 7289-7315. doi: 10.1029/92JD02830

Hennessy, K., Gregory, J., & Mitchell, J. (1997). Changes in daily precipitation under enhanced greenhouse conditions. *Climate Dynamics, 13*(9), 667-680. doi: 10.1007/s003820050189

Holloway, C. E., & Neelin, J. D. (2009). Moisture vertical structure, column water vapor, and tropical deep convection. *Journal of the Atmospheric Sciences, 66*(6), 1665-1683. doi: 10.1175/2008JAS2806.1

Houghton, JT, et al. (1990) *Climate change: the IPCC scientific assessment*. Cambridge, UK: Cambridge University Press.

Hu, Z., Latif, M., Roeckner, E., & Bengtsson, L. (2000). Intensified Asian summer monsoon and its variability in a coupled model forced by increasing greenhouse gas concentrations. *Geophysical Research Letters, 27*(17), 2681-2684. doi: 10.1029/2000GL011550

Huth, R., Kysely, J., & Pokorna, L. (2000). A GCM simulation of heat waves, dry spells, and their relationships to circulation. *Climatic Change, 46*(1-2), 29-60. doi: 10.1023/A:1005633925903

Jiang, J. & Perrie, W. (2007). The Impacts of Climate Change on Autumn North Atlantic Midlatitude Cyclones. *Journal of Climate. 20*. p. 1174-1187.

Johns, T., et al. (2003). Anthropogenic climate change for 1860 to 2100 simulated with the HadCM3 model under updated emissions scenarios. *Climate Dynamics, 20*(6), 583-612. doi: 10.1007/s00382-002-0296-y

Kharin, V., & Zwiers, F. (2000). Changes in the extremes in an ensemble of transient climate simulations with a coupled atmosphere-ocean GCM. *Journal of Climate, 13*(21), 3760-3788. doi: 10.1175/1520-0442(2000)013<3760:CITEIA>2.0.CO;2

Knutson, T.R., et al. (2010). Tropical cyclones and climate change. *Nature Geoscience, 3*(3), 157-163. doi: 10.1038/NGEO779

Knutson, T.R., Sirutis, J. J., Garner, S. T., Vecchi, G. A., & Held, I. M. (2008). Simulated reduction in Atlantic hurricane frequency under twenty-first-century warming conditions. *Nature Geoscience, 1*(6), 359-364. doi: 10.1038/ngeo202

Knutson, T.R., & Manabe, S. (1994). Impact of increased CO2 on simulated ENSO-like phenomena. *Geophysical Research Letters, 21*(21), 2295-2298. doi: 10.1029/94GL02152

Knutson, T.R., Manabe, S., & Gu, D. (1997). Simulated ENSO in a global coupled ocean-atmosphere model: Multidecadal amplitude modulation and CO2 sensitivity. *Journal of Climate, 10*(1), 138-161. doi: 10.1175/1520-0442(1997)010<0138:SEIAGC>2.0.CO;2

Knutson, T.R., & Tuleya, R. (1999). Increased hurricane intensities with CO2-induced warming as simulated using the GFDL hurricane prediction system. *Climate Dynamics, 15*(7), 503-519. doi: 10.1007/s003820050296

Knutson, T. R., & Tuleya, R. (2004). Impact of CO2-induced warming on simulated hurricane intensity and precipitation: Sensitivity to the choice of climate model and convective parameterization. *Journal of Climate, 17*(18), 3477-3495. doi: 10.1175/1520-0442(2004)017<3477:IOCWOS>2.0.CO;2

Knutson, T.R., Tuleya, R., & Kurihara, Y. (1998). Simulated increase of hurricane intensities in a CO2-warmed climate. *Science, 279*(5353), 1018-1020. doi: 10.1126/science.279.5353.1018

Knutson, T.R., Tuleya, R., Shen, W., & Ginis, I. (2001). Impact of CO2-induced warming on hurricane intensities as simulated in a hurricane model with ocean coupling. *Journal of Climate, 14*(11), 2458-2468. doi: 10.1175/1520-0442(2001)014<2458:IOCIWO>2.0.CO;2

Konig, W., Sausen, R., & Seilmann, F. (1993). Objective identification of cyclones in gcm simulations. *Journal of Climate, 6*(12), 2217-2231. doi: 10.1175/1520-0442(1993)006<2217:OIOCIG>2.0.CO;2

Kripalani, R. H., Oh, J. H., Kulkarni, A., Sabade, S. S., & Chaudhari, H. S. (2007). South Asian summer monsoon precipitation variability: Coupled climate model simulations and projections under IPCC AR4. *Theoretical and Applied Climatology, 90*(3-4), 133-159. doi: 10.1007/s00704-006-0282-0

Kug, J., Jin, F., Sooraj, K. P., & Kang, I. (2008). State-dependent atmospheric noise associated with ENSO. *Geophysical Research Letters, 35*(5), L05701. doi: 10.1029/2007GL032017

Kumar, S., Merwade, V., Kinter,James L.,,III, & Niyogi, D. (2013). Evaluation of temperature and precipitation trends and long-term persistence in CMIP5 twentieth-century climate simulations. *Journal of Climate, 26*(12), 4168-4185. doi: 10.1175/JCLI-D-12-00259.1

Lal, M., Meehl, G. A., & Arblaster, J. M. (2000). Simulation of Indian summer monsoon rainfall and its intraseasonal variability in the NCAR climate system model. *Regional Environmental Change, 1*(3-4), 163-179. doi: 10.1007/s101130000017

Lal, M., et al. (2001). Future climate change: Implications for Indian summer monsoon and its variability. *Current Science, 81*(9), 1196-1207.

Lal, M., Whetton, P., Pittock, A., & Chakraborty, B. (1998). The greenhouse gas-induced climate change over the Indian subcontinent as projected by general circulation model experiments. *Terrestrial Atmospheric and Oceanic Sciences, 9*(4), 673-690.

Lambert, S. (1995). The effect of enhanced greenhouse warming on winter cyclone frequencies and strengths. *Journal of Climate, 8*(5), 1447-1452. doi: 10.1175/1520-0442(1995)008<1447:TEOEGW>2.0.CO;2

Lambert, S. (2004). Changes in winter cyclone frequencies and strengths in transient enhanced greenhouse warming simulations using two coupled climate models. *Atmosphere-Ocean, 42*(3), 173-181. doi: 10.3137/ao.420302

Lambert, S., & Fyfe, J. (2006). Changes in winter cyclone frequencies and strengths simulated in enhanced greenhouse warming experiments: Results from the models participating in the IPCC diagnostic exercise. *Climate Dynamics, 26*(7-8), 713-728. doi: 10.1007/s00382-006-0110-3

Lau, N., & Nath, M. J. (2012). A model study of heat waves over North America: Meteorological aspects and projections for the twenty-first century. *Journal of Climate, 25*(14), 4761-4784. doi: 10.1175/JCLI-D-11-00575.1

Lau, W. K. -., Wu, H. -., & Kim, K. -. (2013). A canonical response of precipitation characteristics to global warming from CMIP5 models. *Geophysical Research Letters, 40*(12), 3163-3169. doi: 10.1002/grl.50420

Lee, C. C. (2012). Utilizing synoptic climatological methods to assess the impacts of climate change on future tornado-favorable environments. *Natural Hazards, 62*(2), 325-343. doi: 10.1007/s11069-011-9998-y

Lenderink, G., & Van Meijgaard, E. (2008). Increase in hourly precipitation extremes beyond expectations from temperature changes. *Nature Geoscience, 1*(8), 511-514. doi: 10.1038/ngeo262

Li, J., et al. (2011). Interdecadal modulation of El Nino amplitude during the past millenium. *Nature Climate Change, 1*. p. 114-118.

Li, T., Kwon, M., Zhao, M., Kug, J., Luo, J., & Yu, W. (2010). Global warming shifts pacific tropical cyclone location. *Geophysical Research Letters, 37*, L21804. doi: 10.1029/2010GL045124

Lin, N., Emanuel, K., Oppenheimer, M., & Vanmarcke, E. (2012). Physically based assessment of hurricane surge threat under climate change. *Nature Climate Change, 2*(6), 462-467. doi: 10.1038/NCLIMATE1389

Lorenz, D. J., & DeWeaver, E. T. (2007). The response of the extratropical hydrological cycle to global warming. *Journal of Climate, 20*(14), 3470-3484. doi: 10.1175/JCLI4192.1

Marzban, C., & Schaefer, J. (2001). The correlation between US tornadoes and pacific sea surface temperatures. *Monthly Weather Review, 129*(4), 884-895. doi: 10.1175/1520-0493(2001)129<0884:TCBUST>2.0.CO;2

May, W. (2002). Simulated changes of the Indian summer monsoon under enhanced greenhouse gas conditions in a global time-slice experiment. *Geophysical Research Letters, 29*(7), 1118. doi: 10.1029/2001GL013808

May, W. (2004). Potential future changes in the indian summer monsoon due to greenhouse warming: Analysis of mechanisms in a global time-slice experiment. *Climate Dynamics, 22*(4), 389-414. doi: 10.1007/s00382-003-0389-2

May, W. (2011). The sensitivity of the Indian summer monsoon to a global warming of 2A degrees C with respect to pre-industrial times. *Climate Dynamics, 37*(9-10), 1843-1868. doi: 10.1007/s00382-010-0942-8

McDonald, R., Bleaken, D., Cresswell, D., Pope, V., & Senior, C. (2005). Tropical storms: Representation and diagnosis in climate models and the impacts of climate change. *Climate Dynamics, 25*(1), 19-36. doi: 10.1007/s00382-004-0491-0

McNeill, A. (2012). Annual Disaster/Death Statistics for US Storms. *Wind Science and Engineering Research Center, Texas Tech University.* http://www.depts.ttu.edu/weweb/Research/DebrisImpact/Reports/DDS.pdf

Meehl, G., & Arblaster, J. (2003). Mechanisms for projected future changes in south asian monsoon precipitation. *Climate Dynamics, 21*(7-8), 659-675. doi: 10.1007/s00382-003-0343-3

Meehl, G., Collins, W., Boville, B., Kiehl, J., Wigley, T., & Arblaster, J. (2000). Response of the NCAR climate system model to increased CO2 and the role of physical processes. *Journal of Climate, 13*(11), 1879-1898. doi: 10.1175/1520-0442(2000)013<1879:ROTNCS>2.0.CO;2

Meehl, G., & Tebaldi, C. (2004). More intense, more frequent, and longer lasting heat waves in the 21st century. *Science, 305*(5686), 994-997. doi: 10.1126/science.1098704

Meehl, G., Teng, H., & Branstator, G. (2006). Future changes of El Nino in two global coupled climate models. *Climate Dynamics, 26*(6), 549-566. doi: 10.1007/s00382-005-0098-0

Meehl, G., & Washington, W. (1993). South Asian summer monsoon variability in a model with doubled atmospheric carbon-dioxide concentration. *Science, 260*(5111), 1101-1104. doi: 10.1126/science.260.5111.1101

Meehl, G., Washington, W., Arblaster, J., Bettge, T., & Strand, W. (2000). Anthropogenic forcing and decadal climate variability in sensitivity experiments of twentieth- and twenty-first-century climate. *Journal of Climate, 13*(21), 3728-3744. doi: 10.1175/1520-0442(2000)013<3728:AFADCV>2.0.CO;2

Mendelsohn, R., Emanuel, K., Chonabayashi, S., & Bakkensen, L. (2012). The impact of climate change on global tropical cyclone damage. *Nature Climate Change, 2*(3), 205-209. doi: 10.1038/NCLIMATE1357

Merryfield, W. J. (2006). Changes to ENSO under CO2 doubling in a multimodel ensemble. *Journal of Climate, 19*(16), 4009-4027. doi: 10.1175/JCLI3834.1

Michalon, N. et al. (1999). Contribution to the climatological study of lightning. *American Geophysical Union, 26*(20). p. 3097-3100.

Min, S-K., et al. (2011). Human contribution to more-intense precipitation extremes. *Nature, 470*(7334). p. 378–381.

Mitchell, J., & Ingram, W. (1992). Carbon-dioxide and climate - mechanisms of changes in cloud. *Journal of Climate, 5*(1), 5-21. doi: 10.1175/1520-0442(1992)005<0005:CDACMO>2.0.CO;2

Mizuta, R., Matsueda, M., Endo, H., & Yukimoto, S. (2011). Future change in extratropical cyclones associated with change in the upper troposphere. *Journal of Climate, 24*(24), 6456-6470. doi: 10.1175/2011JCLI3969.1

Mueller, B., & Seneviratne, S. I. (2012). Hot days induced by precipitation deficits at the global scale. *Proceedings of the National Academy of Sciences of the United States of America, 109*(31), 12398-12403. doi: 10.1073/pnas.1204330109

Murakami, H., Mizuta, R., & Shindo, E. (2012). Future changes in tropical cyclone activity projected by multi-physics and multi-SST ensemble experiments using the 60-km-mesh MRI-AGCM. *Climate Dynamics, 39*(9-10), 2569-2584. doi: 10.1007/s00382-011-1223-x

Murakami, H., & Wang, B. (2010). Future change of north Atlantic tropical cyclone tracks: Projection by a 20-km-mesh global atmospheric model. *Journal of Climate, 23*(10), 2699-2721. doi: 10.1175/2010JCLI3338.1

Murakami, H., Wang, B., & Kitoh, A. (2011). Future change of western north pacific typhoons: Projections by a 20-km-mesh global atmospheric model. *Journal of Climate, 24*(4), 1154-1169. doi: 10.1175/2010JCLI3723.1

Murakami, H., et al. (2012). Future changes in tropical cyclone activity projected by the new high-resolution MRI-AGCM. *Journal of Climate, 25*(9), 3237-3260. doi: 10.1175/JCLI-D-11-00415.1

NOAA (2012). Tropical cyclone climatology. http://www.nhc.noaa.gov/climo/ Retrieved on February 16th, 2013.

NOAA (2013). Monthly and annual tornado summaries. http://www.spc.noaa.gov/climo/online/monthly/newm.html Retrieved on April 2nd, 2013.

NOAA (2013). U.S. Tornado Climatology. http://www.ncdc.noaa.gov/oa/climate/severeweather/tornadoes.html Retrieved on July 28th, 2013.

National Research Council. (2011). *Climate Stabilization Targets: Emissions, Concentrations, and Impacts over Decades to Millennia (2011)*. Washington, DC: The National Academies Press, 2011.

Noda, A., Kusunoki, S., Yoshimura, J., Yoshimura, H., Oouchi, K., & Mizuta, R. (2008). In Hamilton K. O.,W. (Ed.), *Global warming projection by an atmospheric general circulation model with a 20-km grid* doi: 10.1007/978-0-387-49791-4_7

Oglesby, R., & Saltzman, B. (1992). Equilibrium climate statistics of a general-circulation model as a function of atmospheric carbon-dioxide .1. geographic distributions of primary variables. *Journal of Climate, 5*(1), 66-92.

O'Gorman, P. A., & Muller, C. J. (2010). How closely do changes in surface and column water vapor follow clausius-clapeyron scaling in climate change simulations? *Environmental Research Letters, 5*(2), 025207. doi: 10.1088/1748-9326/5/2/025207

Oouchi, K., Yoshimura, J., Yoshimura, H., Mizuta, R., Kusunoki, S., & Noda, A. (2006). Tropical cyclone climatology in a global-warming climate as simulated in a 20 km-mesh global atmospheric model: Frequency and wind intensity analyses. *Journal of the Meteorological Society of Japan, 84*(2), 259-276. doi: 10.2151/jmsj.84.259

Peppler, R. (1988). A review of static stability and related thermodynamic parameters. http://www.isws.illinois.edu/pubdoc/MP/ISWSMP-104.pdf Retrieved on February 17th, 2013.

Pinto, J. G., Ulbrich, U., Leckebusch, G. C., Spangehl, T., Reyers, M., & Zacharias, S. (2007). Changes in storm track and cyclone activity in three SRES ensemble experiments with the ECHAM5/MPI-OM1 GCM. *Climate Dynamics, 29*(2-3), 195-210. doi: 10.1007/s00382-007-0230-4

Price, C. (2009). Will a drier climate result in more lightning? *Atmospheric Research, 91*(2-4). p. 479-484.

Radermacher, C., & Tomassini, L. (2012). Thermodynamic causes for future trends in heavy precipitation over europe based on an ensemble of regional climate model simulations. *Journal of Climate, 25*(21), 7669-7689. doi: 10.1175/JCLI-D-11-00304.1

Raisanen, J. (2002). CO2-induced changes in interannual temperature and precipitation variability in 19 CMIP2 experiments. *Journal of Climate, 15*(17), 2395-2411. doi: 10.1175/1520-0442(2002)015<2395:CICIIT>2.0.CO;2

Reed, R. (1988). Advances in knowledge and understanding of extratropical cyclones during the past quarter century - an overview. *Palmen Memorial Symposium on Extratropical Cyclones,* 6-9.

Rice, D. (2011). USA Slammed by 12 disasters that each cost at least &1B. *USA Today.* http://www.usatoday.com/weather/news/story/2011-12-07/billion-dollardisasters/51704362/1

Rind, D., Goldberg, R., Hansen, J., Rosenzweig, C., & Ruedy, R. (1990). Potential evapotranspiration and the likelihood of future drought. *Journal of Geophysical Research-Atmospheres, 95*(D7), 9983-10004. doi: 10.1029/JD095iD07p09983

Rind, D. (1998). Just Add Water Vapor. *Science, 281*(5380). p.1152-1153.

Royer, J., & Chauvin, F. (2009). In Elsner J. J.,TH (Ed.), *Response of tropical cyclogenesis to global warming in an IPCC AR4 scenario*

Sabade, S. S., Kulkarni, A., & Kripalani, R. H. (2011). Projected changes in South Asian summer monsoon by multi-model global warming experiments. *Theoretical and Applied Climatology, 103*(3-4), 543-565. doi: 10.1007/s00704-010-0296-5

Saunders, M. A., Chandler, R. E., Merchant, C. J., & Roberts, F. P. (2000). Atlantic hurricanes and NW pacific typhoons: ENSO spatial impacts on occurrence and landfall. *Geophysical Research Letters, 27*(8), 1147-1150. doi: 10.1029/1999GL010948

Schar, C., Vidale, P., Luthi, D., Frei, C., Haberli, C., Liniger, M., & Appenzeller, C. (2004). The role of increasing temperature variability in European summer heatwaves. *Nature, 427*(6972), 332-336. doi: 10.1038/nature02300

Semenov, V., & Bengtsson, L. (2002). Secular trends in daily precipitation characteristics: Greenhouse gas simulation with a coupled AOGCM. *Climate Dynamics, 19*(2), 123-140. doi: 10.1007/s00382-001-0218-4

Sheffield, J., & Wood, E. F. (2008). Projected changes in drought occurrence under future global warming from multi-model, multi-scenario, IPCC AR4 simulations. *Climate Dynamics, 31*(1), 79-105. doi: 10.1007/s00382-007-0340-z

Sinclair, M., & Watterson, I. (1999). Objective assessment of extratropical weather systems in simulated climates. *Journal of Climate, 12*(12), 3467-3485. doi: 10.1175/1520-0442(1999)012<3467:OAOEWS>2.0.CO;2

Statistical Solutions. (2011). What is Meta Analysis? http://www.statistical-solutionssoftware.com/what-is-meta-analysis/

Stowasser, M., Annamalai, H., & Hafner, J. (2009). Response of the south asian summer monsoon to global warming: Mean and synoptic systems. *Journal of Climate, 22*(4), 1014-1036. doi: 10.1175/2008JCLI2218.1

Stowasser, M., Wang, Y., & Hamilton, K. (2007). Tropical cyclone changes in the western north pacific in a global warming scenario. *Journal of Climate, 20*(11), 2378-2396. doi: 10.1175/JCLI4126.1

Sugi, M., Noda, A., & Sato, N. (2002). Influence of the global warming on tropical cyclone climatology: An experiment with the JMA global model. *Journal of the Meteorological Society of Japan, 80*(2), 249-272. doi: 10.2151/jmsj.80.249

Sugi, M., Murakami, H., & Yoshimura, J. (2009). A reduction in global tropical cyclone frequency due to global warming. *Sola, 5*, 164-167. doi: 10.2151/sola.2009-042

Sugi, M., Murakami, H., & Yoshimura, J. (2012). On the mechanism of tropical cyclone frequency changes due to global warming. *Journal of the Meteorological Society of Japan, 90A*, 397-408. doi: 10.2151/jmsj.2012-A24

Sugi, M., & Yoshimura, J. (2012). Decreasing trend of tropical cyclone frequency in 228-year high-resolution AGCM simulations. *Geophysical Research Letters, 39*, L19805. doi: 10.1029/2012GL053360

Tebaldi, C. (2011). *Climate Stabilization Targets: Emissions, Concentrations, and Impacts over Decades to Millennia (2011)***.** Washington, DC: The National Academies Press, 2011.

Tett, S. (1995). Simulation of el nino-southern oscillation-like variability in a global AOGCM and its response to C)2 increase. *Journal of Climate, 8*(6), 1473-1502. doi: 10.1175/1520-0442(1995)008<1473:SOENSO>2.0.CO;2

Thompson, S., & Pollard, D. (1995). A global climate model (genesis) with a land-surface transfer scheme (lsx) .2. Co2 sensitivity. *Journal of Climate, 8*(5), 1104-1121. doi: 10.1175/1520-0442(1995)008<1104:AGCMWA>2.0.CO;2

Timmermann, A., Jin, F., & Collins, M. (2004). Intensification of the annual cycle in the tropical pacific due to greenhouse warming. *Geophysical Research Letters, 31*(12), L12208. doi: 10.1029/2004GL019442

Timmermann, A., Oberhuber, J., Bacher, A., Esch, M., Latif, M., & Roeckner, E. (1999). Increased el nino frequency in a climate model forced by future greenhouse warming. *Nature, 398*(6729), 694-697.

Trapp, R. J., Diffenbaugh, N. S., Brooks, H. E., Baldwin, M. E., Robinson, E. D., & Pal, J. S. (2007). Changes in severe thunderstorm environment frequency during the 21st century caused by anthropogenically enhanced global radiative forcing. *Proceedings of the National Academy of Sciences of the United States of America, 104*(50), 19719-19723. doi: 10.1073/pnas.0705494104

Trapp, R. J., Diffenbaugh, N. S., & Gluhovsky, A. (2009). Transient response of severe thunderstorm forcing to elevated greenhouse gas concentrations. *Geophysical Research Letters, 36*(1), L01703. doi: 10.1029/2008GL036203

Trenberth, K. (1998). Atmospheric moisture residence times and cycling: Implications for rainfall rates and climate change. *Climatic Change, 39*(4), 667-694. doi: 10.1023/A:1005319109110

Trenberth, K., Fasullo, J., & Smith, L. (2005). Trends and variability in column-integrated atmospheric water vapor. *Climate Dynamics, 24*(7-8), 741-758. doi: 10.1007/s00382-005-0017-4

Trenberth, K. E. (2012). Framing the way to relate climate extremes to climate change. *Climatic Change, 115*(2), 283-290. doi: 10.1007/s10584-012-0441-5

Tsutsui, J. (2002). Implications of anthropogenic climate change for tropical cyclone activity: A case study with the NCAR CCM2. *Journal of the Meteorological Society of Japan, 80*(1), 45-65. doi: 10.2151/jmsj.80.45

Ueda, H., Iwai, A., Kuwako, K., & Hori, M. (2006). Impact of anthropogenic forcing on the asian summer monsoon as simulated by eight GCMs. *Geophysical Research Letters, 33*(6), L06703. doi: 10.1029/2005GL025336

Van Klooster, S. L., & Roebber, P. J. (2009). Surface-based convective potential in the contiguous united states in a business-as-usual future climate. *Journal of Climate, 22*(12), 3317-3330. doi: 10.1175/2009JCLI2697.1

Vecchi, G., Soden, B., Wittenberg, A., Held, I., Leetmaa, A., & Harrison, M. (2006). Weakening of tropical pacific atmospheric circulation due to anthropogenic forcing. *Nature, 441*(7089), 73-76. doi: 10.1038/nature04744

Vecchi, G. A., & Soden, B. J. (2007). Global warming and the weakening of the tropical circulation. *Journal of Climate, 20*(17), 4316-4340. doi: 10.1175/JCLI4258.1

Vecchi, G. A., & Soden, B. J. (2007). Increased tropical Atlantic wind shear in model projections of global warming. *Geophysical Research Letters, 34*(8), L08702. doi: 10.1029/2006GL028905

Vellinga, P. V. et al. (2001). Insurance and Other Financial Services: Chapter 8 in *Climate Change 2001:* Impacts, Vulnerability, and Adaptation. Geneva: Intergovernmental Panel on Climate Change, Geneva: *United Nations and World Meteorological Organization.*

Wang, C., & Wu, L. (2012). Tropical cyclone intensity change in the western north pacific: Downscaling from IPCC AR4 experiments. *Journal of the Meteorological Society of Japan, 90*(2), 223-233. doi: 10.2151/jmsj.2012-205

Wang, G. (2005). Agricultural drought in a future climate: Results from 15 global climate models participating in the IPCC 4th assessment. *Climate Dynamics, 25*(7-8), 739-753. doi: 10.1007/s00382-005-0057-9

Wang, W., Dudek, M., & Liang, X. (1992). Inadequacy of effective Co2 as a proxy in assessing the regional climate change due to other radiatively active gases. *Geophysical Research Letters, 19*(13), 1375-1378. doi: 10.1029/92GL01157

Wang, X. L., Feng, Y., Compo, G. P., Swail, V. R., Zwiers, F. W., Allan, R. J., & Sardeshmukh, P. D. (2013). Trends and low frequency variability of extra-tropical cyclone activity in the ensemble of twentieth century reanalysis. *Climate Dynamics, 40*(11-12), 2775-2800. doi: 10.1007/s00382-012-1450-9

Warren, R. et al. (2010). Increasing impacts of climate change upon ecosystems with increasing global mean temperature rise. *Climate Change, 106.* p. 141-177.

Washington, W. et al. (2000). Parallel climate model (PCM) control and transient simulations. *Climate Dynamics, 16*(10-11), 755-774. doi: 10.1007/s003820000079

Watterson, I. (2006). The intensity of precipitation during extratropical cyclones in global warming simulations: A link to cyclone intensity? *Tellus Series A-Dynamic Meteorology and Oceanography, 58*(1), 82-97. doi: 10.1111/j.1600-0870.2006.00147.x

Watterson, I., Dix, M., Gordon, H., & McGregor, J. (1995). The csiro 9-level atmospheric general-circulation model and its equilibrium present and doubled Co2 climates. *Australian Meteorological Magazine, 44*(2), 111-125.

Weart, S. (2003). *The Discovery of Global Warming***.** Cambridge, U.S.A: Harvard University Press. 240 pages.

Wehner, M. F., Bala, G., Duffy, P., Mirin, A. A., & Romano, R. (2010). Towards direct simulation of future tropical cyclone statistics in a high-resolution global atmospheric model. *Advances in Meteorology,* , 915303. doi: 10.1155/2010/915303

Weinkle, J., Maue, R., & Pielke, R., Jr. (2012). Historical global tropical cyclone landfalls. *Journal of Climate, 25*(13), 4729-4735. doi: 10.1175/JCLI-D-11-00719.1

Wetherald, R., & Manabe, S. (1999). Detectability of summer dryness caused by greenhouse warming. *Climatic Change, 43*(3), 495-511. doi: 10.1023/A:1005499220385

Wetherald, R., & Manabe, S. (2002). Simulation of hydrologic changes associated with global warming. *Journal of Geophysical Research-Atmospheres, 107*(D19), 4379. doi: 10.1029/2001JD001195

Whetton, P., Fowler, A., Haylock, M., & Pittock, A. (1993). Implications of climate-change due to the enhanced greenhouse-effect on floods and droughts in Australia. *Climatic Change, 25*(3-4), 289-317. doi: 10.1007/BF01098378

Yeh, S., & Kirtman, B. P. (2007). ENSO amplitude changes due to climate change projections in different coupled models. *Journal of Climate, 20*(2), 203-217. doi: 10.1175/JCLI4001.1

Yoshimura, J., & Sugi, M. (2005). Tropical cyclone climatology in a high-resolution AGCM -impacts of SST warming and CO2 increase. *Sola, 1*, 133-136. doi: 10.2151/sola.2005-035

Yoshimura, J., Sugi, M., & Noda, A. (2006). Influence of greenhouse warming on tropical cyclone frequency. *Journal of the Meteorological Society of Japan, 84*(2), 405-428. doi: 10.2151/jmsj.84.405

Zelle, H., Van Oldenborgh, G., Burgers, G., & Dijkstra, H. (2005). El Nino and greenhouse warming: Results from ensemble simulations with the NCAR CCSM. *Journal of Climate, 18*(22), 4669-4683. doi: 10.1175/JCLI3574.1

Zhao, M., & Held, I. M. (2012). TC-permitting GCM simulations of hurricane frequency response to sea surface temperature anomalies projected for the late-twenty-first century. *Journal of Climate, 25*(8), 2995-3009. doi: 10.1175/JCLI-D-11-00313.1

Zhao, M., Held, I. M., Lin, S., & Vecchi, G. A. (2009). Simulations of global hurricane climatology, interannual variability, and response to global warming using a 50-km resolution GCM. *Journal of Climate, 22*(24), 6653-6678. doi: 10.1175/2009JCLI3049.1

Zhu, Y. & Toth, Z. Extreme Weather Events and Their Probabilistic Prediction By The NCEP Ensemble Forecast System.http://www.emc.ncep.noaa.gov/gmb/ens/target/ens/albapr/albapr.html

Zwiers, F., & Kharin, V. (1998). Changes in the extremes of the climate simulated by CCC GCM2 under CO2 doubling. *Journal of Climate, 11*(9), 2200-2222. doi: 10.1175/1520-0442(1998)011<2200:CITEOT>2.0.CO;2

Appendix

Table 9. Data gathered for different parameters used in this research. All data correspond to their respective study (left-hand column) and model(s) utilized (middle column) and are converted into changes (percent or absolute) per degree Celsius of global warming (right-hand column).

Global tropical cyclone (TC) frequency		
Study	**Model**	**% change in TC frequency per degree Celsius of global warming**
Held & Zhao. (2011)	GFDL CM2.1 scenario mean	-5.15
Bengtsson et al. (1996)	ECHAM3 (T106)	-41.90
Bengtsson et al. (2007)	ECHAM5 (T63)	-6.12
Bengtsson et al. (2007)	ECHAM5 (T213)	-2.55
Bengtsson et al. (2007)	ECHAM5 (T319)	-3.16
Oouchi et al. (2006)	MRI/JMA20	-12.00
Yoshimura et al. (2006)	AGCM (T106) JMAGSM9603 scenario mean	-8.23
Murakami et al. (2012)	MRI-AGCM20.3.2	-6.08
Murakami et al. (2012)	MRI-AGCM60.3.2	-9.00
Murakami et al. (2012)	MRI-AGCM20.3.1	-9.00
Murakami et al. (2012)	MRI-AGCM60.3.1	-9.15
Murakami et al. (2012b)	MRI-AGCM60.3.2	-8.57
Gualdi et al. (2008)	SINTEX-G mean	-9.40
Haarsma et al. (1993)	UKMO	17.64
Royer & Chauvin. (2009)	Ensemble of 15coupled CGCMs	2.24
Sugi et al. (2009)	MRI-CGCM20.2.3	-29.20
Sugi et al. (2009)	MIROC-HI	-14.34
Yoshimura & Sugi.(2005)	JMAGSM8911 scenario mean	-6.31
McDonald et al. (2005)	HadCM3	-2.00
Sugi et al. (2002)	MRI-CGCM (JMA-GSM8911)	-21.19
Sugi et al. (2012)	MRI-AGCM60.3.2 scenario mean	-8.96
Sugi & Yoshimura (2012)	MRI-CGCM60.3.2	-10.00
Wehner et al. (2010)	fvCAM2.2	11.17
Noda et al. (2008)	20-km mesh high horizontal resolution AGCM	-11.54
Tsutsui (2002)	NCAR CCM2	1.18
Emanuel (2013)	Six CMIP5 model mean	13.89

Intense global tropical cyclone (TC) frequency		
Study	**Model**	**% change in intense global TC frequency per degree Celsius of global warming**
Held & Zhao. (2011)	Mean GFDL CM2.1	-5.15
Bengtsson et al. (1996)	ECHAM3 (T106)	-35.50
Bengtsson et al. (2007)	ECHAM5 (T63)	0.00
Bengtsson et al. (2007)	ECHAM5 (T213)	15.96
Bengtsson et al. (2007)	ECHAM5 (T319)	4.23
Oouchi et al. (2006)	MRI/JMA20	0.00
Yoshimura et al. (2006)	AGCM (T106) JMAGSM9603 scenario mean	15.58
Zhao & Held (2012)	Ensemble of 8 IPCC AR4 models and uniform 2K SST warming	3.02
Zhao et al. (2009)	GFDL CM2.1	-2.40
Zhao et al. (2009)	HadCM3	1.32
Zhao et al. (2009)	ECHAM5	-2.46
Knutson & Tuleya (2004)	9 CMIP2+ models	3.91
Yoshimura & Sugi (2005)	Mean JMAGSM8911	0.00
Sugi et al. (2002)	MRI-CGCM (JMA-GSM8911)	0.00
Noda et al. (2008)	20-km mesh high horizontal resolution AGCM	2.69
Tsutsui (2002)	NCAR CCM2	3.75
Most intense global tropical frequency		
Study	**Model**	**% change in most intense global TC intensity per degree Celsius of global warming**
Bengtsson et al. (1996)	ECHAM3 (T106)	-30.00
Bengtsson et al. (2007)	ECHAM5 (T63)	0.00
Bengtsson et al. (2007)	ECHAM5 (T213)	8.63
Oouchi et al. (2006)	MRI/JMA20	0.06
Zhao et al. (2009)	GFDL CM2.1	0.00
Zhao et al. (2009)	HadCM3	0.00
Zhao et al. (2009)	ECHAM5	0.00
Murakami et al. (2012)	MRI-AGCM20.3.2	0.00
Murakami et al. (2012)	MRI-AGCM20.3.1	0.00
Knutson & Tuleya (2004)	9 CMIP2+ models	7.39
Yoshimura & Sugi (2005)	Mean JMAGSM8911	0.00
Sugi et al. (2002)	MRI-CGCM (JMA-GSM8911)	0.00
Wehner et al. (2010)	fvCAM2	108.10
Noda et al. (2008)	20-km mesh high horizontal resolution AGCM	76.92
Emanuel (2013)	CMIP5 RCP8.5 (6 model mean)	22.22

Global tropical cyclone intensity		
Study	**Model**	**% change in global TC intensity per degree Celsius of global warming**
Held & Zhao. (2011)	Mean GFDL CM2.1	0.92
Bengtsson et al. (2007)	ECHAM5 (T63)	0.00
Oouchi et al. (2006)	MRI/JMA20	4.28
Yoshimura et al. (2006)	AGCM (T106) JMAGSM9603 scenario mean	-7.36
Zhao et al. (2009)	Ensemble	1.64
Murakami et al. (2012)	MRI-AGCM20.3.2	1.60
Murakami et al. (2012)	MRI-AGCM20.3.1	4.31
Gualdi et al. (2008)	SINTEX-G mean	0.00
Haarsma et al. (1993)	UKMO	5.45
Knutson et al. (2001)	GFDL R30	1.89
Knutson & Tuleya. (2004)	9 CMIP2+ models	3.35
Noda et al. (2008)	20-km mesh high horizontal resolution AGCM	6.00
Tsutsui (2002)	NCAR CCM2	0.00
NW Pacific tropical cyclone (TC) frequency		
Study	**Model**	**% change in NW Pacific TC frequency per degree of Celsius global warming**
Stowasser et al. (2007)	NCAR CCSM2	6.67
Bengtsson et al. (1996)	ECHAM3 (T106)	-34.00
Murakami et al. (2011)	MRI-JMA AGCM20	-3.08
Murakami et al. (2012)	MRI-AGCM20.3.1	3.19
Murakami et al. (2012)	MRI-AGCM60.3.1	-7.62
Murakami et al. (2012)	MRI-AGCM20.3.2	-9.04
Murakami et al. (2012)	MRI-AGCM60.3.2	-11.28
Murakami et al. (2012b)	MRI-AGCM60.3.2	-11.52
Oouchi et al. (2006)	20-km mesh AGCM-MRI/JMA	-15.20
Haarsma et al. (1993)	UKMO	19.99
Sugi et al. (2002)	MRI-CGCM (JMAGSM8911)	-41.13
Royer & Chauvin. (2009)	15 coupled CGCMs	3.58
Sugi et al. (2009)	MRI-CGCM20.2.3.	-27.00
Sugi et al. (2009)	MIROC-HI	25.15
McDonald et al. (2005)	HadCM3	-10.00
Li et al. (2010)	ECHAM5 (T319)	7.81
Wehner et al. (2010)	fvCAM2.2	7.82
Noda et al. (2008)	20-km mesh high horizontal resolution AGCM	-14.62

Tsutsui (2002)	NCAR CCM2	6.56
Intense NW Pacific tropical cyclone (TC) frequency		
Study	**Model**	**% change in intense NW Pacific TC frequency per degree Celsius of global warming**
Haarsma et al. (1993)	UKMO	14.55
Zhao & Held (2012)	Ensemble of 8 IPCC AR4 models	-9.06
Zhao et al. (2009)	GFDL CM2.1	3.99
Zhao et al. (2009)	HadCM3	-3.29
Zhao et al. (2009)	ECHAM5	-11.08
Sugi et al. (2002)	MRI-CGCM (JMAGSM8911)	-27.64
Wang & Wu (2012)	CGCM: T47	38.98
Wang & Wu (2012)	CNRM: CM3.0	15.19
Wang & Wu (2012)	GFDL 2.1	25.86
Wang & Wu (2012)	GISS-EH	49.78
Wang & Wu (2012)	F-GOALS	3.99
Wang & Wu (2012)	INM: CM3	1.24
Wang & Wu (2012)	ECHAM5	18.16
Wang & Wu (2012)	HADGEM1	11.63
Most intense NW Pacific tropical cyclone frequency		
Study	**Model**	**% change in most intense NW Pacific TC frequency per degree Celsius of global warming**
Knutson et al. (1998)	GFDL R30	6.80
Stowasser et al. (2007)	NCAR CCSM2	22.22
Haarsma et al. (1993)	UKMO	12.00
Wang & Wu (2012)	CGCM (T47)	38.98
Wang & Wu (2012)	CNRM CM3.0	15.19
Wang & Wu (2012)	GFDL2.1	25.86
Wang & Wu (2012)	GISS-EH	49.78
Wang & Wu (2012)	FGOALS	3.99
Wang & Wu (2012)	INM CM3	1.24
Wang & Wu (2012)	ECHAM5	18.16
Wang & Wu (2012)	HADGEM1	11.63

NW Pacific tropical cyclone (TC) intensity		
Study	**Model**	**% change in NW Pacific TC cyclone intensity per degree Celsius of global warming**
Knutson et al. (1998)	GFDL R30	4.29
Knutson & Tuleya. (1999)	GFDL R30/GFDL Hurricane Prediction System	2.86
Stowasser et al. (2007)	NCAR CCSM2	11.11
Knutson & Tuleya. (2004)	9 CMIP2+ models	3.35
Murakami et al. (2011)	MRI-JMA AGCM20	1.02
Murakami et al. (2012)	MRI-AGCM20.3.1	6.96
Murakami et al. (2012)	MRI-AGCM20.3.2	2.84
Oouchi et al. (2006)	20-km mesh AGCMMRI/JMA	1.68
Haarsma et al. (1993)	UKMO	5.45
Noda et al. (2008)	20-km mesh high horizontal resolution AGCM	0.88
Tsutsui (2002)	NCAR CCM2	0.00
Wang & Wu (2012)	CGCM: T47	5.08
Wang & Wu (2012)	CNRM: CM3.0	4.43
Wang & Wu (2012)	GFDL 2.1	5.17
Wang & Wu (2012)	GISS-EH	8.23
Wang & Wu (2012)	F-GOALS	-0.17
Wang & Wu (2012)	INM: CM3	1.24
Wang & Wu (2012)	ECHAM5	4.73
Wang & Wu (2012)	HADGEM1	3.72
Atlantic tropical cyclone (TC) frequency		
Study	**Model**	**% change in Atlantic TC frequency per degree Celsius of global warming**
Bengtsson et al. (1996)	ECHAM3 (T106)	-13.00
Oouchi et al. (2006)	20-km mesh high-resolution global atmospheric model of MRI/JMA	13.60
Murakami et al. (2012)	MRI-AGCM20.3.1	3.19
Murakami et al. (2012)	MRI-AGCM60.3.1	-0.62
Murakami et al. (2012)	MRI-AGCM20.3.2	-11.56
Murakami et al. (2012)	MRI-AGCM60.3.2	-15.60
Murakami et al. (2012b)	MRI-AGCM60.3.2	-12.14
Knutson et al. (2008)	18 CMIP3 model ensemble from IPCC AR4	-13.39
Royer & Chauvin. (2009)	15 coupled CGCMs	-1.19

Murakami & Wang. (2010)	18 CMIP3 model ensemble from IPCC AR4	1.89
Haarsma et al. (1993)	UKMO	23.03
Andre et al. (2008)	ARPEGE-Climat	-13.71
Sugi et al. (2002)	MRI-CGCM	28.50
Sugi et al. (2009)	MRI-CGCM20.2.3	53.60
McDonald et al. (2005)	HadCM3	-10.67
Bender et al. (2010)	GFDL CM2.1	-1.30
Bender et al. (2010)	MRI-CGCM	-7.69
Bender et al. (2010)	MP1-ECHAM5	-8.23
Bender et al. (2010)	HadCM3	-13.07
Zhao et al. (2009)	GFDL CM2.1	-15.97
Zhao et al. (2009)	HadCM3	-17.76
Zhao et al. (2009)	ECHAM5	8.00
Wehner et al. (2010)	fvCAM2.2	19.55
Noda et al. (2008)	High-horizontal resolution AGCM	13.08
Tsutsui (2002)	NCAR CCM2	-8.63
Intense global tropical cyclone frequency		
Study	**Model**	**% change in intense Atlantic TC frequency per degree Celsius of global warming**
Zhao & Held (2012)	Ensemble of 8 IPCC AR4 models and uniform 2K SST warming	-7.55
Knutson et al. (2008)	18 CMIP3 model ensemble from IPCC AR4	-5.36
Bender et al. (2010)	GFDL CM2.1	-2.44
Bender et al. (2010)	MRI-CGCM	-8.39
Bender et al. (2010)	MP1-ECHAM5	-9.98
Bender et al. (2010)	HadCM3	-16.00
Zhao et al. (2009)	GFDL CM2.1	6.39
Zhao et al. (2009)	HadCM3	-17.11
Zhao et al. (2009)	ECHAM5	0.00
Most intense Atlantic tropical cyclone frequency		
Study	**Model**	**% change in most intense Atlantic TC frequency per degree Celsius of global warming**
Knutson et al. (2008)	18 CMIP3 model ensemble from IPCC AR4	-2.38
Haarsma et al. (1993)	UKMO	6.22
Bender et al. (2010)	GFDL CM2.1	51.95
Bender et al. (2010)	MRI-CGCM	62.94

Bender et al. (2010)	MP1-ECHAM5	19.95
Bender et al. (2010)	HadCM3	-16.00
Atlantic tropical cyclone (TC) intensity		
Study	**Model**	**% change in Atlantic TC intensity per degree Celsius of global warming**
Knutson & Tuleya. (2004)	9 CMIP2+ models	3.35
Oouchi et al. (2006)	20-km mesh high-resolution global atmospheric model of MRI/JMA	4.48
Murakami et al. (2012)	MRI-AGCM20.3.1	1.88
Murakami et al. (2012)	MRI-AGCM60.3.1	3.85
Knutson et al. (2008)	18 CMIP3 model ensemble from IPCC AR4	0.86
Haarsma et al. (1993)	UKMO	5.45
Noda et al. (2008)	High-horizontal resolution AGCM	7.77
Tsutsui (2002)	NCAR CCM2	0.00
South Asian Summer monsoon zonal wind		
Study	**Method**	**Absolute change in S. Asian Summer monsoon zonal wind (m/s) per degree Celsius of global warming**
May (2004)	ECHAM4/OPYC3	-0.90
Ashrit et al. (2003)	CNRM	0.00
May (2011)	Mean ECHAM5/MPI-OM	-1.08
Ueda et al. (2006)	INM CM3.0	-0.59
Ueda et al. (2006)	CNRM.CM3	-0.15
Ueda et al. (2006)	ECHAM5/MPI-OM	-0.21
Ueda et al. (2006)	F-GOALS	-0.18
Ueda et al. (2006)	GFDL CM.2.0	-0.15
Ueda et al. (2006)	MIROC3.2 MEDRES	-0.50
Ueda et al. (2006)	MRI CGCM2.3.2	-0.26
Dairaku & Emori (2006)	Ensemble of 7 models	-0.64
South Asian Summer monsoon rainfall		
Study	**Model**	**% change in Summer (JJAS) monsoon rainfall per degree Celsius of global warming**
Dai et al. (2001)	PCM	18.75
Meehl et al. (2000)	NCAR CSM	8.11

Meehl et al. (2000)	NCAR DOE	0.40
Meehl et al. (2000b)	DOE PCM	-10.33
May (2004)	ECHAM4/OPYC3	3.52
Ashrit et al. (2001)	ECHAM4/OPYC3	13.05
Ashrit et al. (2003)	CNRM	2.44
Hu et al. (2000)	ECHAM4/OPYC3	8.28
May (2002)	ECHAM4/OPYC3	4.38
May (2011)	Mean ECHAM5/MPI-OM	1.79
Meehl & Washington (1993)	GCM	4.94
Bhaskaran et al. (1995)	UKMO HadCM2	0.00
Kripalani et al. (2007)	CCCma CGCM3.1	3.50
Kripalani et al. (2007)	CNRM3 CM3	2.84
Kripalani et al. (2007)	MPI-ECHAM5	0.91
Kripalani et al. (2007)	MIROC-HI	2.92
Kripalani et al. (2007)	MIROC-MED	2.55
Kripalani et al. (2007)	Model ensemble	2.44
Kripalani et al. (2007)	CNRM3 CM3	-0.32
Kripalani et al. (2007)	ECHAM5/MPI-OM	3.85
Kripalani et al. (2007)	INM CM3	1.94
Kripalani et al. (2007)	IPSL CM4	2.70
Kripalani et al. (2007)	GFDL CM2.0	2.66
Kripalani et al. (2007)	GFDL CM2.1	4.65
Kripalani et al. (2007)	GISS-EH	6.86
Kripalani et al. (2007)	GISS-ER	5.71
Kripalani et al. (2007)	F-GOALS-g1.0	0.26
Kripalani et al. (2007)	CSIRO Mk3	7.61
Kripalani et al. (2007)	ECHO-G	3.32
Kripalani et al. (2007)	MIROC3.2-HI	2.03
Kripalani et al. (2007)	MIROC3.2-MED	3.12
Kripalani et al. (2007)	MRI-CGCM 2.3.2	2.24
Kripalani et al. (2007)	NCAR PCM	0.31
Kripalani et al. (2007)	NCAR CCSM3	0.99
Kripalani et al. (2007)	UKMO HadGEM	7.54
Sabade et al. (2011)	Model mean (IPCCAR4)	8.27
Lal et al. (1998)	DKRZO	4.52
Lal et al. (1998)	UKMOH	2.54
Lal et al. (1998)	CCC	3.95
Lal et al. (1998)	BMRC	-1.38
Lal et al. (1998)	CSIRO9	1.21
Lal et al. (1998)	UKMO	2.47
Lal et al. (1998)	GFDLQ	9.05

Lal et al. (1998)	GFDLH	6.38
Lal et al. (1998)	DKRZL	3.98
Lal et al. (2001)	Mean CCRS/NIES1	2.95
Meehl & Arblaster (2003)	Mean PCM	6.73
Ueda et al. (2006)	INM CM3.0	3.68
Ueda et al. (2006)	CNRM.CM3	0.90
Ueda et al. (2006)	ECHAM5/MPI-OM	3.78
Ueda et al. (2006)	F-GOALS	1.57
Ueda et al. (2006)	GFDL CM.2.0	1.83
Ueda et al. (2006)	MIROC3.2 MEDRES	2.79
Ueda et al. (2006)	MRI CGCM2.3.2	4.30
Dairaku & Emori (2006)	Ensemble of 7 models	1.29
Stowasser et al. (2009)	GFDL CM2.1	3.40
Global precipitation		
Study	**Model**	**% change in global precipitation per degree Celsius of global warming**
Bengtsson et al. (2009)	ECHAM5	1.59
Bengtsson et al. (2007)	ECHAM5 (T213)	1.73
Bengtsson et al. (2007)	ECHAM5 (T63)	1.62
Wetherald & Manabe (2002)	Coupled oceanic and atmospheric GCMs	2.26
Bengtsson et al. (1996)	ECHAM3 (T106)	0.00
Sugi et al. (2002)	MRI-CGCM (JMA-GSM8911)	1.25
Gordon et al. (1992)	CSIRO4	1.93
Johns et al. (2003)	Mean HadCM3 scenarios	1.02
Houghton et al. (1990)	UKHI	2.57
Hennessy et al. (1997)	CSIRO9	2.08
Hennessy et al. (1997)	UKHI	2.86
Thompson & Pollard (1995)	Genesis GCM v1.02	1.37
Thompson & Pollard (1995)	Genesis v1.02 (PRESP)	1.39
Thompson & Pollard (1995)	Genesis v1.02 (PRESC)	1.44
Thompson & Pollard (1995)	Genesis v1.02 (OLDP)	1.78
Thompson & Pollard (1995)	Genesis v1.02 (OLDC)	1.68
Thompson & Pollard (1995)	Genesis v1.02 (EARL)	1.89
Raisanen (2002)	BMCR	0.82
Raisanen (2002)	CCCma	0.68
Raisanen (2002)	CCSR1	0.67
Raisanen (2002)	CCSR2	1.82
Raisanen (2002)	CERFACS	2.26

Raisanen (2002)	CSIRO	1.80
Raisanen (2002)	ECHAM3	1.84
Raisanen (2002)	ECHAM4	-0.14
Raisanen (2002)	GFDL (R15)	2.14
Raisanen (2002)	GFDL (R30)	2.33
Raisanen (2002)	GISS	1.31
Raisanen (2002)	HadCM2	1.71
Raisanen (2002)	HadCM3	0.88
Raisanen (2002)	IAP/LASG	0.55
Raisanen (2002)	LMD/IPSL	1.26
Raisanen (2002)	MRI1	2.48
Raisanen (2002)	MRI2	1.30
Raisanen (2002)	NCAR-CSM	1.46
Raisanen (2002)	NCAR/DOM-PCM	1.53
Gualdi et al. (2008)	SINTEX-G scenario mean	0.87
Semenov & Bengtsson (2002)	ECHAM4/OPYC3	0.56
Henderson-Sellers et al. (1993)	NCAR CCM1-OZ	2.36
Hart et al. (1990)	BMRC	1.24
Wang et al. (1992)	CCM1W	1.93
Oglesby & Saltzman (1992)	NCAR CCM1	1.38
Watterson et al. (1995)	CSIRO9	2.21
Kharin & Zwiers (2000)	Mean CGCM1	0.00
Boer et al. (2000)	CCCma	0.79
Boer et al. (1992)	CCC GCMII	1.09
Boer et al. (2000b)	CCCma	2.77
Dai et al. (2001)	Mean NCAR CSM	1.91
Dai et al. (2001)	PCM	1.65
Dai et al. (2004)	PCM	0.00
Meehl et al. (2000)	Mean NCAR CSM	1.68
Meehl et al. (2000)	Mean DOE	0.88
Zwiers & Kharin (1998)	CCC GCM2	1.10
Gregory et al. (1997)	Coupled GCMs	-1.76
Held & Zhao. (2011)	Mean GFDL CM2.1	1.07

Global precipitable water

Study	Model	% change in global precipitable water per degree Celsius of global warming
Bengtsson et al. (2009)	ECHAM5	6.85
Bengtsson et al. (2007)	ECHAM5 (T63)	7.12

Sugi et al. (2002)	MRI-CGCM (JMA-GSM8911)	8.75
Gordon et al. (1992)	CSIRO4	6.25
Held & Soden (2006)	PCMDI AR4 model1	6.25
Held & Soden (2006)	PCMDI AR4 model2	6.47
Held & Soden (2006)	PCMDI AR4 model3	7.65
Held & Soden (2006)	PCMDI AR4 model4	8.18
Held & Soden (2006)	PCMDI AR4 model5	8.48
Held & Soden (2006)	PCMDI AR4 model6	5.90
Held & Soden (2006)	PCMDI AR4 model7	6.67
Held & Soden (2006)	PCMDI AR4 model8	7.75
Held & Soden (2006)	PCMDI AR4 model9	8.04
Held & Soden (2006)	PCMDI AR4 model10	8.25
Held & Soden (2006)	PCMDI AR4 model11	6.67
Held & Soden (2006)	PCMDI AR4 model12	7.39
Held & Soden (2006)	PCMDI AR4 model13	7.71
Held & Soden (2006)	PCMDI AR4 model14	8.57
Held & Soden (2006)	PCMDI AR4 model15	8.20
Held & Soden (2006)	PCMDI AR4 model16	7.54
Held & Soden (2006)	PCMDI AR4 model17	8.14
O'Gorman & Muller (2010)	Model mean	7.09
Global convection precipitation		
Study	**Model**	**% change in global convective rainfall per degree Celsius of global warming**
Gordon et al. (1992)	CSIRO4	5.75
Mitchell & Ingram (1992)	UKMI (low resolution version)	2.86
Johns et al. (2003)	Mean HadCM3 scenarios	1.02
Hennessy et al. (1997)	CSIRO9	6.25
Hennessy et al. (1997)	UKHI	8.57
Gualdi et al. (2008)	SINTEX-G scenario mean	-1.92
Lau et al. (2013)	14 CMIP5 model ensemble	18.28
Northern hemisphere (NH) annual mid-latitude cyclone frequency		
Study	**Model**	**% change in annual NH mid-latitude cyclones per degree Celsius of global warming**
Konig et al. (1993)	ECHAM2	-0.58
Sinclair & Watterson (1999)	CSIRO9 Mk2	-1.57
Lambert (2004)	CCCma CGCM1	-1.36
Lambert (2004)	CCCma CGCM2	-1.71

Watterson (2006)	CSIRO Mk2	-1.15
Bengtsson et al. (2009)	ECHAM5	-0.87
Bengtsson et al. (2006)	MPI-OM	0.00
Northern hemisphere (NH) cool season mid-latitude cyclone frequency		
Study	**Model**	**Absolute change in NH cool season mid-latitude cyclone frequency (per Winter) per degree Celsius of global warming**
Geng & Sugi (2003)	JMA forecast model (GSM8911)	-0.23
Carnell & Senior (1998)	HadCM2 scenario mean	-3.25
Mizuta et al. (2011)	MRI-AGCM20.3.1	-238.00
Mizuta et al. (2011)	MRI-AGCM60.3.1 scenario mean	-18.73
Finnis et al. (2007)	NCAR CCSM3	-0.86
Catto et al. (2011)	HadGEM scenario mean	-1.33
Pinto et al. (2007)	ECHAM5/MPI-OM1 scenario mean	-65.60
Lambert (1995)	CCCma CGCM2	-30.11
Lambert (2004)	CCCma CGCM1	-74.57
Lambert (2004)	CCCma CGCM2	-94.44
Bengtsson et al. (2006)	MPI-OM	-0.10
Lambert (2006)	CCCma (T47)	-53.57
Lambert (2006)	CNRM: CM3	-33.99
Lambert (2006)	MIROC HI	-33.72
Lambert (2006)	MIROC MED	-53.02
Lambert (2006)	GFDL 2.0	-47.51
Lambert (2006)	GFDL 2.1	-72.15
Lambert (2006)	GISS ER	-59.67
Lambert (2006)	GISS AOM	-59.57
Lambert (2006)	IPSL CM4	-39.62
Lambert (2006)	INM CM3	-21.47
Lambert (2006)	MRI CGCM2.3.2	-47.10
Lambert (2006)	NCAR CCSM3	-32.54
Lambert (2006)	ECHAM5	-38.36
Northern hemisphere (NH) intense cool season cyclone frequency		
Study	**Model**	**Absolute change in intense NH cool season cyclone frequency (per Winter) per degree Celsius of global warming**
Geng & Sugi (2003)	JMA forecast model (GSM8911)	-0.01

Carnell & Senior (1998)	HadCM2 scenario mean	-1.97
Mizuta et al. (2011)	MRI-AGCM20.3.1	-7.10
Mizuta et al. (2011)	MRI-AGCM60.3.1 scenario mean	-18.79
Catto et al. (2011)	HadGEM scenario mean	0.00
Lambert (1995)	CCCma CGCM2	8.00
Lambert (2004)	CCCma CGCM1	40.67
Lambert (2004)	CCCma CGCM2	101.25
Bengtsson et al. (2009)	ECHAM5	-1.39
Bengtsson et al. (2006)	MPI-OM	0.00
Lambert (2006)	CCCma (T47)	6.66
Lambert (2006)	CNRM: CM3	1.00
Lambert (2006)	MIROC HI	4.34
Lambert (2006)	MIROC MED	1.93
Lambert (2006)	GFDL2.0	3.29
Lambert (2006)	GFDL2.1	7.82
Lambert (2006)	GISS ER	2.47
Lambert (2006)	GISS AOM	1.40
Lambert (2006)	IPSL CM4	1.82
Lambert (2006)	INM CM3	-3.07
Lambert (2006)	MRI CGCM2.3.2	2.90
Lambert (2006)	NCAR CCSM3	0.70
Lambert (2006)	ECHAM5	6.75

Southern hemisphere (SH) annual mid-latitude cyclone frequency

Study	Model	% change in SH annual mid-latitude cyclone frequency per degree Celsius of global warming
Konig et al. (1993)	ECHAM2	-0.77
Sinclair & Watterson (1999)	CSIRO9 Mk2	-1.91
Watterson (2006)	CSIRO Mk2	-1.43
Bengtsson et al. (2009)	ECHAM5	0.26
Bengtsson et al. (2006)	MPI-OM	0.00
Fyfe (2003)	CCCma CGCM1	-7.89

Southern hemisphere (SH) mid-cool season latitude cyclone frequency		
Study	**Model**	**Absolute change in SH cool season mid-latitude cyclone frequency (per Winter) per degree Celsius of global warming**
Geng & Sugi (2003)	JMA forecast model (GSM8911)	-0.34
Konig et al. (1993)	ECHAM2	-24.19
Lambert (2004)	CCCma CGCM1	113.58
Lambert (2004)	CCCma CGCM2	89.45
Bengtsson et al. (2006)	MPI-OM	-0.05
Lambert (2006)	CCCma (T47)	-194.81
Lambert (2006)	CNRM:CM3	-40.27
Lambert (2006)	MIROC HI	-54.59
Lambert (2006)	MIROC MED	-59.51
Lambert (2006)	GFDL 2.0	-49.71
Lambert (2006)	GFDL 2.1	-61.51
Lambert (2006)	GISS ER	-87.45
Lambert (2006)	GISS AOM	-44.68
Lambert (2006)	IPSL CM4	-47.81
Lambert (2006)	INM CM3	-29.14
Lambert (2006)	MRI CGCM2.3.2	-42.21
Lambert (2006)	NCAR CCSM3	-41.69
Lambert (2006)	ECHAM5	-57.54
Southern hemisphere (SH) intense cool season cyclone frequency		
Study	**Model**	**Absolute change in intense SH cool season mid-latitude cyclone frequency (per Winter) per degree Celsius of global warming**
Geng & Sugi (2003)	JMA forecast model (GSM8911)	-0.01
Lambert (1995)	ECHAM2	4.31
Lambert (2004)	CCCma CGCM1	34.57
Lambert (2004)	CCCma CGCM2	90.00
Bengtsson et al. (2006)	MPI-OM	0.13
Lambert (2006)	CCCma (T47)	29.22
Lambert (2006)	CNRM: CM3	45.77
Lambert (2006)	MIROC HI	58.39
Lambert (2006)	MIROC MED	23.14

Lambert (2006)	GFDL2.0	22.41
Lambert (2006)	GFDL2.1	27.97
Lambert (2006)	GISS ER	18.00
Lambert (2006)	GISS AOM	6.38
Lambert (2006)	IPSL CM4	15.73
Lambert (2006)	INM CM3	14.57
Lambert (2006)	MRI CGCM2.3.2	9.96
Lambert (2006)	NCAR CCSM3	92.83
Lambert (2006)	ECHAM5	27.51
European soil moisture		
Study	**Model**	**% change in European soil moisture per degree Celsius of global warming**
Dai et al. (2001)	PCM scenario mean	-2.50
Wetherald & Manabe (1999)	GFDL (R15)	-13.33
Wetherald & Manabe (2002)	Coupled GCMs	-2.17
Gregory et al. (1997)	Coupled GCMs	-7.06
Boer et al. (2000b)	CCCma	-14.00
Wang (2005)	CCSM3	-0.99
Wang (2005)	GFDL CM2.1	-15.74
Dai (2013)	11 CMIP5 model mean	-3.43
North American soil moisture		
Study	**Model**	**% change in North American soil moisture per degree Celsius of global warming**
Dai et al. (2001)	PCM scenario mean	-0.5
Wetherald & Manabe (1999)	GFDL (R15)	-13.3
Wetherald & Manabe (2002)	Coupled GCMs	-2.2
Gregory et al. (1997)	Coupled oceanic and atmospheric GCMs	-8.8
Boer et al. (2000b)	CCCma	-15.0
Diffenbaugh et al. (2005)	HadCM3	-7.7
Dai (2013)	11 CMIP5 model mean	-2.86
European 30 Celsius days		
Study	**Model**	**% change in European 30 Celsius days per degree Celsius of global warming**
Beniston et al. (2007)	HIRHAM4	140.60

Beniston & Diaz (2004)	HIRHAM4	123.46
Beniston (2004)	HIRHAM4	115.74
Fischer & Schaer (2009)	Average HadCM3	11.59
Huth et al. (2000)	ECHAM3	250.91
U.S. vertical wind shear		
Study	**Model**	**% change in U.S. vertical wind shear per degree Celsius of global warming**
Trapp et al. (2009)	Model mean	-1.66
Trapp et al. (2007)	HadCM3	-4.03
Held & Zhao. (2011)	GFDL CM2.1 scenario mean	-1.12
McDonald et al. (2005)	HadCM3	0.00
Vecchi & Soden (2007)	Multi-model	-2.11
U.S. severe thunderstorm development days		
Study	**Model**	**% change in U.S. severe thunderstorm development days per degree Celsius of global warming**
Trapp et al. (2009)	Model mean	12.30
Trapp et al. (2007)	HadCM3	7.14
Trapp et al. (2007)	GFDL CM2.1	14.29
Trapp et al. (2007)	MPI-ECHAM5	9.97
Trapp et al. (2007)	NCARCCSM3	2.56
Lee (2012)	NCAR CCSM3 scenario mean	2.35
Lee (2012)	CCCma CGCM3 scenario mean	3.59
Del Genio (2007)	GISS Model EGCM	0.00
El Nino Southern Oscillation (ENSO) amplitude		
Study	**Model**	**% change in ENSO variability per degree Celsius of global warming**
Washington et al. (2000)	PCM scenario mean	-2.44
Meehl et al. (2006)	PCM scenario mean	-3.05
Meehl et al. (2006)	CCSM3 scenario mean	-5.90
Collins (2000)	HadCM2 scenario mean	-3.39
Collins (2000)	HadCM3	-1.24
Knutson et al. (1997)	GFDL (R15) scenario mean	-3.44
Merryfield (2006)	CCCma CGCM3.1 (T47)	-0.40

Merryfield (2006)	MIROC3.2-MED	-5.83
Merryfield (2006)	CNRM3 CM3	-2.96
Merryfield (2006)	GFDL CM2.0	5.82
Merryfield (2006)	GFDL CM2.1	12.19
Merryfield (2006)	GISS-EH	-0.31
Merryfield (2006)	GISS-ER	-9.27
Merryfield (2006)	F-GOALS-g1.0	-17.21
Merryfield (2006)	IPSL CM4	1.19
Merryfield (2006)	INM CM3	-6.45
Merryfield (2006)	ECHAM5/MPI-OM	14.84
Merryfield (2006)	MRI-CGCM2.3.2	10.81
Merryfield (2006)	NCAR CCSM3	-5.48
Merryfield (2006)	NCAR PCM	-2.02
Merryfield (2006)	MO/HadCM3	5.19
Knutson et al. (1994)	GFDL	-3.43
Bengtsson et al. (2006)	MPI-OM	0.00
Zelle et al. (2005)	NCAR CCSM1.4	0.00
Timmermann et al. (1999)	ECHAM4/OPYC3	10.90
Tett (1995)	UKMO	0.00
An et al. (2008)	MRI-CGCM2.3.2a scenario mean	-2.92
Yeh & Kirtman (2007)	GFDL 2.0	0.00
Yeh & Kirtman (2007)	MIROC3.2 MEDRES	0.00
Yeh & Kirtman (2007)	GISS ER	0.00
Chen et al. (2005)	MIROC3.2	10.70
El Nino Southern Oscillation (ENSO) period		
Study	**Model**	**% change in ENSO period per degree Celsius of global warming**
Collins (2000)	HadCM2 scenario mean	-8.49
Collins (2000)	HadCM3	0.00
Merryfield (2006)	CCCma CGCM3.1 (T47)	-0.44
Merryfield (2006)	MIROC3.2-MED	-13.89
Merryfield (2006)	CNRM3 CM3	-3.55
Merryfield (2006)	GFDL CM2.0	5.48
Merryfield (2006)	GFDL CM2.1	-7.10
Merryfield (2006)	GISS-EH	-1.57
Merryfield (2006)	GISS-ER	-8.61
Merryfield (2006)	F-GOALS-g1.0	-4.29
Merryfield (2006)	IPSL CM4	-2.10
Merryfield (2006)	INM CM3	-1.40

Merryfield (2006)	ECHAM5/MPI-OM	-4.52
Merryfield (2006)	MRI-CGCM2.3.2	5.52
Merryfield (2006)	NCAR CCSM3	-4.06
Merryfield (2006)	NCAR PCM	-7.69
Merryfield (2006)	MO/HadCM3	2.36
Zelle et al. (2005)	NCAR CCSM1.4	0.00
Timmermann & Collins (2004)	ECHAM4/OPYC3	-9.93